



Study the Effect of Prosthetic Foot Type on the Vibration and Stresses Subjected on Below Knee Prosthetic Limp

A THESIS
SUBMITTED TO THE COLLEGE OF ENGINEERING
UNIVERSITY OF BASRAH
IN PARTIAL FULFILLMENT
OF
THE REQUIREMENTS FOR THE DEGREE
OF MASTER OF SCIENCE
IN
MECHANICAL ENGINEERING

BY
Hayder Raheem Ma'ebid
(B.SC. MECH. ENG.)
February, 2025

بِسْمِ اللَّهِ الرَّحْمَنِ الرَّحِيمِ

﴿وَقُلِ اعْمَلُوا فَسَيَرَى اللَّهُ عَمَلَكُمْ وَرَسُولُهُ وَالْمُؤْمِنُونَ وَسَتُرَدُّونَ إِلَى

عَالِمِ الْغَيْبِ وَالشَّهَادَةِ فَيُنَبَّئُكُمْ بِمَا كُنْتُمْ تَعْمَلُونَ ﴾¹⁰⁵

صدق الله العلي العظيم

سورة التوبة

آية 105

Dedication

This work is dedicated to the Almighty God, without whom nothing is possible. I also dedicate this work to my lovely family for their unwavering support and encouragement.

To my beloved wife, whose steadfast support, patience, and encouragement have been my greatest strength throughout this journey. Also, Thanks to the patient who stayed with me for all the experimental work to complete this thesis. Thank you for believing in me and for your endless love and understanding. This thesis is a testament to your inspiration and the sacrifices you have made. I am forever grateful.

Acknowledgements

First of all, all thanks goes to **Allah** the great engineer of the universe for helping to finishing this work .

First and foremost, I extend my deepest thanks to my supervisors, **Proof. Dr Jumaa S. chiad** and Assit.Proof.Dr **Hassanein I. Khalaf**, for their invaluable guidance, expertise, and encouragement. Your feedback has been instrumental in shaping my research and helping me grow as a scholar.

I am also grateful to my **committee members**, for their insightful comments and constructive criticism, which have greatly enhanced the quality of this work.

A special thank you goes to my **colleagues and friends** in the mechanical department, whose camaraderie and collaboration made this process more enjoyable. I appreciate the stimulating discussions and shared experiences that kept me motivated.

I also wish to express my sincere gratitude to the head of the **Mechanical Engineering department** and the **dean of the Engineering College** for their leadership and support throughout my academic journey. Your commitment to fostering a conducive learning environment has been invaluable.

Lastly, I am profoundly thankful to my **wife** and my **parents**, for her unwavering support and love. Your belief in me has been a source of strength, and I could not have completed this journey without you.

Thank you all for being part of this significant chapter in my life.

Abstract

This study aims to provide insights that can lead to advancements in prosthetic technology, ultimately enhancing the overall user experience for below-knee amputees, by investigating how different prosthetic foot types affect vibrations and stresses in below-knee amputees. A 34-year-old male participant, who lost his left foot in 2016, was assessed through a CT scan at Kadhimiya Teaching Hospital to determine the dimensions of the amputated portion. This technique utilizes a narrow beam of X-rays that rotates around the body to generate cross-sectional images.

To assess the forces on three prosthetic foot types—SACH, single-axis, and multi-axis—ground reaction force was measured using the Tekscan Walkway. Interface pressure distribution was measured with an F-socket sensor between the socket and residual limb. Muscle stress in the amputated leg was analyzed using EMG Myotrace 400 sensors affixed to the thigh. Acceleration values were converted to vibration values using Fast Fourier Transform (FFT) and analyzed via Root Mean Square (RMS) for comparison across foot types. Additionally, numerical modeling and simulations were performed using ABAQUS 6.5 software alongside real-world testing.

The SACH foot recorded the lowest minimum GRF value (663.116 N), while the multi-axis foot demonstrated the highest maximum GRF (703.024 N). This suggests that the multi-axis foot may provide better energy absorption and distribution during gait, which could enhance performance characteristics, which may lead to improved mobility and quality of life for users.

The F-socket test measured maximum concentrated pressures: 33 psi (227.53 kPa) for the SACH foot, 40 psi (275.79 kPa) for the single-axis foot, and 35 psi (241.3 kPa) for the multi-axis foot. These results indicate that the multi-axis foot is the best choice among the three due to its superior pressure

distribution, dynamic performance, and comfort, making it better suited for adapting to various surfaces essential for an active lifestyle.

The EMG analysis reveals that muscle activity in the lower limb, particularly in the rectus femoris, is not significantly affected by the type of prosthetic foot used.

The RMS values of vibration showed that the SACH foot is the best option for minimizing excessive motion and providing stability, especially in the lateral and vertical directions. Its lower RMS values in the Y and Z axes indicate better performance than the Single and Multi-feet. While the Single foot excels in the X-axis, it does not match the SACH foot's overall stability. Ultimately, the best choice depends on individual needs and walking conditions, but the SACH foot is the superior option for stability and comfort.

The study simulated stress distribution in a prosthetic socket under three loading conditions: SACH Foot at 227.53 kPa, Multi-axis foot at 241.3 kPa, and single-axis foot at 275.79 kPa. The Single Axis Foot showed the highest stresses, with mean values of (9.3, 10.1, and 11.2) in the X, Y, and Z axes due to limited mobility. The Multi-Axis Foot exhibited moderate stresses (7.4, 7.9, and 8.3) from effective force distribution but lacked shock absorption. The SACH Foot had the lowest stresses (6.3, 6.8, and 7.1) due to its shock-absorbing design. This analysis highlights the importance of choosing the right prosthetic foot based on activity level and the balance between stress distribution and functionality.

In conclusion, the Multi-Axis Foot is the best overall option for biomechanical performance and comfort, unless stability is prioritized, in which case the SACH foot is preferable.

Contents

Title	Page No.
Acknowledgements	I
Certification	II
Committee Report	III
Abstract	IV
Contents	VII
Nomenclatures	X
Abbreviations	XI
Chapter One: Introduction	
1.1 Amputation	1
1.2 Prosthetic	3
1.3 Types of artificial limbs	5
1.4 Lower limb prostheses	8
1.4.1 The Amputation of Foot	8
1.4.2 Transtibial (below knee)	8
1.4.3 Knee disarticulation	8
1.4.4 Transfemoral (above knee)	8
1.4.5 Hip disarticulation	9
1.5 Transtibial (below knee)	9
1.5.1 Socket	10
1.5.2 Suspension	10
1.5.3 Shin piece	11
1.5.4 Ankle Foot Assembly	11
1.5.4.1 SACH Foot	11
1.5.4.2 Single Axis Foot	12
1.5.4.3 Multi-axis Foot	13
1.6 Vibration in Prosthetic Limbs	13
1.7 Objectives	15
1.8 Framework of the Thesis	15
Chapter Two: Literature Review	
2.1 Introduction	17
2.2 Prosthetics Limb below Knee	21
2.3 Types of Prosthetic Foot	26
2.4 Vibrations	30
2.5 Summary	32
Chapter Three: Theoretical Analysis	
3.1 Introduction	36

3.2	General equations	36
3.3	Numerical work	38
3.3.1	Force Balance	39
3.3.2	Simulation Model and Boundary Conditions	39
3.3.2.1	Abaqus Model	39
3.3.2.2	Boundary Conditions	40
3.3.2.3	Mesning and Element Type.	41
Chapter Four: Experimental Work		
4.1	Introduction	45
4.2	Measurement devices	46
4.2.1.	Tekscan Walkway	46
4.2.2.	F-Socket	48
4.2.3.	The EMG Myotrace 400	50
4.2.4.	HEX dual electrodes	52
4.2.5.	VERNIER GO DIRECT ACCELERATION SENSOR	53
4.2.6.	3DMA Rizzoli gait analysis	55
4.3	Measurement tests	58
4.3.1.	Measurement of ground reaction force (GRF)	58
4.3.2.	Measurement of socket pressure distribution (F-Socket)	58
4.3.3.	Muscle stress of the lower muscles of the limbs	59
4.3.4.	Acceleration measurement	61
4.3.5.	Gait analysis	63
Chapter Five: Results and Discussion		
5.1	Introduction	65
5.2	Ground Reaction Force (GRF) and Knee Force Results	65
5.3.	F-Socket results	74
5.4.	EMG Activity of the lower limb Muscles results	80
5.5.	Acceleration results	87
5.6.	Vibration results	94
5.7.	3DMA Rizzoli Gait Analysis	101
5.7.1.	Gait cycle analysis	102
5.7.2.	Pelvis Angle Results	104
5.7.3.	Hips Angle Results	109
5.7.4.	Knee Angle Results	114
5.7.5.	Ankle Flexion Angle Results	118
5.7.6.	Foot Direction Angle Results	123
5.8	Simulation and results analysis	125
5.8.1.	Introduction	125

5.8.2.	Finite Element Model	126
5.8.2.1.	Model geometry	126
5.8.2.2.	Mesh generation	127
5.8.3.	Model Development	127
5.8.4.	Boundary Condition Impact	128
5.8.5.	Loading Conditions	128
5.8.6.	Computational Analysis	128
5.8.7.	Results and Discussion	129
5.8.7.1.	Detailed Stress Analysis	131
5.8.7.2.	Deflection (Displacement) Analysis	132
5.8.7.3.	Safety Factor Assessment	134
Chapter six: Conclusions and Recommendations		
6.1	Conclusions	136
6.2	Recommendations	138
References		140

Nomenclature

Symbol	Description	Unit
a	Acceleration	m/s^2
A	Surface area of the prosthetic foot	m^2
AC	Alternating Current	Ampere
B	The strain-displacement matrix	
D	The material property matrix	
E	The Young's modulus of material	Pa
F	Force	N
f	The force vector	
G	Ground reaction force	N
IP	interface pressure	Pa
K	Stiffness matrix	
L	Length	m
m	Mass	Kg
P	The applied pressure	Pa or MPa
u	The displacement	m
U	Strain energy density	J/m ³
V	Volume	m^3

Greek Symbols

Symbol	Description	Unit
ϵ	The strain	
$\Delta\epsilon$	The change in strain during cyclic loading	
σ	The stress	Pa or MPa
$\Delta\sigma$	The change in stress during cyclic loading	Pa or MPa
ΔL	The change in length	

Subscripts

Symbol	Description
o	Original
1, 2, 3	The principal stress vector
ankle	Description of the physical parameters of the ankle
foot	Description of the physical parameters of the foot
g	Gravity
knee	Description of the physical parameters of the knee
shank	Description of the physical parameters of the shank
x, y, z	Cartesian Coordinates

Abbreviations

Symbol	Description
3DMA	Three-Dimensional Analysis
AC	Alternating Current
CT scan	Computed Tomography Scan
EMG	Electromyography
ESAR	Energy Saving and Return
FBG	Fibber Bragg Grating
FEM	Finite Element Methods
FFT	Fast Fourier Transform
GRF	Ground Reaction Force
HDPE	High Density Polyethylene
HEX	Hexokinase
HS	Hydrostatic Socket
PLC	Programmable logic controller
PTB	Patellar Tendon Bearing
RMS	Root Mean Square
SA	Single Axis Foot
SACH	Solid Ankle Cushion Heal
SG	Strain Gauge
TSB	Total Surface Bearing
TTAS	Transtibial amputations
VAS	Vacuum Assisted Suction

Chapter One

Introduction

Chapter One

Introduction

1.1 Amputation

Amputation refers to the surgical removal of a part or parts of the body, which can be caused by a traumatic event or planned surgical measure. Traumatic amputation can place a burden on families, society, and medical facilities. Depending on the cause of amputation, it may be performed as a planned surgery to address pain or a disease process in the affected limb, such as malignancy or gangrene [1].

The typical forms of amputation can be classified to [2][3]:

- a. Upper-limb amputation.
- b. Lower-limb amputation.

Lower-limb amputations occur more frequently than upper-limb amputations, and most amputations occur in older adults, particularly as a complication of diabetes mellitus. However, amputations can also be performed for a variety of other reasons, such as congenital limb deficiencies, vascular insufficiency, cancer, and traumatic injuries. Amputees must undergo significant physical, social, and emotional adjustments, but the degree of adaptation can vary greatly among individuals.

Individuals who have lost a limb due to acquired amputation or congenital deficiency often use prosthetic limbs to improve the function and/or appearance of the missing limb. Prosthetic limbs are designed to restore or simulate some of the capabilities and aesthetics of a natural limb. [4].

Following the arm or leg amputation, you may be eligible for a prosthetic limb. These artificial limbs are designed to imitate the movements of natural limbs, although it may take some time to adjust to them. A physical therapist will guide you through exercises to help you become accustomed to the prosthetic limb. Generally, the fitting process for a prosthetic limb takes place six to eight weeks after surgery, once the incision has fully healed [2].

The individuals who undergo lower limb amputation tend to experience more significant life changes following the procedure [1]. In the present study, the focus will be on the prosthetic limb below the knee.

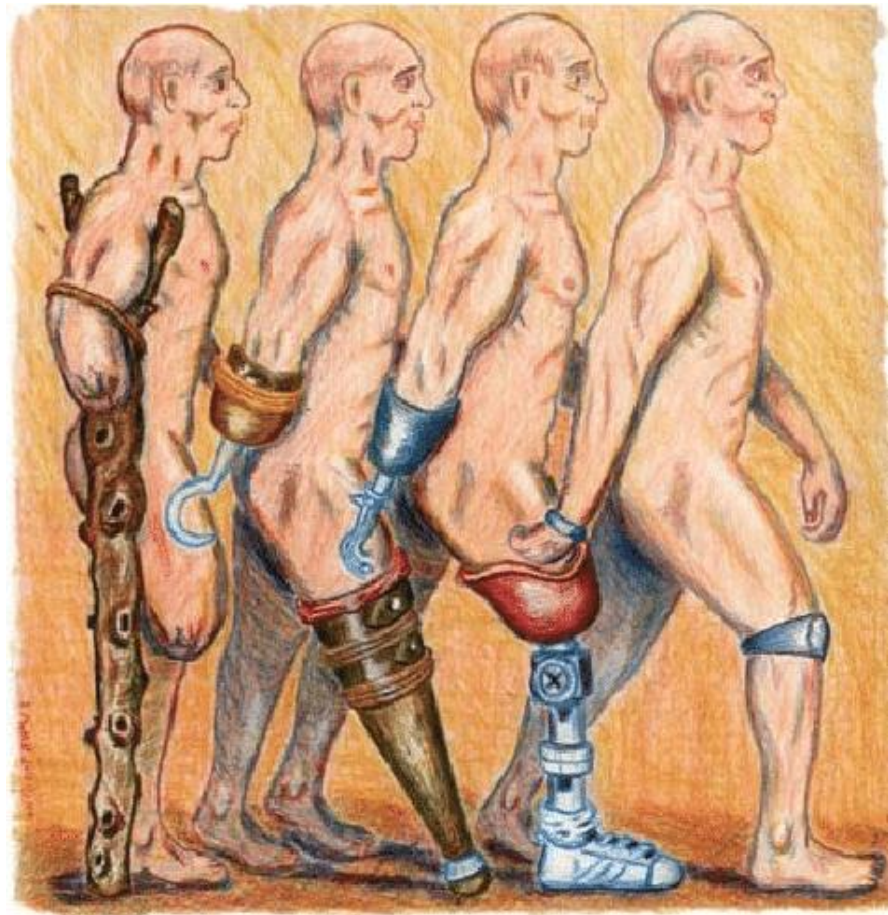


Figure (1-1) History of Prosthetics [5].

1.2 Prosthetic

The term "prosthetic" has its roots in the Greek language, meaning "the systematic pursuit of adding on to." Prosthetics specifically refer to the application or addition of an artificial device, known as prosthesis, to the body. This prosthesis serves to either partially or completely replace any missing extremities. Prostheses are medical devices designed to restore function to a body part that has been lost due to disease or accident. Doctors often recommend the use of prostheses to patients who have undergone amputations, as they allow for a return to normal activities. In addition to restoring function and aesthetics, the use of prostheses aims to improve the quality of life for prosthetic users. The issue of metabolic energy consumption during walking is also crucial in the design of transtibial bionic prostheses as it affects the user's comfort. [6].

In the latter half of the 20th century, significant advancements in prosthetics have been made, including the use of improved materials, utilizing the labs of modern gait, and developing reliable surgical procedures to create the best functioning residual limb. The overall functional improvement for individuals who have experienced limb loss depends on various factors, such as the patient's overall condition, the quality of the residual limb, the fit of the prosthesis, and the suitability of the prosthesis itself. In particular, the individual's choice of prosthesis has consistently been identified as a crucial factor in prosthetic acceptance.

In recent decades, significant progress has been made in prosthetic technology to aid individuals with missing limbs. Recent advancements have focused on improving the designs of prostheses for both upper and lower extremity. Myoelectric technologies and targeted muscle reinnervation are two examples of recent innovations that have shown potential in improving upper extremity

prostheses, specifically at the transhumeral and shoulder disarticulation levels. A more natural and adaptable gait for individuals with transfemoral-level limb loss has been attributed to improved socket design and microprocessor knees [7].

In essence, lower-limb prostheses serve two primary functions: enabling a person to stand and walk. However, the demands placed on upper-limb prostheses are significantly different [8].

Prostheses can restore appearance, functionality, or both to a lost or missing limb, with the prosthesis specific type depending on the location of the missing limb. Great technological advancements in prosthetics have driven the market to considerable growth, gratitude to innovative evolutions that cater to the specific needs of patients. Today's prosthetic devices, ranging from traditional knees to energy-storing feet, provide a more normal and productive life for amputees. In the coming years, technology will continue to have a tremendous impact on the market, with novel technologies invention such as bionic, sensor, artificial intelligence and micro mechatronics driving further advancements. A growing market for amputee products is driving the demands of market for a better life quality, and innovation is addressing these needs. “Every component--whether the socket, knee, or foot--involved in the prosthesis has undergone immense research and development” says Frost & Sullivan Research Analyst Archana Swathy. “Furthermore, the use of novel materials has further redefined the potential of prosthetic devices.” The classification of prostheses can be based on both their functionality and the amputation level, as shown in the Figure (1-2) [9].

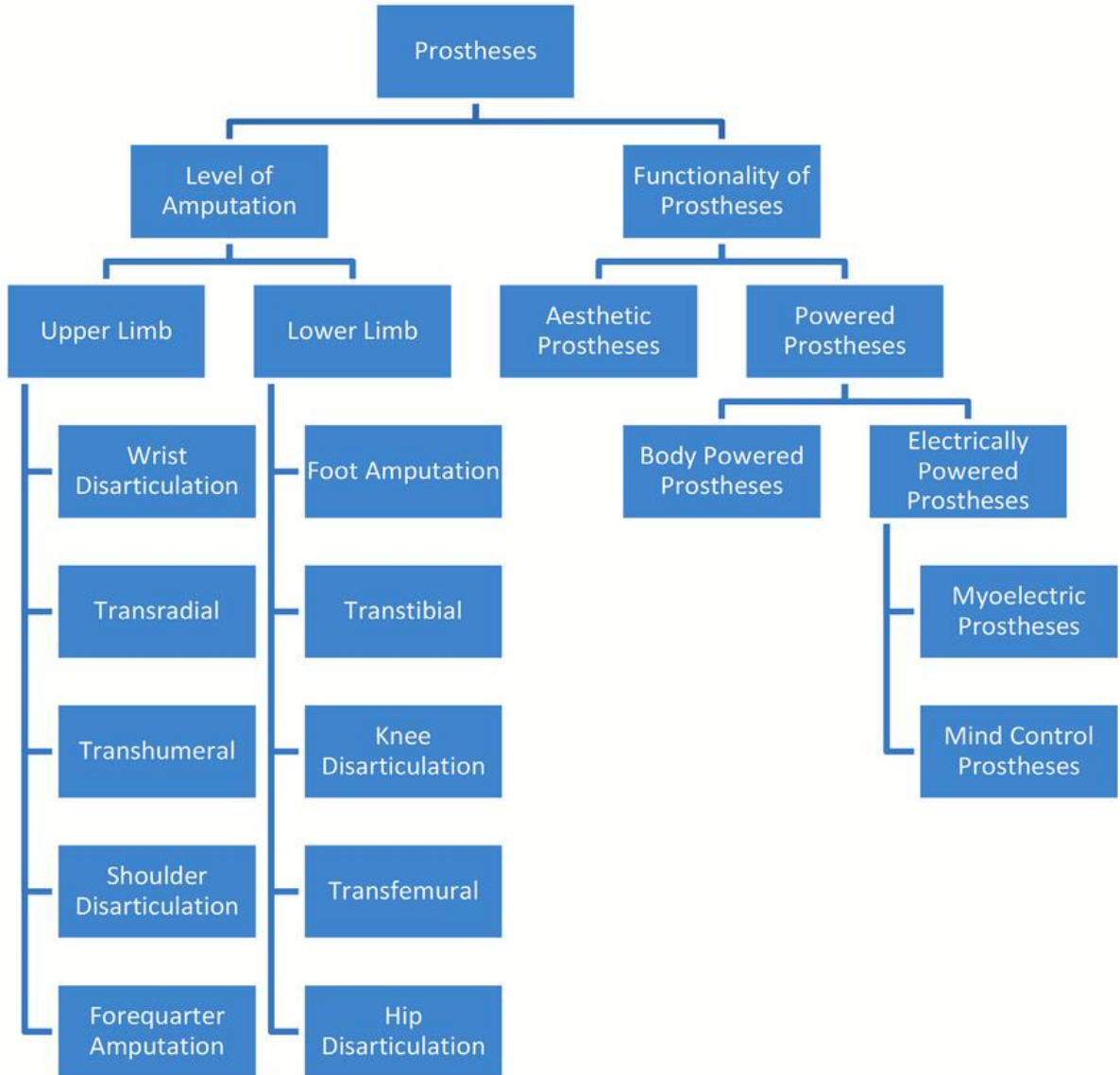


Figure (1-2) Classification of prostheses [9]

1.3 Types of artificial limbs

The design of prosthesis may vary depending on the level of amputation. For instance, if the pinky finger of right hand has been lost, an aesthetic prosthesis may suffice. However, if the amputation level is at the wrist, the prosthesis needs to

replicate all fingers function, including the thumb to enable the person to grip or hold effectively an object. This portion discusses the amputation level for both upper limbs and lower limbs, artificial limbs fall into four main categories identified: transtibial, transfemoral, transradial, and transhumeral prostheses, [10]:

1. Transradial Prosthesis (Below-Elbow Prosthetics):

Transradial prosthesis is a type of artificial limb that replaces an arm missing below the elbow. There are two main types of prosthetics available: cable-operated limbs and myoelectric arms. Cable-operated limbs function by attaching a harness and cable around the opposite shoulder of the damaged arm, while myoelectric arms work by sensing muscle movement in the upper arm through electrodes, which cause an artificial hand to open or close.

2. Transhumeral Prosthesis (Above -Elbow Prosthetics):

Transhumeral prosthesis is an artificial limb designed to replace an arm missing above the elbow. Transhumeral amputees face similar challenges to those with transfemoral amputations, as the movement of the elbow is complex and difficult to replicate with an artificial limb.

3. Transtibial Prosthesis (Below-Knee Prosthetics):

An artificial limb that replaces a leg below the knee is transtibial prosthesis. Compared to individuals with a transfemoral amputation, transtibial amputees are often able to regain normal movement more easily, primarily because they retain the knee joint, which enables the ability to move more easily as shown in Figure (1-3).

4. Transfemoral Prosthesis (Above-Knee Prosthetics) :

Transfemoral prosthesis is an artificial limb designed to replace a leg missing above the knee. Individuals with transfemoral amputations often face significant challenges in regaining normal movement, as the complexities associated with the knee joint make it difficult to replicate natural movement patterns. In general, a person with a transfemoral amputation requires approximately 80% more energy to walk than an individual with two intact legs. However, newer and more advanced designs have incorporated technologies such as hydraulics, carbon fiber, mechanical linkages, motors, computer microprocessors, and innovative combinations of these technologies to provide greater control to the user and improve overall functionality as shown in Figure (1.3).

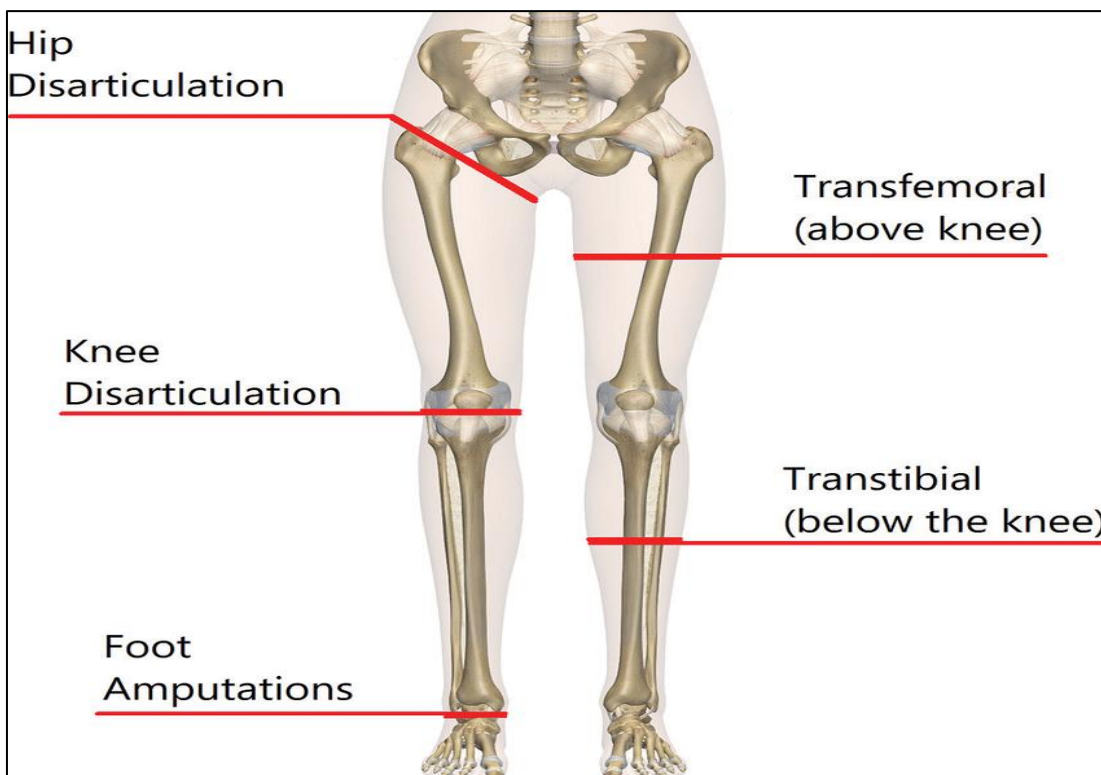


Figure (1-3) Amputation level of the lower limb [9].

1.4 Lower limb prostheses

The design of lower limb prostheses varies depending on the level of amputation. Figure (1.3) illustrates the five major levels of lower limb amputation, while Figure (1.4) depicts the corresponding types of prostheses for each level of amputation. [11].

1.4.1 The Amputation of Foot

Foot amputation can occur at any point below the ankle, and in such cases, a durable aesthetic prosthesis is typically all that is required to assist with walking [11].

1.4.2 Transtibial (below knee)

Transtibial amputation involves the loss of a limb between the ankle and knee, and in many cases, the residual muscles and bones can be utilized to power the prosthesis, thereby improving the quality of life for the amputee [11].

1.4.3 Knee disarticulation

Knee disarticulation involves amputation at the knee joint, resulting in the loss of muscles and bones below the knee. However, the muscles responsible for leg movement remain intact in this type of amputation. [11].

1.4.4 Transfemoral (above knee)

Transfemoral amputation involves the loss of most leg muscles and bone between the knee and hip. Prostheses designed for this type of amputation must incorporate knee and ankle movements to enable the amputee to perform a range of activities [11].

1.4.5 Hip disarticulation

Hip disarticulation results in the complete amputation of the leg, which may render the amputee unable to perform hip movements. To recover from this disability, the amputee may require fully functional biomimetic leg prosthesis. [11].



Figure (1-4) the different types of prostheses for the lower limb [13].

1.5. Transtibial (below knee)

Transtibial amputation represents the majority (59%) of lower limb amputations, and as such, the current study will be focused on prostheses designed for this type of amputation [12].

Components of transtibial prosthesis, as shown in figure 1.5, include [13]:

- a) Socket
- b) Suspension
- c) Shin piece
- d) Foot piece.

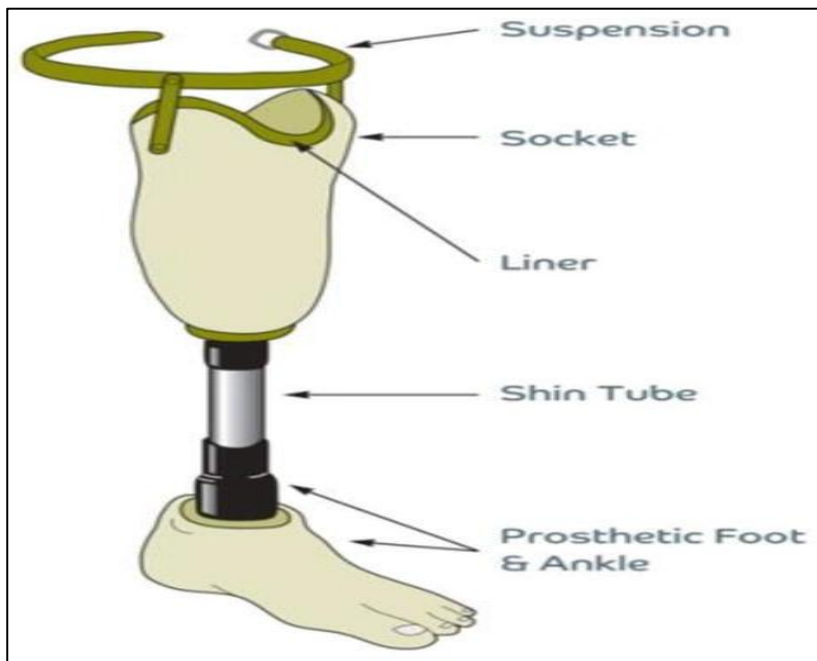


Figure (1-5) components of lower limb prostheses [13].

1.5.1 Socket

There are several types of sockets, and the names of prostheses are determined by the type of socket used in them. The socket is the portion of the prosthesis that surrounds the stump and creates a connection between the residual limb and the artificial limb [12].

1.5.2. Suspension

Suspension refers to the mechanism that keeps the socket in place on the residual limb, preventing it from falling off when the leg is lifted or moved during

walking. Effective suspension is crucial for optimizing energy transfer, enhancing prosthesis control, and reducing discomfort or abrasions [12].

1.5.3. Shin piece

This component is situated between the socket and the prosthetic foot, and is typically constructed from strong and lightweight materials like carbon fiber, aluminum, or titanium [12].

1.5.4. Ankle Foot Assembly

Three types of feet are available for transtibial prostheses [12]:

1. The foot of SACH.
2. The foot of Single - axis.
3. The foot of Multi - axis.

1.5.4.1 SACH Foot

The most commonly used foot type even in western countries for transtibial prosthesis is the solid ankle cushion heel (SACH) foot. This type of foot has several characteristics as shown in figure 1.6, including [12]:

- a) The heel is a solid piece that is in direct connection with the ankle block without a joint at the ankle. It is made of wood or metal.
- b) Cushion heels are typically made of rubber wedges or layers of hard and soft rubber alternating. Depending on the patient's weight and the level of activity that he or she engages in, the cushion heel may have a different compressibility, and it compresses during heel strike to simulate plantar flexion.
- c) A molded cosmetic forefoot that may or may not include separate finger.

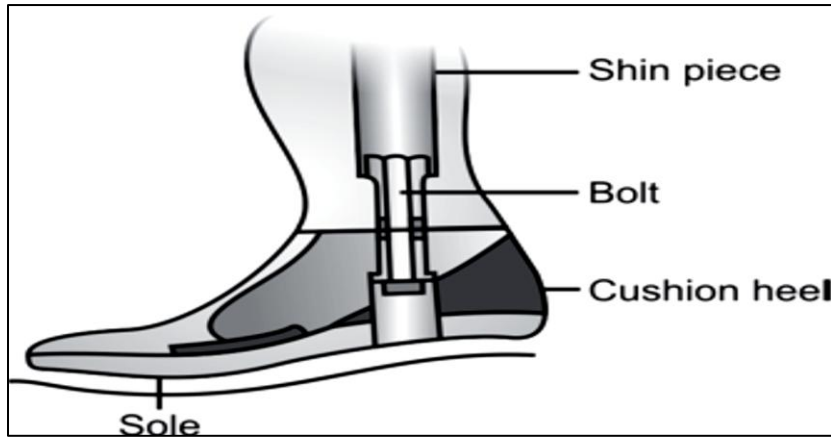


Figure (1-6) foot of SACH [12].

1.5.4.2 Single Axis Foot

This type of foot permits restricted dorsiflexion and plantar flexion through the use of hard rubber bumpers. When the heel makes contact with the ground, the plantar flexion bumper compresses, leading to plantar flexion, followed by the foot flattening. This quick transition to a flat foot increases the extension of knee and promotes the stability of prosthetic. As a result, it is commonly used in above-knee prostheses. As shown in figure 1.7 [12].

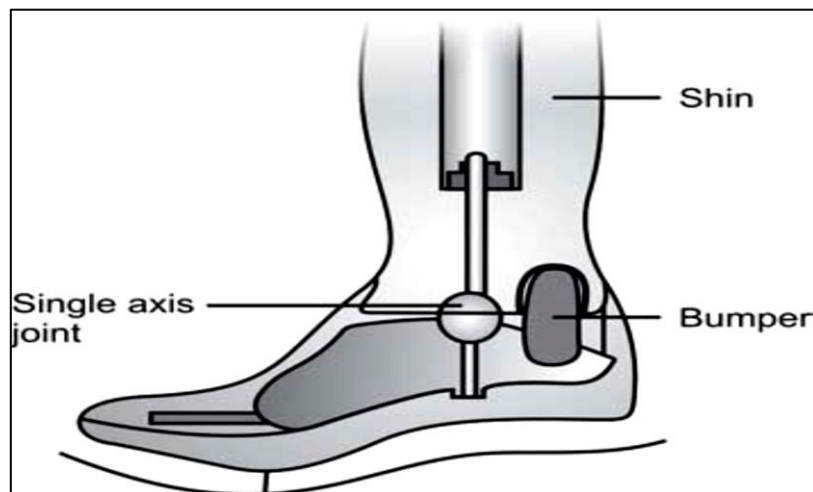


Figure (1-7) Single Axis Foot [12].

1.5.4.3 Multi-axis Foot

This type of foot allows for dorsiflexion, plantar flexion, inversion, and eversion, providing effective shock absorption. It is particularly useful for walking on uneven surfaces and for individuals with excessively scarred stumps. Figure 1.8 illustrates this type of foot [12].

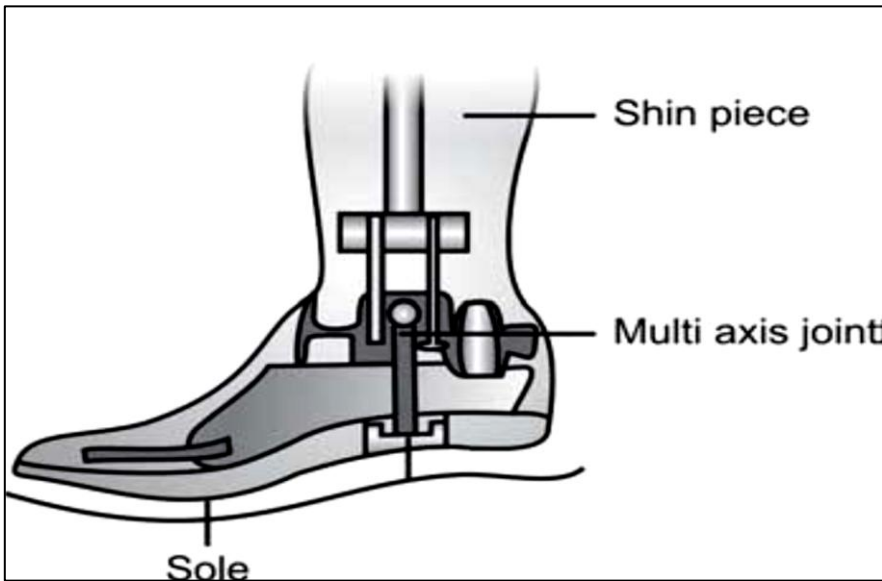


Figure (1-8) Multi-axis Foot [12].

1.6 Vibration in Prosthetic Limbs

Prosthetic limbs are designed to replace missing body parts and improve the quality of life for amputees. However, one common problem with prosthetic limbs is the occurrence of vibration, which can cause discomfort and reduce function.

Vibration can occur in prosthetic limbs for several reasons, including poor fit, improper alignment, and inadequate suspension. Poor fit can cause the prosthetic limb to move around excessively, leading to vibration and discomfort. Improper alignment can also cause vibration, as it can result in uneven weight distribution and excessive pressure on certain parts of the prosthetic limb.

Additionally, inadequate suspension can cause the prosthetic limb to bounce and vibrate during movement.

Vibration can have several negative effects on prosthetic limb users, including discomfort, reduced function, and skin irritation. Discomfort from vibration can make it difficult to use the prosthetic limb for extended periods of time or to perform certain activities. Vibration can also reduce function by decreasing stability and balance. Finally, prolonged exposure to vibration can cause skin irritation and other health problems.

Several solutions have been proposed to reduce or eliminate vibration in prosthetic limbs. These include using advanced sensors and control systems to improve alignment and stability, incorporating damping materials to reduce vibration, and using better suspension systems to prevent excessive movement. Additionally, proper fit and alignment are essential for reducing vibration and ensuring optimal function [15].

Vibration in prosthetic limbs is a common problem that can cause discomfort and reduce function. However, with proper fit, alignment, and suspension, as well as the incorporation of advanced technologies and materials, it may be possible to reduce or eliminate vibration and improve the quality of life for prosthetic limb users [16].

1.7 Objectives

The main objectives of the present work are:

1. An experimental work will be conducted involving five tests on three types of prosthetic feet (SACH, single-axis, and multi-axis) to measure and estimate the ground reaction force, pressure distribution, vibration effects, muscle activities, and gait analysis.
2. The results obtained from the F-socket test for the three types of feet will be inputted into a 3D numerical model of the prosthetic socket using Abaqus software version 6.5 to calculate stress distribution, deformation, and the safety factor versus stress.
3. Provide a recommendation for choosing the suitable type of prosthetic foot for an amputee with a below-knee prosthetic limb according to their lifestyle, by making a comparison between the three types of feet based on the results of experimental and numerical work.

1.8 Framework of the Thesis

The current thesis comprises six chapters, outlined as follows:

1. Chapter One: provides a general introduction to amputation and its various types, prosthetics, types of artificial limbs, lower limb prostheses, transtibial (below knee) amputations, vibration, vibration in prosthetic limbs, and the significance and rationale of the study.
2. Chapter Two: critically examines the existing scholarly literature relevant to the research topic, and concludes by summarizing the major findings in it.
3. Chapter Three: describes the equations of theory, transtibial (below knee) prosthesis geometry, and the procedure of numerical solutions.

4. Chapter Four: demonstrates the model validation, grid independence, and the numerical and empirical results emerged from the research.
5. Chapter Five: focuses on the practical aspect of this thesis, presenting the laboratory measurements and corresponding results.
6. Chapter six: provides a summary of the work main conclusions and offers guidance for further research.

At the thesis end, list of relevant references are included.

Chapter Two

Literature Review

Chapter Two

Literature Review

2.1 Introduction

Lower limb prostheses are an indispensable device that extends the movement of lower limb amputee individuals to perform daily life routines and experience mobility in everyday life as part of modern health services. Choosing the proper components of the prosthetic device is crucial to its success since it determines both the functioning of the device and the quality of life of the patient.

Lower limb prostheses perform many functions — including bearing weight, absorbing shock and providing stability during a range of activities.

Many studies have been published on how each element affects the properties and functions of the prosthetic device over the years. Establishing selection of their prosthesis such as socket, foot and ankle can yield profound effects on gait trunk control energy demand and comfort. Therefore, it is important to study and develop in this field to improve lower limb prostheses function and efficiency

Therefore, many complete investigations have been conducted in the last few years in this context, while others have also pursued complete reviews of these studies and classified them by some particularities to create a summary of the findings, one of this reviews was conducted by **Andrysek (2010)** [17] included 106 articles since 1994–2010, analyzed different categories of prosthetic technologies, which included (materials, structures, alignment techniques, feet, ankles, knees, sockets, and suspension system). Additionally, the articles were classified into three

categories: technical evolution, clinical (laboratory) testing, and the studies of clinical field testing, in the case of countries of developing countries.

Designing prosthetic technologies for developing countries is a complex challenge. The components must be functional for active individuals while also being affordable, highly durable, and culturally and environmentally appropriate.

The findings highlight significant efforts made in the development and implementation of standardized outcome measures for field testing. This enables the evaluation of various prosthetic technologies concerning their usage, functionality, strength, and another relevant element. While advancement has been made in treating the prosthetic technologies limitations, further research and evolution are still needed.

Voinescu et al., (2012) [18] estimating the forces generated by the thigh muscles of transtibial amputees, and comparing them to the forces generated by the thigh muscles of normal subjects. The muscle forces originating from the femur are crucial for the gait of transtibial amputees, serving as the primary means of propulsion. This study estimates and compares the forces generated by the thigh muscles of amputees with those of able-bodied individuals to assess the energy requirements for prosthetic devices. Two transtibial amputees and four similarly sized normal subjects were analyzed while walking on level ground. Using inverse dynamics and a muscle recruitment algorithm from anybody Technology, muscle activation patterns and forces were calculated, distinguishing between anterior and posterior muscle groups. Results indicated that amputees generate significantly higher forces in their posterior muscles during walking, increasing the metabolic cost per step. The findings highlight compensatory mechanisms used by amputees for support and movement, providing data consistent with previous research on muscular forces in gait.

Ferreira et al., (2015) [19] presents a rehearsal of the key control strategies employed in leg prostheses, specifically focusing on the controllers utilized in energy-assiste prosthesis, which use to replace a leg missing above the knee or below the knee. Prosthesis of lower limb consists of three primary categories: passive, semi-active or variable damping, and powered or intelligent. Through this literature review, it has been determined that the main limitation of lower limb prostheses lies in the controller, as the mechanical systems have undergone significant refinement. However, there is still no consensus on the optimal type of control that should be employed to more accurately replicate the biomechanics of human lower limbs. Powered devices have the capability to achieve such performance levels. Simultaneously, they decrease the metabolic energy consumed during walking and have the potential to restore symmetric gaits, as well as alleviate issues such as osteoarthritis in the joints of the unaffected limb. After the passage of one year, **Windrich et al. (2016) [20]** provide an overview of the design challenges and corresponding solutions faced by active leg prosthetics. This is based on a systematic review of the literature using a comprehensive search strategy. A total of 21 distinct active prosthetic devices were identified, including 8 above-knee prosthetics, 9 below-knee prosthetics, and 4 combined knee and ankle prosthetics.

Despite promising results from tests indicating the potential for restoring functional performance in amputees across several preliminary studies, the development of active prosthetics remains a challenging task. Therefore, it is essential to continue conducting further research, including comprehensive clinical evaluations, to effectively address this challenge. Another review was conducted by **Frossard et al., (2018) [21]** to examines the present status of biomechatronic advancements in upper and lower limb prostheses, emphasizing the hurdles

associated with amputation and the clinically significant outcomes. The reviewed article highlights that the most advanced technologies discussed might enable individuals with limb amputation to participate in a broader range of activities in a more natural manner. Nevertheless, it is worth noting that the majority of publications reviewed primarily relied on laboratory-based outcomes and had limited subject samples. Additionally, there was a lack of consistency in the outcome measures and assessment tools employed across the publications, as each study focused on specific design or functional aspects of the examined devices or technologies.

A more recent review by **Asif, et al., (2021)** [22] explored various aspects of lower limb prostheses. This includes the study of lower limb amputations, their design and development, control strategies, machine learning algorithms, as well as the psychological and social impact on prosthetic users, and the prevailing design trends found in patents. They also created an open-source database dedicated to patents, highlighting design trends and advancements in lower limb prosthetics from 1970 to 2020.

Although there are many reviews addressing the needs of users regarding upper limb prosthetics, there is currently no comprehensive summary available for individuals affected by lower limb loss. Therefore, **Manz et al. (2022)** [23] conducted a thorough literature review to analyze the fundamental needs expressed by lower limb prosthetic users. This review included 56 articles that explicitly documented the desires, wishes, and needs reported by a total of 8,149 individuals with lower limb amputations.

The authors found that identifying user needs is a crucial stage in the development of advanced lower limb prosthetics aimed at improving users' quality of life. However, this task is complex due to the interconnectedness of needs and

their dependency on various factors such as mobility level, age, and gender. Moreover, these needs evolve over time in response to device usage. Therefore, innovative assessment methods are necessary to comprehensively evaluate the system's impact, considering objective outcomes as well as the overall user experience and satisfaction within their daily life environment.

2.2Prosthetics Limb below Knee

The idea of artificial limbs has existed for centuries, with the first examples emerging in ancient Egyptian tombs and Roman dig sites. But it wasn't until the mid-20th century that prosthetic limb manufacturing saw major improvements. World War II acted as a boom for innovation in many areas, including prosthetics, because thousands of veterans returning from war had been victims of amputation that necessitate the use of functional, economical artificial limbs.

The below knee prosthetic field has seen great developments recently through many technologies, robotics, 3D printing and advanced materials technologies. All of these innovations have enhanced the functionality, comfort, and aesthetics of below knee prosthetic limbs, enabling amputees to participate in a greater variety of activities with increased ease and confidence.

The study (**Kendell et al., (2010)**) [24] highlights these differences between the intact and prosthetic limbs and between conditions and the able-bodied population compared to subjects using lower-limb prosthesis, and this is important for the understanding of the active use or how to improve the behavior of these individuals, since the rate of falling between this population is significant, the understanding here helps strengthen the knowledge of factors related to dynamic stability, especially in this population.

The results consistently indicated lower outcomes for the prosthetic limb, suggesting the utilization of a gait strategy that prioritizes dynamic stability on the prosthetic limb while the intact limb undergoes adaptation.

The authors suggest that future research should focus on optimizing parameter calculations for unilateral transtibial prosthesis users and establishing the correlations between the potential for falls and dynamic stability measures.

Transtibial amputees have access to multiple options when it comes to prosthetic suspension systems. Prosthetists would find it easier to make selections when they possess greater knowledge about suspension systems. The review conducted by **Gholizadeh, et al., (2013)** [25], which analyzed 22 articles (15 prospective studies and 7 surveys), aimed to identify scientific evidence regarding different transtibial suspension systems in order to offer clinicians selection criteria, there is currently no clinical evidence to support the notion of a universally applicable "standard" suspension system for all transtibial amputees. Nonetheless, among the different suspension systems available for transtibial amputees, the Iceross system was preferred by a majority of users in terms of functionality and comfort.

Another study conducted by **Arifin, et al., (2014)** [26] utilized the Biomed stability system to examine the impact of various prosthetic feet on the control of postural stability. The investigation involved comparing three types of prosthetic feet: solid ankle cushion heel (SACH) foot, single-axis (SA) foot, and energy-saving and return (ESAR) foot among a group of 10 transtibial amputees. A comparison was made between the results of the study and those of able-bodied participants.

The mean overall stability index score of the SACH foot was significantly lower than that of the ESAR foot on the compliant surface when participants stood on the compliant surface in the study. Each of the prosthetic foot groups exhibited a significantly greater mediolateral stability index score than did the able-bodied group. Furthermore, the total stability score was significantly greater in the foam specific to the ESAR foot. The results showed that amputees had greater postural instability mediolaterally than those who were able-bodied.[35] Hence, this study highlights the importance of rehabilitation programs to target frontal plane stability and proprioceptive improvement of the residual limb.

One year later, A comparison study was performed by **Paradisi et al., (2015,)** [27] on a group of 20 hypomobile transtibial amputees (TTAs) who had their usual SACH foot replaced with a multiaxial foot, focusing on mobility, balance, and quality of life. Their finding was that, following the substitution of the SACH foot with a multiaxial foot, patients have consistently sustained their level of stability and perceived safety. Moreover, there has been a notable yet slight enhancement observed in various crucial clinical facets of daily living for transtibial amputees (TTAs). These include overall mobility, balance, general comfort, and the satisfaction they perceive with their prosthetic device.

During the same year, a review study conducted by **Safari and Meier, (2015)** [28] aimed to unravel the intricacies of transtibial prosthetic socket fit and potentially identify indications of the most suitable prosthetic socket type for specific situations. This study presents the findings derived from a systematic review of quantitative outcomes, encompassing a total of 27 articles, exhibit varying degrees of methodological rigor, ranging from low to moderate. The majority of studies focused on patellar tendon bearing PTB and total surface bearing TSB sockets, while only a limited number of studies examined vacuum-

assisted suction VAS and hydrostatic socket HS designs. Notably, the VAS socket demonstrated the most effective suspension among all the reported socket designs. With limited studies available on VAS sockets, the available evidence suggests that they have a positive impact on gait symmetry, effectively control fluctuations in residual limb volume, and potentially promote better residual limb health when compared to other socket designs.

The allocation of stress at the interface between a transtibial amputee's residual limb and the prosthetic socket has been widely regarded as a direct measure of the fit and comfort quality of the socket. Therefore, researchers have shown significant interest in quantifying these interface stresses, **Al-Fakih, et al., (2016) [29]** conducted a review study to examine a variety of measurement systems have been developed over the course of five decades to investigate the interface normal and shear stresses in transtibial prosthetic sockets. These systems have significantly contributed to facilitating a clear understanding of the mechanical interplay between the residual limb and the socket.

At the same year another review study by **Chatterjee, et al., (2016) [30]** extensively examines 49 papers on the biomechanics and pathomechanics of prosthetic gait, thoroughly investigating the mechanical and associated medical issues, as well as proposing potential solutions.

The main findings from this review study, Achieving proper fit and comfort with trans-tibial prostheses can be difficult, impacting functionality and usability. Additionally, inadequate socket design can lead to discomfort, pressure sores, and reduced prosthetic performance. On the other hand, maintaining good residual limb health is crucial for optimal prosthesis usage, considering concerns such as skin breakdown and potential infections.

Trans-tibial prostheses may cause gait deviations and increased energy expenditure during walking, which can affect mobility and quality of life. However, accurate alignment and effective suspension systems are vital for stability, comfort, and improved functional outcomes of trans-tibial prostheses.

After the passage of one year, eleven studies were found through a systematic literature search by **Davenport, et al., (2017)** [31], focusing on investigating the alterations in prosthetic socket pressure distribution in unilateral transtibial amputees due to device alignment. The reports varied significantly in their approaches to measurement, and there are notable gaps in the measurement of various alignment configurations. A majority of the studies had deficiencies in their design and description, with the quality of evidence supporting their conclusions rated no higher than moderate and often deemed low.

Considering the limited existing research, the authors strongly suggest conducting regular updates of this literature assessment due to the increased feasibility of measurement techniques and the significant clinical relevance of the subject. This approach would help gain insights into the implications of prosthesis design decisions.

The work conducted by **Liu, et al., (2021)** [32] provided a comprehensive review and analysis of ankle-foot prostheses developed after 2000. In this systematic review, the authors briefly described and compared the mechanical design characteristics of 91 ankle-foot prostheses, which were categorized into 11 sub classifications. Their findings revealed a significant increase in the development of powered ankle-foot prostheses over the past two decades. This development showcased the emergence of alternative modes, transitioning from

pneumatic or hydraulic drivers to motorized drivers, and from rigid transmissions to elastic actuators.

Measuring interface pressure is vital for amputee patients. The cavity of prosthetic limbs supports the weight of the trunk during walking, necessitating an assessment of the pressure exerted on the residual limb's tissues. **Aboud and Rasan (2021)** [33] conducted a review study to measure interface pressure for below-knee prosthetic sockets. They analyzed five methods for measuring interface pressure, which are: vacuum diaphragm and liquid sensor, displacement sensor, force sensing resistors and strain gauges, tactile pressure sensor, and piezoelectric sensor, and Fiber Bragg grating (FBG) sensors).

Their results refers to that, different methods for measuring interface pressure in below-knee prosthetic sockets have disadvantages such as neglecting shear stress, limited impact resistance, hysteresis, measuring pressure at a single point, dependence on socket deformation, temperature sensitivity, limited flexibility, high cost, and challenges in differentiating temperature and strain effects.

Researchers and developers should consider these drawbacks when selecting and utilizing interface pressure measurement methods to ensure accurate and reliable results.

2.3 Types of Prosthetic Foot

Since the 1980s, various classifications have been used to categorize different types of feet for prosthetics. These classifications include the single-axis foot, SACH (Solid Ankle Cushion Heel) foot, multi-axis foot, and dynamic response foot. Over the years, many different types of artificial foot structures have been designed for usage with prosthetic devices. In summary, these designs fall into two top-level

categories: articulated feet with moving joints, and non-articulated feet without moving joints. However, articulated feet including single-axis foot and multi-axis foot do show specific behavior & are also considered high maintenance than non-articulated foot.

The single-axis foot consists of one quotaable joint and generally has two rubber bumpers. The multi-axis foot, on the other hand, moves in three axes, allowing patients to swivel the foot. It is good for walking on unlevel ground. on a downside the multi-axis foot is bit heavier than the single-axis foot and needs lot more maintenance.

The authors, **Goh and co-workers(1984)** [34], introduced a method to assess the performance of two different types of prosthetic feet (SACH and uniaxial). This included a clinical examination by an orthopod and a biomechanical assessment of foot function and its influence on kinematics and kinetics of the lower limb. Methods of data collection included three Bolex H16 cine cameras and two Kistler force plates. Neither of the types of prosthetic foot was found to have clear subjective assessment preference. Overall, the amputees favored the foot they were used to. In terms of kinematic analysis, it was observed that the uniaxial foot closely resembled the natural foot in providing plantar flexion during early stance. However, when examining ground force actions, it was found that the SACH foot facilitated a smoother transition from heel-strike to toe-off. There were no meaningful differences in whole body kinetics, despite these differences.

Huang et al., (2001) [35] studied the dynamic gait characteristics and energy cost of six male below-knee amputees. Three types of foot were tested: SACH, single-axis foot, and multiple-axis foot. Data was collected using six-camera motion analysis, a metabolic measurement cart, and a beast of a treadmill (Tuff Tread).

Their results are based on that, the SACH foot is appropriate for lower-activity-level amputees in need of reduced dorsiflexion.

It is recommended to use a single-axis foot for individuals with amputated limbs who walk on slopes or uneven terrain, or for those with higher activity levels that require greater ankle movement. The increased ankle mobility in a single-axis foot helps adapt better to various walking surfaces and speeds, enhancing symmetry between the healthy limb and the prosthetic one. Therefore, it is considered a good option for moderately active individuals who do not have specific walking issues or concerns. In contrast, a multi-axis foot is more suitable for moderately active individuals, as it meets the demands for increased ankle range of motion, including changes in walking speed and walking on slopes.

According to **Powelson and Yang, (2012) [36]**, the objective of this systematic review is to conduct a technical survey of transtibial prosthetics, which consist of four major components: the socket, suspension system, pylon, and prosthetic foot. Over the past 50 years, significant advancements have been made in prosthetic technology. Some of these advancements have benefited the general group of individuals who have undergone below-knee amputations includes techniques such as vacuum-assisted suspension systems, single-axis feet, and TSB bags. Mobility for more active prosthetic users has been enhanced by the introduction of features that were previously unavailable to them. Examples of these advancements include running-specific feet, shock-absorbing pylons, and multi-axis feet.

The objective of **Pirouzi, et al., (2014) [37]** review was to conduct a comprehensive examination and assessment of research conducted over the past few decades concerning socket design, measurement of interface pressure within the socket, and the biomechanics of the socket. A total of 19 articles were chosen

for analysis, divided into four groups depending on what they study: the use of Finite Element Methods (FEM) for Socket Pressure Measurement, Deep-Tissue Damage, Sensing Pressure, and Socket Design and Pressure Distribution. Numerous studies have yielded positive outcomes in terms of modeling, experimentation, and the application of technical and mechanical equations. However, these findings prove impractical due to the need for eliminating or treating certain assumptions as fixed in computerized modeling. For instance, the modeling of friction tends to yield unreliable results due to the limitations of current software in accommodating various parameters. Consequently, the skin and underlying tissues bear the brunt of the pressure for now. In fact, there exists a trade-off between the benefits and potentialities of an artificial leg. Therefore, it is crucial for all studies to focus on minimizing these drawbacks while maximizing the advantages in order to achieve an optimal end product.

Systematic review by **Resan, et al., (2023)** [38] the objective of it is to assess the various types of artificial feet and their compatibility with amputees, taking into consideration different factors such as return energy, age, dorsiflexion, effective length ratio, and gait stability. The findings indicate that traditional prosthetic feet are suitable for initial amputation training or for elderly individuals, as they are not designed to accommodate high speeds. The selection of an appropriate prosthetic foot depends on the specific needs and activities of the amputee.

2.4 Vibrations

In the design, in addition to the choice of suitable prosthetic components, vibration's impact on lower limb prostheses design and development of prosthetic device is an important consideration. Vector Information From Storage Gradient Vibration in Prosthetic Use: A Challenge for The Agency on Residual Limb Tissue and the Device. Several studies revealed higher energy expenditure, lesser gait stability and decreased control of balance for prosthetic users due to excessive vibration on prosthetic limbs [3,4]. The vibration can also have an adverse effect on the function and lifespan of prosthetic components, including the socket and foot, causing premature wear and failure, which may result in the need for an early replacement. In order to mitigate these problems, have been various methods aimed at reducing vibration transmission in lower limb prosthetics, including; shock-absorbing materials, alignment and suspension adjustments, and implementing active vibration control systems. This is a brief analysis only, and it has been yet to prove that lessening vibration influences the lower limb prostheses can be a highly comfortable, stable, and mobile experience specifically in those individuals who have undergone the loss of lower limbs—consequently, in the long run, increasing the overall quality of life for those people with limb differences.

Puers, et al., (2000) [39] study, a novel implantable system is presented for detecting hip prosthesis loosening using vibration analysis. The detection of loosening is achieved through a miniature accelerometer placed in the head of the hip prosthesis. The collected data from the implant is wirelessly transmitted and analyzed using a computer. The power consumption of the system is 22.5 mW, supplied through an inductive link. Promising results have been obtained from

cadaver experiments, and further clinical tests are planned to assess the effectiveness of this system.

Experimental work as conducted by **Bedaiwi and Chiad, (2012) [40]** aims to test the effect of vibration on the comfort of amputees. The study focuses specifically, firstly, on free and forced vibration transmission from the artificial limb to the human body. For the experiment a setup was designed including a shaking table with cam mechanism, an AC motor, a proportional-integral-derivative (PID) speed variator, and the necessary springs. Displacement, velocity, and acceleration were measured as the user activated the interface and walked on a flat surface with the use of a prosthetic limb, and were taken from various points along the prosthetic limb and the healthy limb using a measuring device connected to the computer interface. This research concluded that vertical vibration intensames when the liner moves away from the amputee. Furthermore, in varied rotary motor velocity and excitation, the prosthetic limb demonstrated a maximum frequency that was higher than that of the healthy limb (both with and without liner). The frequency ranges for each part of the limb were 7-55 Hz for the foot, 10-50 Hz for the ankle, 7-45 Hz for the leg, 4-40 Hz for the knee, and 3-15 Hz for the hip. Additionally, both the Block RMS and V RMS of acceleration are greater in the healthy limb than the prosthetic limb regardless of the presence or absence of the liner.

Another work was by **(Jweeg and Jaffar, 2016) [41]**, is an Experimental work in which using of empirical approach to measure the pressure distribution and Ground Reaction Force (GRF) in old and new patient's prostheses. The interface pressure (IP) at the level of the leg and socket was measured by the F-Socket sensor. In the case of the natural frequency, the impact hammer test was used, while for the position of vibration (acceleration and frequency) it was collected in different places of the gait cycle. GRF (ground reaction force) during the gait cycle resulted

in a mean duration of 1.50 seconds and 1.58 seconds for left and right leg respectively. The maximum interface pressure (IP) of 408 KPa was observed in the regions of the Tensor fascia lata of the thigh. The new prosthesis showed the maximum vibration data at the thigh portion and acceleration and frequency were 2.09 Hz and 2.66 Hz respectively. The maximum vibration data for the thigh region of the old prosthesis was found to be 4.44 Hz (acceleration) and 3.12 Hz (frequency). The first mode natural frequency calculated in hammer test mode for the prosthesis was 33.2 Hz for the old prosthesis and 46.8 Hz for the designed prosthesis.

2.5 Summary

Multiple reviews and investigations have been conducted on prosthetic socket biomechanics, prosthetic technologies, control strategies, and user needs for lower limb prostheses.

1. The socket, foot/ankle mechanism, and suspension system critically influence gait, stability, and comfort. Developing countries require prostheses that are affordable, durable, and culturally adaptable (Andrysek, 2010).
2. Transtibial amputees exert higher posterior thigh muscle forces during walking, increasing metabolic cost (Voinescu et al., 2012). Compensatory mechanisms lead to asymmetric gait and higher energy demands.
3. Powered prostheses show promise in restoring natural gait symmetry and reducing joint strain (Ferreira et al., 2015).
4. No consensus exists on optimal control strategies, necessitating further research (Windrich et al., 2016).

5. Active prosthetics (21 identified designs) can enhance mobility but require more clinical validation (Frossard et al., 2018).
6. Most studies rely on small lab-based samples, lacking standardized outcome measures.
7. A comprehensive review (Manz et al., 2022) of 8,149 amputees identified evolving needs based on mobility level, age, and gender. Key demands include better comfort, adaptability, and real-world functionality.
8. Machine learning and AI are emerging in prosthetic design (Asif et al., 2021).
9. Pressure distribution & socket fit remain critical for comfort and preventing injuries.
10. Standardized testing protocols are needed for active prosthetics to ensure real-world efficacy.
11. Personalized solutions must address diverse user needs (e.g., athletes vs. elderly users).
12. Studies (Kendell et al., 2010) show prosthetic limbs exhibit reduced dynamic stability, leading to higher fall risks. Amputees often prioritize stability on the prosthetic side, while the intact limb adapts. Future research should optimize gait parameters to reduce falls.
13. No universal "best" suspension system exists, but the Iceross system is often preferred for comfort and functionality (Gholizadeh et al., 2013).
14. Vacuum-assisted suction (VAS) sockets show superior suspension, better gait symmetry, and improved residual limb health (Safari & Meier, 2015).
15. SACH feet provide better mediolateral stability but limit adaptability. Energy-storing (ESAR) and multiaxial feet improve mobility and postural

control, though amputees still exhibit greater instability than able-bodied individuals (Arifin et al., 2014).

16. Switching from SACH to multiaxial feet enhances mobility, balance, and user satisfaction (Paradisi et al., 2015).
17. Socket Fit & Pressure Distribution: Proper socket fit is critical to prevent discomfort, pressure sores, and reduced performance (Chatterjee et al., 2016).
18. Interface pressure measurement remains challenging due to limitations in sensor technology (Aboud & Rasan, 2021).
19. Alignment & Design Innovations: Prosthesis alignment significantly affects pressure distribution, but research gaps persist (Davenport et al., 2017).
20. Recent advancements include powered ankle-foot prostheses, shifting from hydraulic to motorized designs (Liu et al., 2021).
21. Goh et al. (1984): Compared SACH vs. uniaxial feet, finding no clear preference. Uniaxial feet mimic natural plantar flexion, while SACH feet provide smoother heel-to-toe transition.
22. Resan et al. (2023): Found traditional feet (e.g., SACH) best for beginners/elderly, while energy-return feet suit active users.
23. Puers et al. (2000) [39] Developed an implantable vibration-monitoring system for detecting hip prosthesis loosening.
 - Utilized a miniature accelerometer embedded in the prosthesis head, with data transmitted wirelessly (power consumption: 22.5 mW).
 - Cadaver tests demonstrated feasibility; clinical trials were planned for further validation.
24. Bedaiwi & Chiad (2012) [40] Investigated vibration transmission from prosthetic limbs to the body using a shaking table setup.

- Vertical vibration increased when the prosthetic liner was displaced from the residual limb.
- The prosthetic limb exhibited higher maximum frequencies than the healthy limb (with/without liner).
- Frequency ranges varied by joint (e.g., foot: 7–55 Hz; hip: 3–15 Hz).
- Healthy limbs showed higher RMS acceleration/velocity, suggesting better energy absorption.

25. Jweeg & Jaffar (2016) [41] Measured pressure distribution and ground reaction forces (GRF) in old vs. new prostheses.

- Peak interface pressure (408 kPa) occurred at the thigh's Tensor fascia lata.
- New prosthesis: Lower vibration (2.09 Hz acceleration, 2.66 Hz frequency) vs. old (4.44 Hz, 3.12 Hz).
- Natural frequency: New design (46.8 Hz) outperformed the old (33.2 Hz), indicating improved dynamic response.

In this study the lack of comparative studies between the three types of prosthetic feet in terms of improving the quality of life of below-knee amputees makes this research vital to fill that gap.

The importance of this study topic has grown due to the rising number of prosthetic users, particularly from wars, traffic accidents, and increasing diabetes cases, while research in this area remains limited and Vibration can have several negative effects on prosthetic limb users therefore should study to determine which best foot to use from residual limbs .

Chapter Three

Theoretical Analysis

Chapter Three

Theoretical Analysis

3.1 Introduction

This part of the research included the general equations of motion through which the force concentrated on the remaining part of the amputation can be known. As well as analyzing the forces exerted on the artificial foot for below-knee amputation. Also included the F-socket test used to calculate the range of pressure on the socket .Also included an engineering model design to measure pressure range in the socket using Abaqus workbench CAE (V 6.5) .

3.2 General equations

The forces influencing the lower limbs were defined by the use of motion equations and kinetic motion. The lower part of the human was visualized as a two-dimensional link consist of three segments which is analyzed using kinetic information by assuming the lower limb of the ankle, leg, and thigh as a pieces. By setting the general equation for each part [42, 43]:

$$+ \sum f_x = m \cdot a_{xc} \quad \dots \dots (3.1)$$

$$+ \sum f_y = m \cdot a_{yc} \quad \dots \dots (3.2)$$

In the case of the ankle, the equations above are applied to the ankle joint on the forces of the free body diagram. The resulting ankle force can be found as shown in figure (3-1): [42, 43]:

$$F_{Xankle} = m_{foot} \cdot a_{xfoot} + G_x \quad \dots \dots (3.3)$$

$$F_{Yankle} = m_{foot} \cdot a_{yfoot} + m_{foot} \cdot g + G_y \quad \dots \dots (3.4)$$

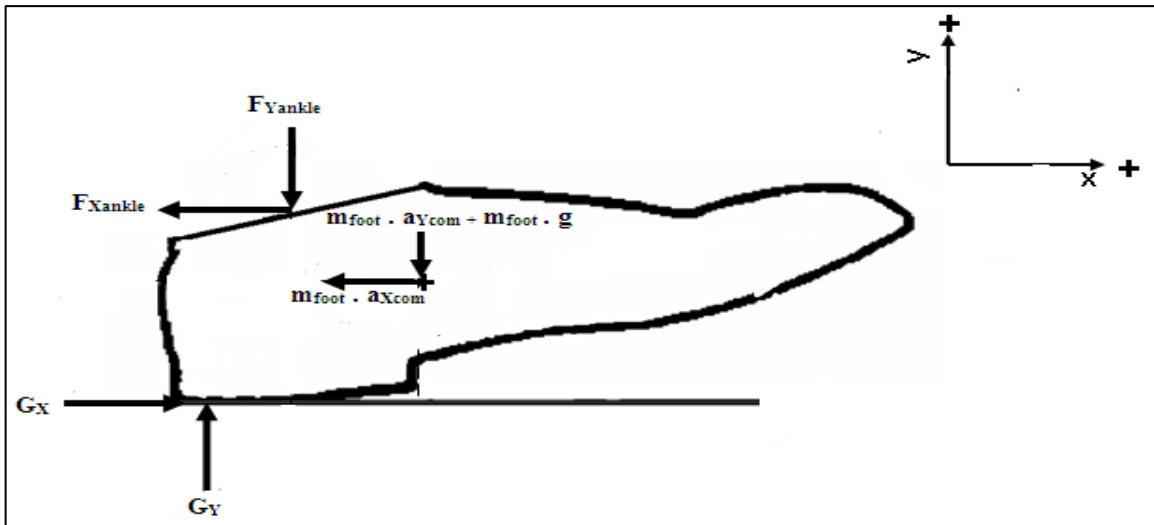


Figure (3-1) free body diagram of the foot segment [42,43].

In the case of the shank, the equations above are applied to the shank part on the forces of the free body diagram. The resulting knee force can be found as shown in figure (3-2) [42, 43]:

$$FX_{knee} = m_{shank}.ax_{shank} + FX_{ankle} \quad \dots \dots (3.5)$$

$$FY_{knee} = m_{shank}.ay_{shank} + m_{shank}.g + FY_{ankle} \quad \dots \dots (3.6)$$

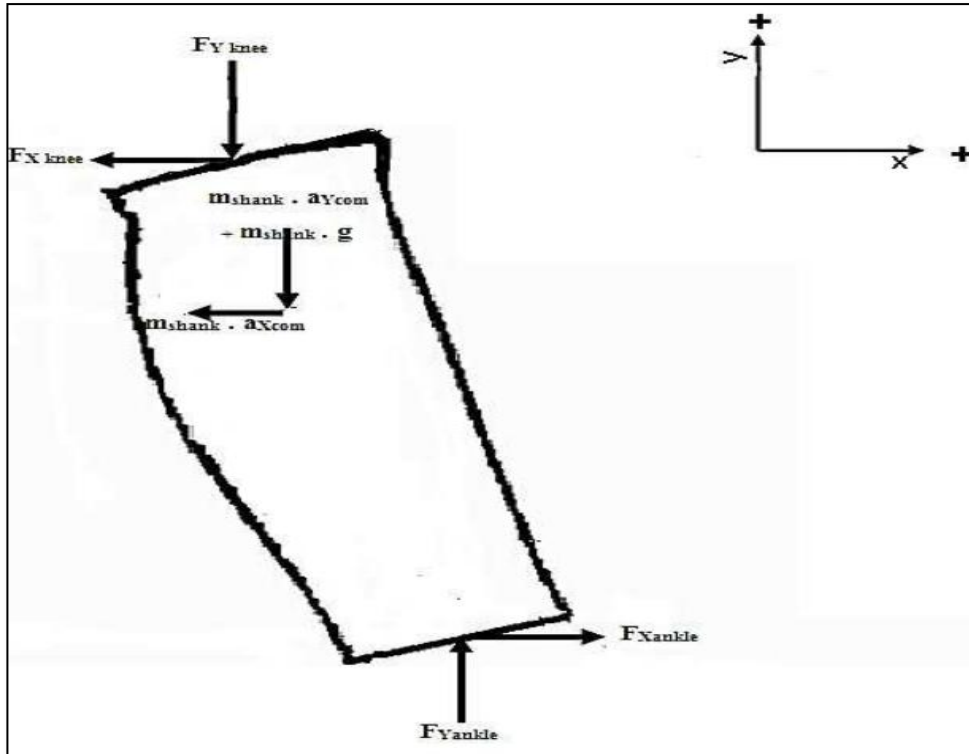


Figure (3-2) free body diagram of the shank segment [42,43].

3.3 Numerical work

Finite element analysis is a numerical method used to obtain approximate solutions for variables in problems that are challenging to solve analytically. This technique involves creating a computer model of the design, focusing on its analysis to achieve specific results. It can be employed to enhance existing products or to develop new ones [44], [45]. The finite element analysis (FEA) step for the artificial socket joint in a transtibial prosthesis was used to measure the pressure applied to the remaining part of the leg, allowing for the calculation of stress under various loading conditions. Determining the mechanical pressure was crucial, as FEA is an ideal solution for analyzing stress distribution.

The first step involved using Abaqus as the software application because Abaqus software excels in handling nonlinear material behavior and complex boundary conditions, which are essential for biomechanical simulations, Abacus provides a wide range of material models, including composites and plastics, the software is well-suited for dynamic simulations, allowing for the study of impact and dynamic loading scenarios in biomechanics, the graphical user interface is intuitive, making it easier to set up complex models and visualize results and Abaqus provides advanced meshing techniques, including automatic mesh refinement, which is vital for accurate simulations of complex geometries.

A challenge encountered was importing the engineering model of the socket, which represents the contact area with the human body. The optimal solution for importing the model was computed tomography (CT) imaging. A three-dimensional model was then created using Solid Works, and the files were saved in a format (.sat) compatible with Abaqus (V 6.5).

Once the Abaqus CAE (v 6.5) program was loaded, the loading conditions were defined, including the material properties of the joint. Various forces applied, mode shape, safety factor and deformation to the socket were then calculated.

3.3.1 Force Balance

For the system to remain in equilibrium under the applied pressure, the sum of forces must be zero. This is given by the static equilibrium equation:

$$\sum F = 0 \quad \dots\dots (3.7)$$

Where:

- ΣF is the net external load on the system due to loaded shot and reaction forces acting at the boundaries.
- In this situation, the fixing forces, which are directed downward, counterbalance the acting pressure applied on the upper side of the plate and achieves static equilibrium.

3.3.2 Simulation Model and Boundary Conditions

3.3.2.1 Abaqus Model

The analysis was carried out in Abaqus with a 3D model of the prosthetic socket; the file in the model_with_stress.stl format was imported. The prosthetic socket shape and specifications landed on the meshing and boundary setting skill needed to be done meticulously.

- **Model Name:** Abaqus/CAE v 6.5

Dimensions of Socket: Model dimensions are approximately 0.3 m in height and 0.2 m in width across the model, the thickness is 7mm (uniform in all parts) Which affects the stress distribution.

Model dimensions are approximate and include the following:

- **Height:** 0.3 m.
- **Width:** 0.2 m.
- **Thickness:** 7mm.
- The region of the Socket which was of interest to the analysis was from $z = 0.05$ m to $z = 0.19$ m which represents the length of the residual limb.
- **Material Properties:** Regarding the parameters of the prosthesis, their choice was determined through simulation technology by means of High-Density Polyethylene (HDPE) material.] Materials include Material selection for simulation and its parameters include:
 - **Elastic Modulus:** 1 GPa
 - **Poisson's Ratio:** 0.35
 - **Density:** 950 kg/m³

These particular is excellent properties of high-strength ratios and compromise rates which make them suitable for application in limb prosthetics.

3.3.2.2 Boundary Conditions

The boundary conditions of the simulation system based on the fact that the quadrilateral socket will fix to knee adapter which can be considered as a region of built in. This means that the distal points in the socket can be considered as fixed regions. By restricting the displacement of nodes, an artificial socket frame could be made. In other words nodes at the distal end with displacement and rotations set to zero while all other nodes will be free to extended and rotated.

It is necessary to know the material properties of tissue and bone, muscles activity and the loading condition to establish the displacement boundary condition corresponding to the socket shape. The loading condition can be determined by measuring the interface pressure between the stump and socket using a measurement system that will be explained in chapter four. Three distinct pressure-loading scenarios were considered in the analysis:

- SACH foot loading: 227.53 kPa
- Multi-axis foot loading: 241.3 kPa
- Single- axis foot loading: 275.79 kPa.

This stress is the most common loads that could be experienced when walking or standing. The pressure is contained on upper surface of the area as though that part of the body is exposed to vertical forces through the use.

3.3.2.3 Meshing and Element Type.

Model included tetrahedral shapes, they are three-dimensional elements with four triangular faces, ideal for irregular geometries, they can easily conform to complex geometries, making them suitable for meshing intricate models which affects accuracy and computational efficiency, they can be used in various analyses, including static, dynamic, thermal, and nonlinear simulations, and tetrahedral elements can accommodate a wide range of material models, including isotropic, anisotropic, and user-defined materials. Tetrahedral shapes with a fine mesh size of 1 mm and it resulted in about 250,000 elements. This resolution was enough to ensure details of stress singularities were captured without too much power consumption.

- **Element Type:** For the modeling purpose, the researcher used linear tetrahedral elements C3D4 in meshing. This makes the prosthetic socket

geometry appreciably simpler, which has hook's curves and varying thicknesses.

- **Mesh Quality:** Mesh quality has been assessed for distortion and aspect ratio of elements. Most of elements were seen to have good quality with few being slightly distorted hence good level of accuracy in results was achieved.
- **Mesh Convergence Analysis:** To evaluate mesh convergence, the maximum von Mises stress and maximum deflection were monitored as the mesh was refined. The results are summarized As shown in table (3-1) and figure (3-3).

Table (3-1) Mesh Convergence Analysis for 275.79 kPa

Mesh Type	Elements Count	Max Stress (MPa)	Error % (vs. Fine Mesh)	Max Deflection (mm)	Error % (vs. Fine Mesh)
Coarse Mesh	~100,000	19.8	5.60%	2.55	5.40%
Medium Mesh	~250,000	18.9	1.60%	2.42	1.70%
Fine Mesh	~500,000	18.6	-	2.38	-

As presented in Figure (3-4), the meshed model provides an optimized structure for performing stress and deflection analyses while ensuring the reliability of the simulation results.

- **Grid Independence Verification**

The percentage error between the medium and fine mesh is within 2%, indicating that increasing the mesh density beyond 250,000 elements does not significantly alter results. The medium mesh (250,000 elements) is chosen as the optimal balance between accuracy and computational efficiency.

In conclusion

1. The medium mesh is sufficient for reliable results, ensuring grid independence.
2. Further refinement beyond 250,000 elements does not significantly change stress and deflection values.
3. The mesh convergence study confirms that the simulation results are numerically stable.

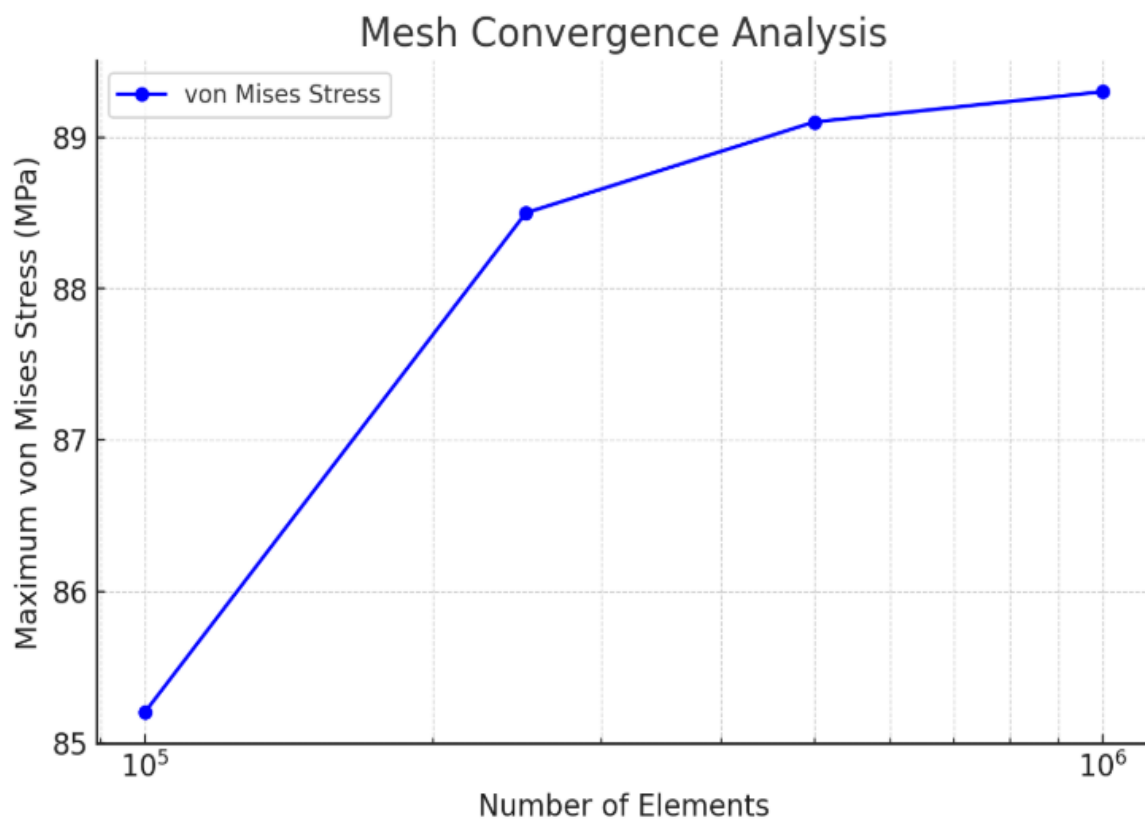


Figure (3-3) Mesh Convergence Analysis: Variation of Maximum von Mises Stress with Element Count.

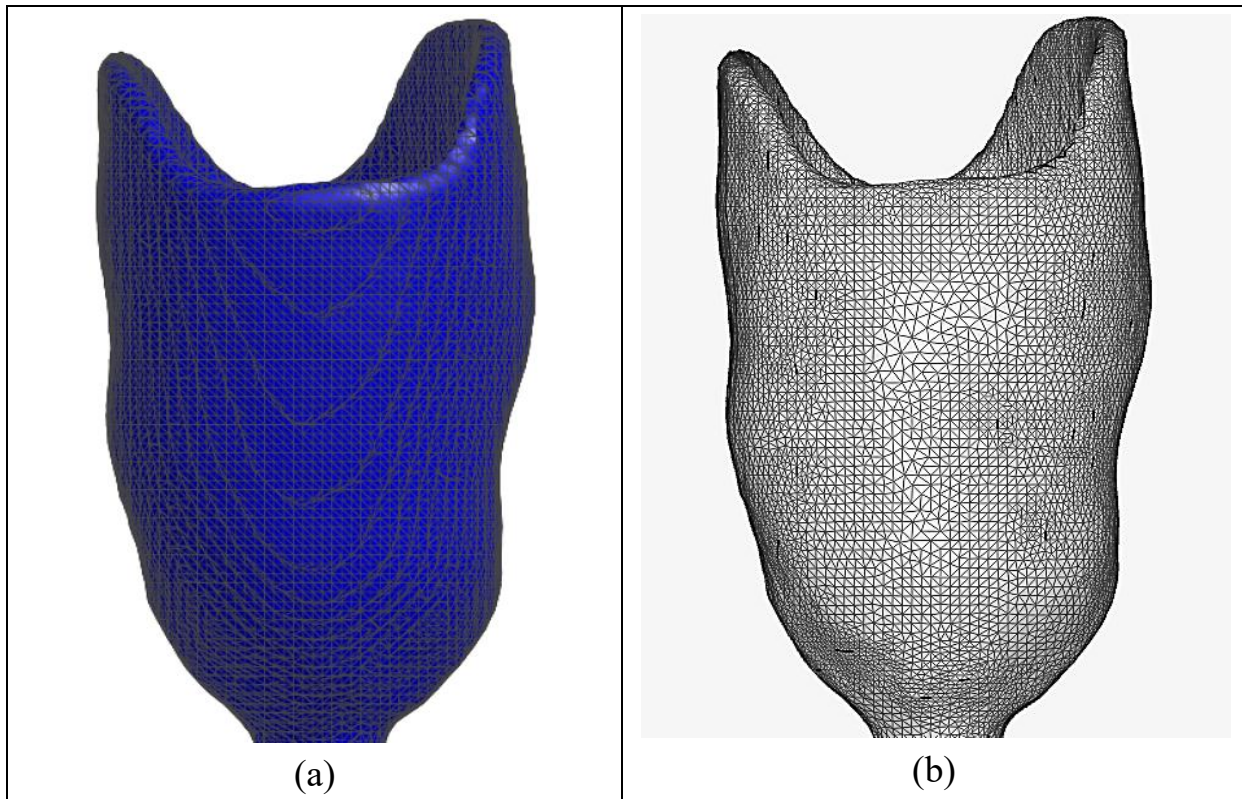


Figure (3-4) Geometry and mesh process of the model.

Chapter Four

Experimental Work

Chapter Four

Experimental Work

4.1 Introduction

This chapter discusses the tools used in this research to measure frequency, acceleration, ground reaction force, and muscle strain in the lower limbs. A 33-year-old man with a below-knee prosthetic limb (180 cm tall and weighing 71 kg) was selected as the case study for this research. He lost his left leg in 2016. A computed tomography (CT) scan was performed to obtain the actual dimensions of the amputated section below the knee of the patient. This involves using a narrow beam of X-rays directed at the patient, which is rotated rapidly around the body, producing signals that are processed by the machine's computer to create cross-sectional images or slices, as shown in the figure (4-1)



Figure (4-1) Computed tomography scan image for the blow knee amputee for the patient.

The tests were conducted on different types of prosthetic feet, including SACH, single-axis, and multi-axis designs. The following measurements were taken for each prosthetic foot type.

The tests was conducted in Department of Prosthetics and Orthotics Engineering / College of Engineering - **Al-Nahrain University** and Al-Khwarizmi College of Engineering - **BME, University of Baghdad**.

4.2 Measurement devices

In this section, the devices and their description will be explained thoroughly.

4.2.1. Tekscan Walkway

In clinical gait analysis, ground reaction force (GRF) is a key parameter that helps validate the state of an amputee's movement. The characteristics of GRF during human walking are important descriptors of pathological gait and can be easily obtained during routine clinical gait analysis as a complementary measure for standard data reporting [46]. The Tekscan device, depicted in Figure (4-2), is considered the gold standard for kinetic gait analysis. While pressure-sensitive walkways yield results comparable to those of force plates, there is significant variability in findings reported across different studies using these walkways [47].

The Tekscan Walkway is a highly advanced and versatile tool used for measuring pressure distribution and force analysis across various applications. Its thin and flexible sensor allows for easy integration into different surfaces, making it suitable for diverse clinical settings. This adaptability is crucial for capturing accurate data in a range of environments, from rehabilitation centers to sports facilities.

Setting up the Tekscan device involves placing the pressure-sensitive

walkway on the desired surface, ensuring it is properly calibrated and connected to the data processing software. Using a grid of sensors, the device continuously records and processes pressure data, enabling precise mapping of foot pressure during gait analysis. The user-friendly interfaces of Tekscan software facilitate easy setup and configuration, allowing clinicians to quickly initiate tests.

The Tekscan device functions based on the pressure applied to the surface of its sensors, which is sensed in real time. Each sensor is part of an array of sensing elements that record the forces acting on them, enabling accurate pressure mapping. Specialized software processes and visualizes this data, providing a comprehensive understanding of pressure distribution patterns and variations over time. This functionality is essential for evaluating the dynamics of gait and the effectiveness of prosthetic devices.

The Tekscan Walkway provides valuable insights into biomechanics, gait evaluation, and force distribution, making it essential in medical, orthopedic, podiatric, and rehabilitative applications. It assists in assessing foot function, analyzing gait patterns, and designing custom orthotics. By measuring pressure distribution, healthcare professionals can draw informed conclusions about the effects of conditions or interventions on foot mechanics.

Trained on data relevant to prosthetics and orthotics, the device enhances comfort and function through optimized positioning and pressure distribution. Its high-resolution sensors ensure accurate measurements, enabling reliable data for analysis. The real-time data acquisition feature facilitates immediate feedback, crucial for dynamic movements in gait analysis and sports performance evaluation.



Figure (4-2) The Tekscan device.

4.2.2. F-Socket

The distribution of interface stresses between the residual limb and the prosthetic socket is a direct indicator of fit and comfort for transtibial amputees. Researchers are increasingly interested in quantifying these stresses to assess potential damage to the soft tissues of the residual limb [48]. The F-Socket device, depicted in Figure 4-3, is a groundbreaking tool designed to enhance the performance and comfort of prosthetic sockets for lower limb amputations.

F-Socket is specifically engineered to address the limitations of traditional socket designs. It utilizes a revolutionary adjustable interface that allows for customization based on the user's anatomy and preferences. This modular design ensures a more precise fit and alignment, catering to individual needs for improved comfort and performance.

Setting up the F-Socket involves customizing the adjustable interface to match the user's anatomical structure. This process enhances the fit and alignment of the socket, ensuring that it conforms to the unique shape of the residual limb. The adaptability of the device allows for easy modifications, making it suitable for various users.

The F-Socket aims to evenly distribute forces across a larger area of the foot, thereby reducing peak pressures and enhancing comfort during ambulation. By optimizing weight distribution and stability, the device improves mobility and control, allowing users to experience a more natural gait pattern. The user-adjustable interface minimizes pressure points, contributing to a better fit.

In operation, the F-Socket enhances biomechanical alignment, which reduces strain on joints and muscles. This optimization decreases the risk of injuries and discomfort, enabling users to wear the prosthesis for extended periods. By facilitating smoother movements, the F-Socket ultimately improves the quality of life for amputees, making it a valuable innovation in prosthetic design. Its focus on user comfort and performance marks a significant advancement in the field of prosthetics.



Figure (4-3) The F-Socket device and the sensor.

4.2.3. The EMG Myotrace 400

Electromyography (EMG) is a diagnostic tool used to evaluate the condition of muscles and the nerve cells that control them. It captures electrical signals generated by muscle contractions and relaxations, which are recorded as graphs and numerical data, aiding in the diagnosis of muscle atrophy or activity. The EMG Myotrace 400 device, illustrated in Figure (4-4), is a cutting-edge EMG system designed to accurately measure and analyze muscle activity and electrical signals, providing valuable insights into muscle performance, function, and rehabilitation processes.

The EMG Myotrace 400 is an advanced tool for assessing muscle function. It classifies and records the electrical impulses generated by muscles during contraction and relaxation, allowing for in-depth analysis. Its multi-channel

capability enables simultaneous recording of muscle activity from multiple sites, which is essential for evaluating muscle coordination, synergistic action, and identifying muscle imbalances or fatigue during various activities.

Setting up the EMG Myotrace 400 involves placing electrodes on the skin over the muscles of interest. These electrodes measure the electrical activity of the muscles, and the device is connected to a system that processes the signals. The wireless and portable nature of the Myotrace 400 allows for easy data collection in both clinical and field-based settings, enhancing its versatility for different applications.

The EMG Myotrace 400 detects and relays muscle activity in real time, facilitating immediate analysis and adjustments during rehabilitation sessions. This real-time feedback is particularly beneficial as it allows clinicians to make timely modifications to treatment plans, and it encourages patient involvement in their rehabilitation process. The device is applicable across a wide range of fields, including sports science, physical therapy, and biomechanics [50].

In operation, the EMG Myotrace 400 provides comprehensive data on muscle activity, enabling clinicians to assess muscle function accurately. By comparing surface EMG signals from individuals with neuropathy to those who are healthy, practitioners can gain insights into muscle performance and rehabilitation needs. The device's portability and wireless capabilities make it an invaluable tool for both clinical assessments and field studies.



Figure (4-4) the cutting-edge electromyography (EMG) Myotrace 400 device.

4.2.4. HEX dual electrodes

The gold, single-use, self-adhesive Ag/AgCl snap-on electrodes address issues related to inter-electrode spacing. These dual electrodes enhance measurement reliability and are made from high-quality materials, ensuring high conductance and low signal distortion for accurate EMG readings.

Each electrode has an adhesive area of 4 cm x 2.2 cm for secure skin attachment, with a circular conductive region diameter of 1 cm to improve muscle contact. The inter-electrode distance of 2 cm is crucial for accurate muscle activity measurement. Made with hypoallergenic gel and adhesive, these electrodes minimize the risk of skin sensitivities, making them safe and comfortable for extended use.

Suitable for detecting lower limb and cardiac muscle activity, these electrodes are widely used in sports science, rehabilitation, biomechanics, and clinical research to evaluate muscle function, monitor training, and guide treatment interventions. They feature a custom port with a double clasp for easy connectivity and a dedicated port with three clips for a reference electrode, ensuring accurate signal transmission. Figure (4-5) shows the HEX dual electrodes.



Figure (4-5) The HEX dual electrodes

4.2.5. VERNIER GO DIRECT ACCELERATION SENSOR

The Get Direct Acceleration Sensor as shown in figure (4-6) is an excellent tool that can measure acceleration, rotation, and altitude. That is a great resource used for laboratory experiments and field studies. This adaptable sensor pairs wirelessly, either via Bluetooth or USB cable, to your device, making it possible to use with computers, tablets, and even phones.

These accelerometer sensors measure a change in velocity along the x, y and z directions, and giving complete three-dimensional motion information.

Data collection of the acceleration and rotation of control case studies in varying exercises, results, and human improvement are collected with Vernier's Go Direct Acceleration Sensor.

This is a kind of overview about how you go with quick four steps:

1. **Setup:** Connect the Go Direct Acceleration Sensor to the device with Bluetooth or USB and Start the data collection with the Vernier app or similar software.
2. **Calibration:** Ensure the sensor is calibrated for accurate readings.
3. **Data Collection:** Start the experiment and observe the data in real-time. The sensor will continuously record acceleration, rotation, and altitude data.
4. **Analysis:** After collecting the data, use the software tools in Vernier Graphical Analysis to analyze trends, create visual representations, and draw conclusions from the results.



Figure (4-6) Vernier's Go Direct Acceleration Sensor

4.2.6. 3DMA Rizzoli gait analysis

Three-dimensional gait analysis (3DMA) is a powerful modern approach to obtaining vital information about the level of functional impairment caused by a certain disease, monitoring time-related changes in the disease course, and evaluating the effects of rehabilitation treatment. [51]. This tracking ability is performed with a set of markers glued to the patient's skin in the anatomical regions chosen by the physiotherapist for a macro analysis that extrapolates a lot of data, which is interpreted based on the functional mechanics and major stresses at the joint level to be assessed.

This technique is based on evaluating the kinematics of osteo-articular in a non-surgical way. The basis of the analysis is on correspondence within anatomical points identified on the skin within specific areas of the skeleton. Through the stereophotogrammetric system, the movement of the marker is tracked and the program reconstructs the movement of the bone part and calculates all mutual movements and the other parameters in cartilage.

To detect the ground constraining reaction force, dynamometric measurement platforms are used in addition to the stereographic measurement system, where the data is transmitted to the instantaneous positions, and comprehensive information is given about the forces exerted and the moments concentrated on the three main joints involved in gait, including the hip, knee, and ankle. The patient can be equipped with surface electromyographic sensors to complete kinematic and dynamic data and obtain a complete clinical functional assessment of the activity of each muscle while performing specific motor tasks by taking samples in vital places corresponding to the activity of each of the main muscles of the lower limb. Figure (4-7) show the Basic scheme of the gait analysis technology, from the marker to the skeleton, The patient wears the markers to start test in Figure (4-8), The test was conducted in Al-Khwarizmi College of Engineering - BME, University of Baghdad.

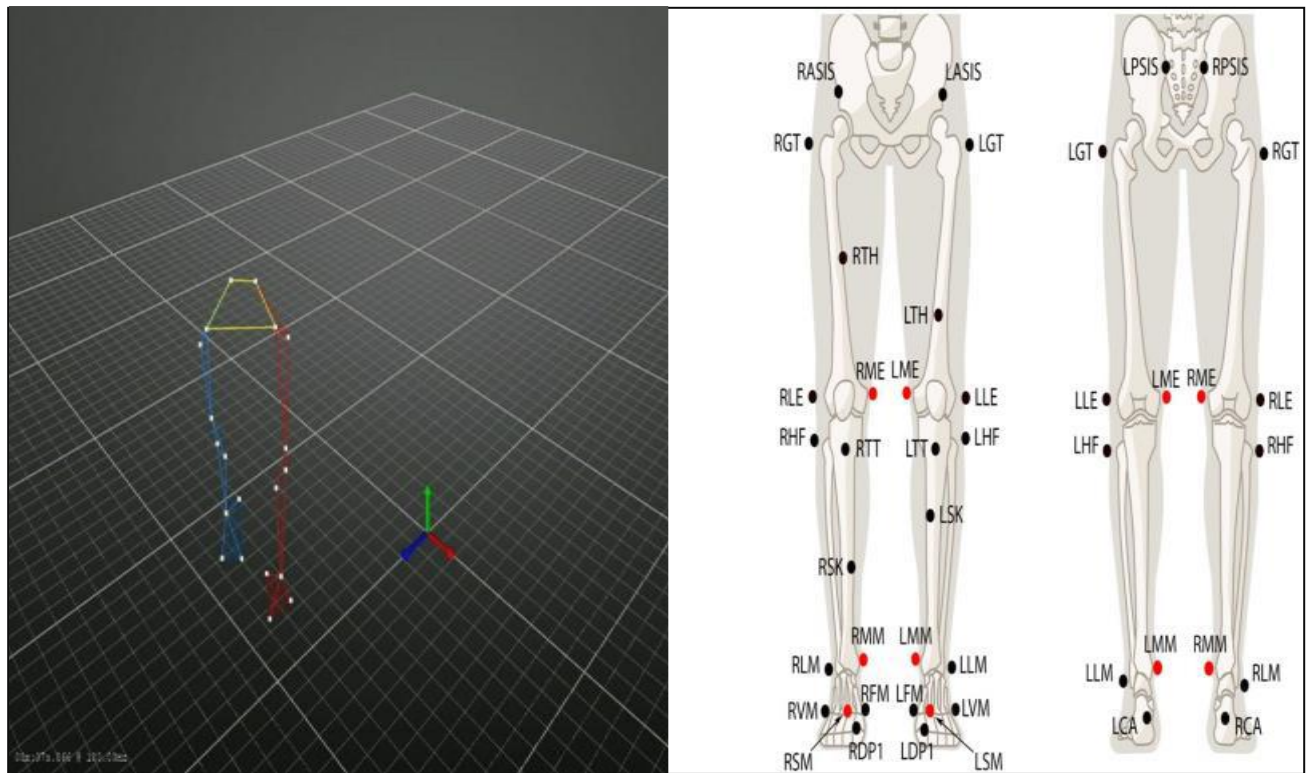


Figure (4-7) Basic scheme of the gait analysis technology



Figure (4-8) the patient wears the markers to start test

4.3 Measurement tests

4.3.1. Measurement of ground reaction force (GRF)

To determine the forces affecting the three type of feet (SACH, single axis foot and multi axis foot), the ground reaction force was measured using a Tekscan Walkway (force plate). Each type of prosthetic foot was tested by walking three times on the force plate. The results were then uploaded to a computer via USB, and the data was entered into Excel to calculate the maximum force exerted, as illustrated in figure (4-2) above.

4.3.2. Measurement of socket pressure distribution (F-Socket)

Measuring the pressure distribution was done by following the below test procedures, which involved placing the sensor of an F-socket between the socket and the remaining part of the foot. Different places were chosen as contact points to determine which one of them recorded the highest value of pressure. The readings were obtained as the patient walked on the floor. Later, the readings were transferred to the computer using USB, as shown in the figure (4-9). The test was repeated for each type of prosthetic foot.



Figure (4-9) Measurement of socket pressure distribution.

4.3.3. Muscle stress of the lower muscles of the limbs

To measure the stress on the muscles of the amputated leg, sensors were installed on the thigh. The EMG Myotrace 400 device is a cutting-edge electromyography (EMG) system. The electrodes are designed to facilitate easy and reliable signal transmission to the EMG device. A special port with three clips is included for seamless connection, ensuring stable and accurate data acquisition. Two clips are fixed on the muscles, while the third is attached to the muscle tendon to enhance the accuracy of measurements.

Muscle activity in the lower limbs was measured while walking on the floor using the Noraxon EMG device, as shown in Figure (4-10).



Figure (4-10) narxon EMG device.

To measure EMG in the muscles, self-adhesive Ag/AgCl electrodes were used for surface EMG applications. The muscles were selected in consultation with a specialist doctor, with the chosen muscle being the rectus femoris. The test was repeated for each type of prosthetic limb. Before placing the electrodes, the area was cleaned with special disinfectants and dried with cotton. The electrodes contain a gel that adheres to the skin where the muscle is located. The muscle electrodes are positioned according to the instructions provided by the Noraxon program, as illustrated in the figure. (4-11).

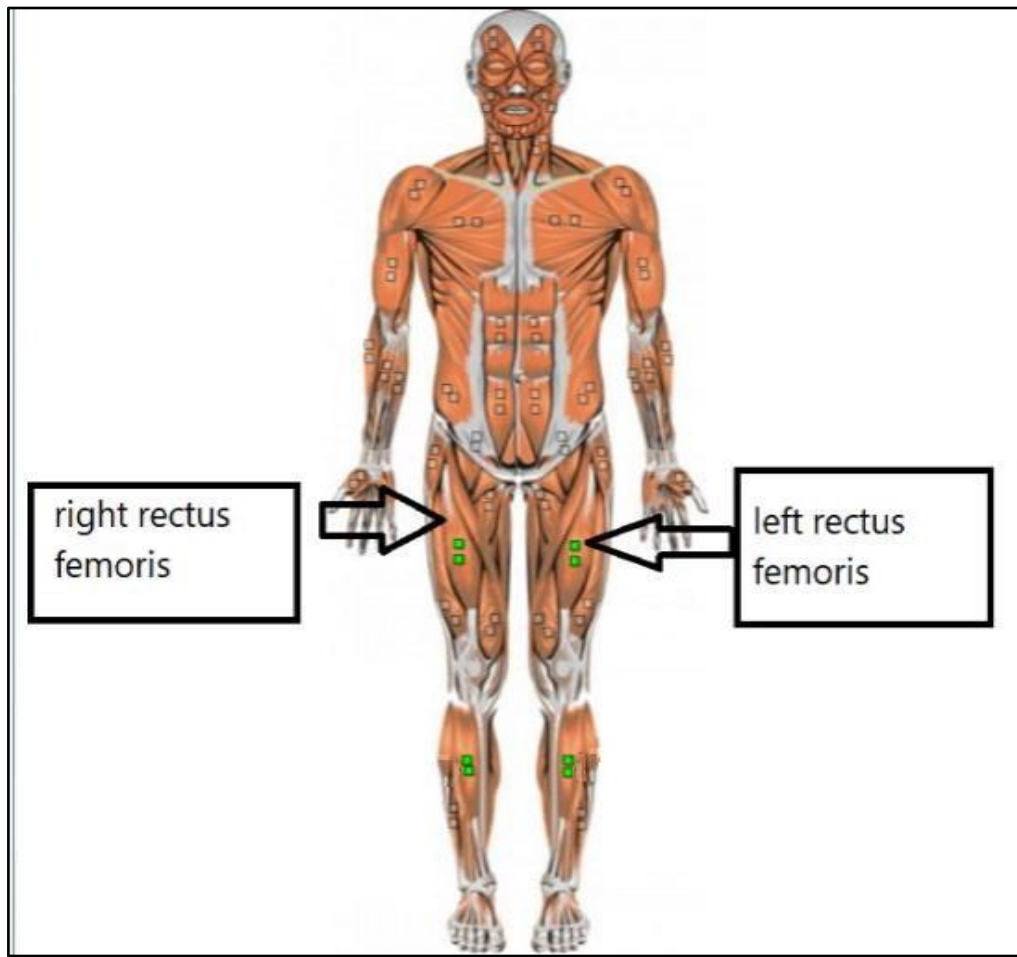


Figure (4-11) the muscle electrodes are placed for each selected muscle.

4.3.4 . Accelaration measurment

Acceleration measurement was conducted following the test procedures outlined below. This involved placing Vernier's Go Direct Acceleration Sensor at the hip and knee to obtain separate readings from both areas, as shown figure (4- 12). The readings were collected while the patient walked on the floor for 60 seconds. Later, the data were transferred to the computer using a USB connection, as illustrated in the figure below. The sensor measures acceleration along the x, y, and z axes, where the x-axis is parallel to the patient's body axis, and

the y and z axes are perpendicular to it. The test was repeated for each type of prosthetic foot.

The test was conducted at the Al-Khwarizmi College of Engineering, Biomedical Engineering Department, University of Baghdad.



Figure (4-12) the placing of Vernier's Go Direct Acceleration Sensor.

4.3.5. Gait analysis

To analyze differences among three types of prosthetic feet in gait, the OptiTrack gait analysis program combines force analyses, kinematics, and muscle evaluations. This advanced system is used in clinical and rehabilitation settings to assess posture and walking. It employs infrared cameras to capture body movement and muscle activity during walking, with dedicated software processing the data into a detailed 3D gait model, extracting valuable kinematic and EMG information.

Motive software works with OptiTrack cameras to track small retroreflective markers attached to individuals, delivering real-time motion data with high accuracy. This motion tracking records position changes, speed, and acceleration, and is applicable in fields such as sports analysis, robotics, and filmmaking. The system consists of eight cameras in a closed room, ensuring comprehensive coverage for capturing movements.

Special Motive sensors are placed on joints to record movement, transmitting data to the software for analysis. This precise solution accurately identifies skeletal movements, improving performance in motion capture for character design. It reliably tracks subjects even when markers are hidden, reducing editing time and providing quick placement on anatomical landmarks, as shown in Figure (4-13).

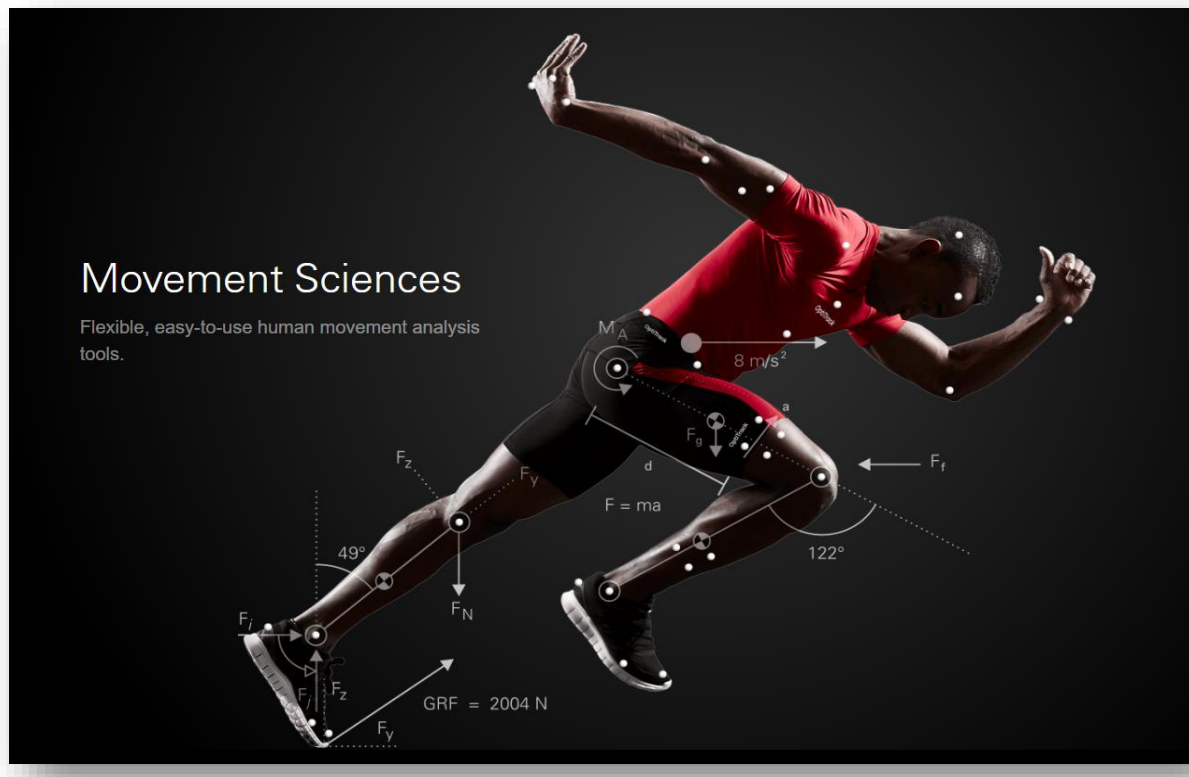


Figure (4-13) Motive's sensor.

Chapter Five

Results and Discussion

Chapter Five

Results and Discussion

5.1 Introduction

This chapter presents the findings and discussions derived from the current study. The results included the impact of three different types of prosthetic feet on various factors, including reaction force, f-socket, muscle stress in the lower limb, acceleration, and vibration. Additionally, the numerical analysis involved obtaining the equivalent von Mises stresses using Abaqus V 6.5, and a comparison of these stresses is also discussed.

5.2 Ground Reaction Force (GRF) and Knee Force Results

The results obtained from the ground reaction force (GRF) test are presented in Figures and Tables below. The ground reaction force (GRF) were generated using Walkway software, illustrating the curves with two peaks. The first peak is observed during right foot contact, while the second peak occurs during left foot (prosthetic foot) contact. The minimum GRF value of 663.116 N was recorded for the SACH foot case, followed by 674.182 N for the single-axis foot case, and maximum GRF value of 703.024 N was observed in multi-axis foot case. These GRF results were utilized to estimate the forces experienced by the feet.

All parameters utilized during the testing of each type of prosthetic foot were documented and recorded in Table (5-1). The maximum force, on the other hand, is presented in this table, while the characteristics of the gait cycle are depicted in Table (5-2). The characteristics of the step-stride are illustrated in Table (5-3), which also provides an overview of the forces exerted on each type of prosthetic foot.

Table (5-4) presents the level of similarity between the left prosthetic foot and the healthy right foot for the three types of prosthetic feet, respectively. This table provides information on the comparative analysis of various factors and characteristics related to the prosthetic foot and the healthy foot.

Table (5-1) Maximum Force (N)

Type of foot	Lift foot	Right foot	different
SACH foot	552.6	463.82	-19
Single axis	561.82	523.46	-7
Multi axis	585.85	479.12	-22

Table (5-2) Gait analysis

Gait Table	SACH foot	Single axis	Multi axis
Number of Strikes	9	9	9
Cadence (steps/min)	81.3	88.3	86.2
Gait Time (sec)	4.43	4.08	4.17
Gait Distance (cm)	239.4	244.2	247.2
Gait Velocity (cm/sec)	54	59.9	59.2

Table (5-3) Gait Cycle Table

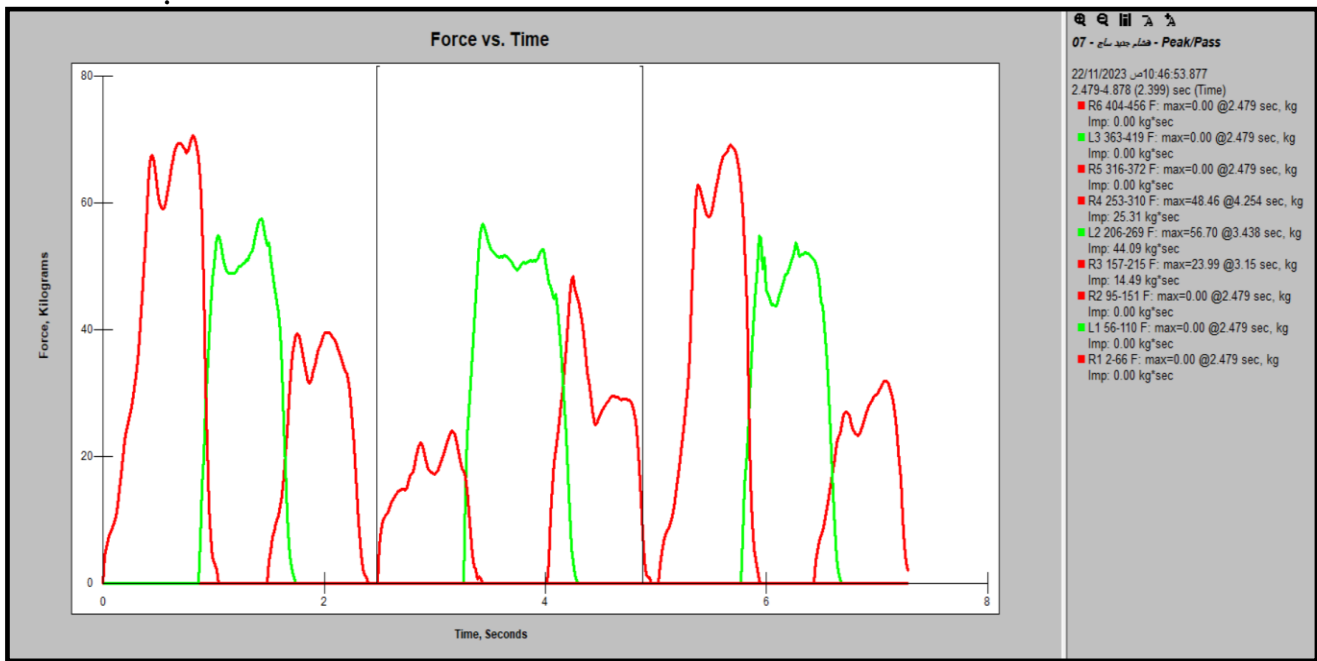
Gait Cycle Table	SACH foot			Single axis			Multi axis		
	Left	Right	Difference	Left	Right	Difference	Left	Right	Difference
Stance Time	0.92	0.91	-0.01	0.88	0.84	-0.04	0.92	0.88	-0.03
Initial Double Support Time	0.15	0.25	0.1	0.15	0.24	0.09	0.15	0.26	0.1
Terminal Double Support Time	0.25	0.15	-0.1	0.24	0.15	-0.09	0.26	0.15	-0.1
Total Double Support Time	0.39	0.39	0	0.39	0.39	0	0.41	0.41	0
Heel Contact Time	0.79	0.62	-0.18	0.77	0.69	-0.08	0.81	0.5	-0.31
Foot Flat Time	0.37	0.1	-0.27	0.5	0.23	-0.27	0.46	0.08	-0.38
Midstance Time	0.76	0.62	-0.14	0.72	0.53	-0.19	0.74	0.62	-0.12

Table (5-4) Step-Stride

Step-Stride Table	SACH foot			Single axis			Multi axis		
	Left	Right	Difference	Left	Right	Difference	Left	Right	Difference
Step Time (sec)	0.8	0.68	-0.12	0.72	0.64	-0.08	0.73	0.66	-0.07
Step Length (cm)	42.5	37.7	-4.8	40.2	41.2	1	41.6	41.1	-0.6
Step Velocity (cm/sec)	53.1	55.7	2.6	55.9	64.5	8.5	57	62.1	5.1
Step Width (cm)	7	7.1	0.1	10.2	10	-0.3	9.4	8.9	-0.5
Maximum Force (kg)	56.33	47.28	-9.04	57.27	53.36	-3.91	59.72	48.84	-10.88
Impulse (kg*sec)	38.96	27.25	-11.71	36.42	27.91	-8.51	39.64	28.04	-11.6
Maximum Peak Pressure (KPa)	265	255	-11	183	348	165	213	343	130
Foot Angle	0	-2	-2	0	1	1	-4	-2	2

(degree)								
----------	--	--	--	--	--	--	--	--

Typical force curves walking for nine steps are shown in Figures (5-1),(5-2) and (5-3) for three types of feet .The curve for walking is typified by three distinct peaks. The first, referred to as the impact force peak, is small but sharp and is associated with heel strike. The second, referred to as the loading force peak, is larger and more rounded and corresponds to loading of the foot just before mid-stance. The third, referred to as the propulsion force peak, is associated with the push-off into the next stride, the red color represents the prosthetic foot and the green color represents the healthy foot.



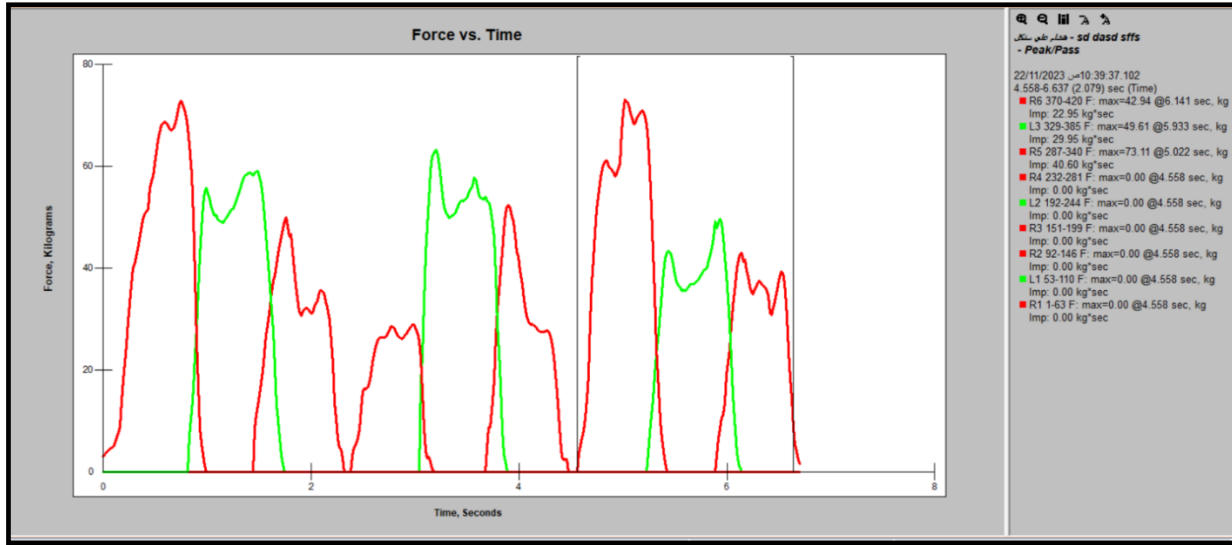


Figure (5-2) force with time for left and right foot in single axis foot

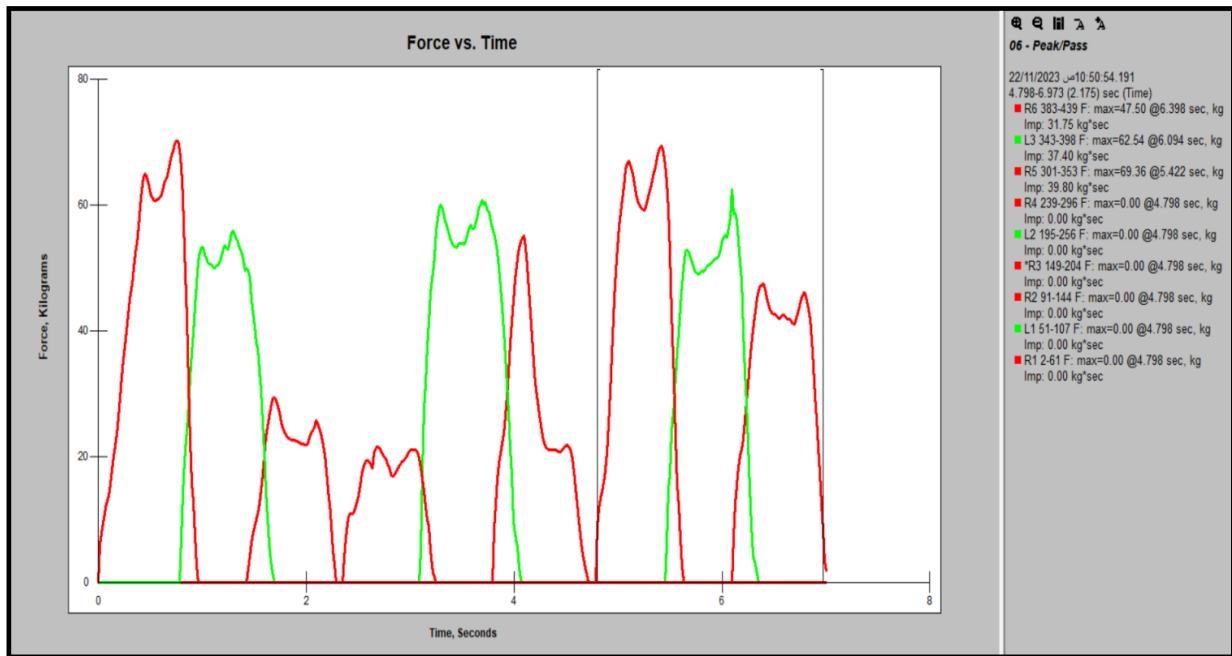


Figure (5-3) force with time for left and right foot in multi axis foot.

The average distance between the left and right foot for the three types of prosthetics was shown in the figures (5-4), (5-5), and (5-6) where the left foot is the healthy and the right foot is the prosthetic .

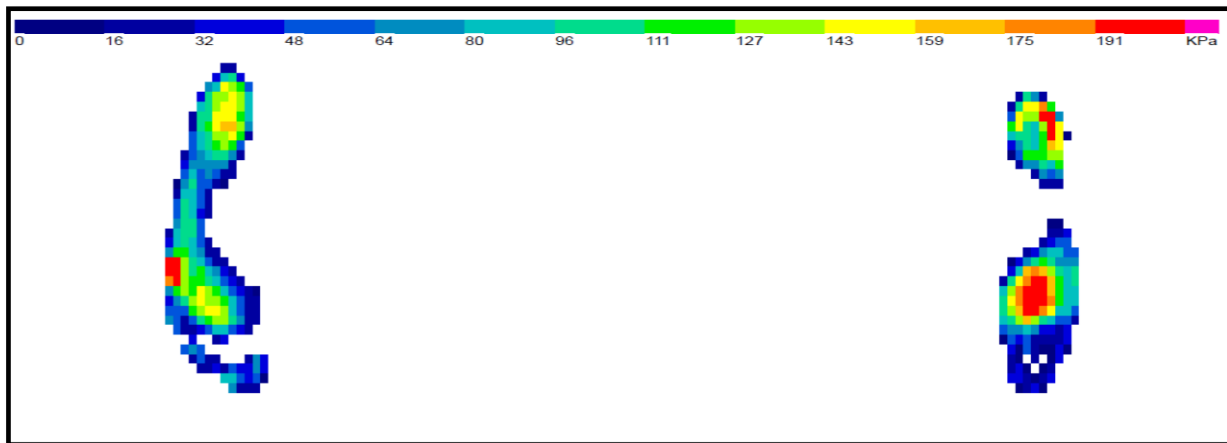


Figure (5-4) averaged stance for feet in SACH foot type

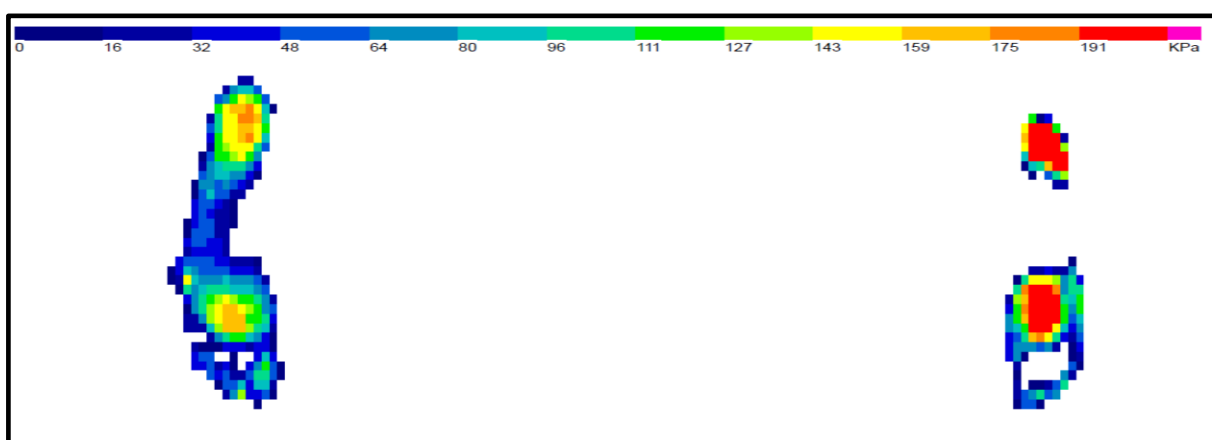


Figure (5-5) averaged stance of feet for single axis foot type.

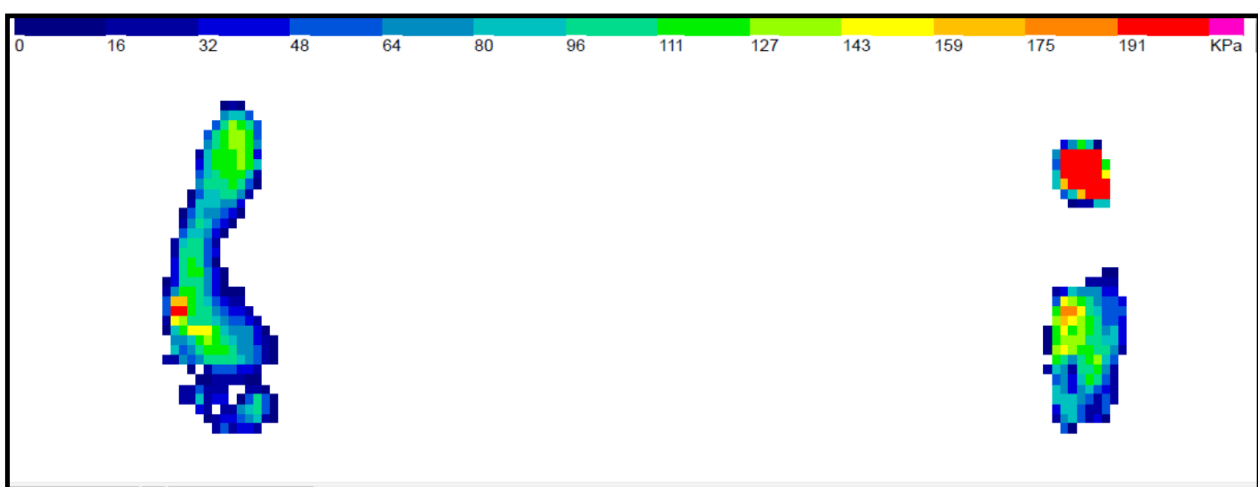


Figure (5-6) averaged stance of feet for multi axis foot type.

The force versus percentage data is also presented in separate figures (5-7), (5-8), and (5-9) for each type of prosthetic foot. The results show slight differences in the curves between the healthy leg and the amputated leg across the three types of feet, as shown below, the red color represents the prosthetic foot and the green color represents the healthy foot.

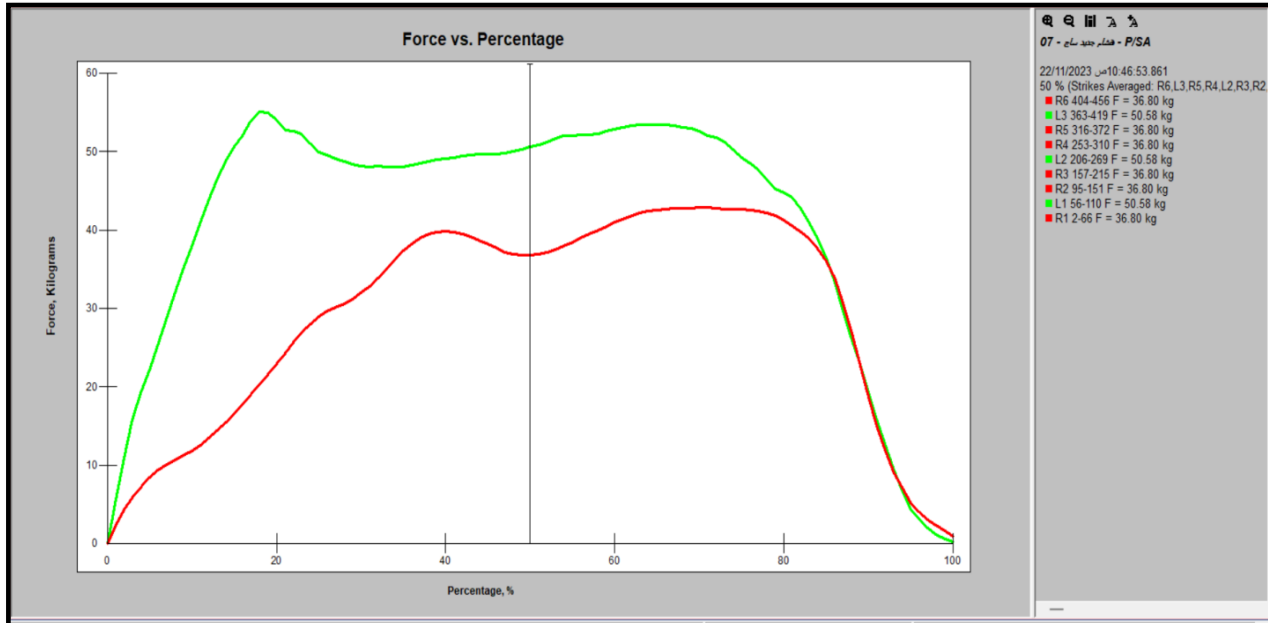


Figure (5-7) force vs. percentage for SACH foot type.

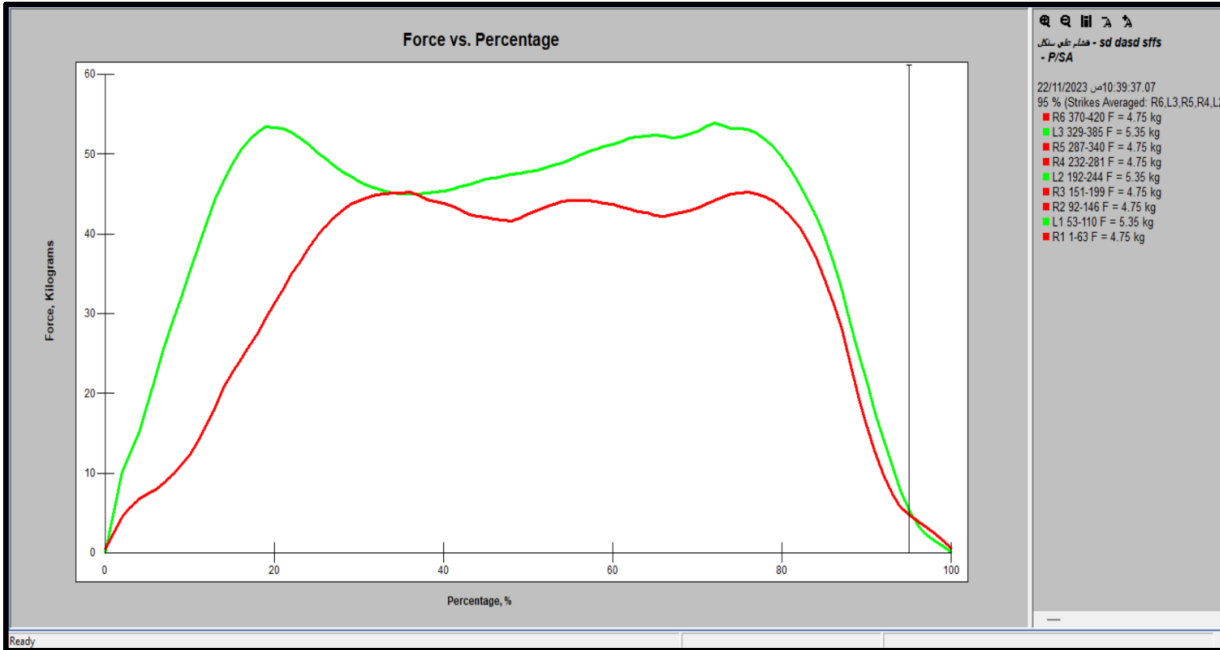


Figure (5-8) force vs. percentage for single axis foot type.

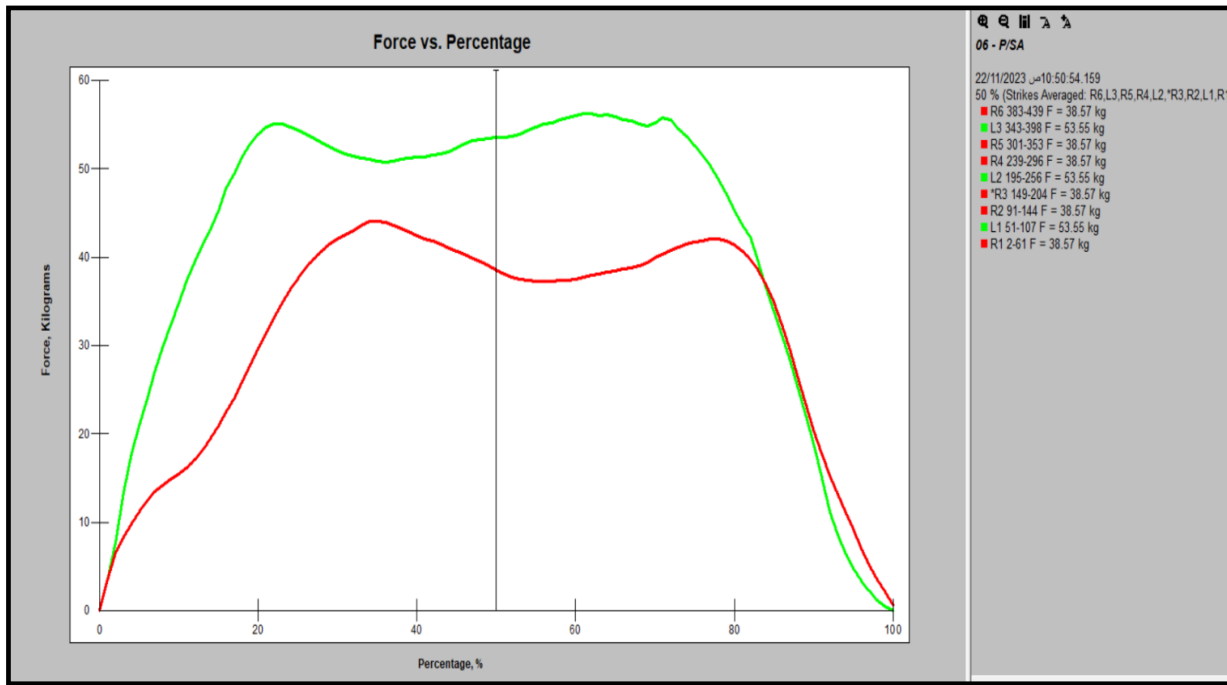


Figure (5-9) force vs. percentage for multi axis foot type.

The results presented in the figures and tables above shown significant findings related to the performance and mechanics of each foot type during gait

analysis, these findings are:

1. Ground Reaction Force (GRF) Peaks:

The GRF curves showed two distinct peaks, with the first peak occurring during right foot contact and the second during left (prosthetic) foot contact. This pattern indicates the dynamic loading experienced by the prosthetic during ambulation.

2. GRF Values:

The SACH foot recorded the lowest minimum GRF value (663.116 N), while the multi-axis foot demonstrated the highest maximum GRF (703.024 N). This suggests that the multi-axis foot may provide better energy absorption and distribution during gait, which could enhance user comfort and stability.

3. Pressure Measurements:

The pressure distribution obtained from the indicative figures for various types of foot showed a difference in terms of load for the left prosthetic foot and the healthy foot on right. Analyzing this aspect is important to evaluate how well prosthetic designs mimic normal motion.

4. Comparative Analysis:

The similarities and differences between the force exert by prosthetic foot versus the healthy foot are presented in table (5-4). The lift force provided by the multi-axis foot was the highest (585.85 N) among the three types of foot, suggesting that this type of foot might provide better performance than the other types.

5. Gait Characteristics:

The foot types in gait analysis tables (5-2 and 5-3) have differing values of cadence, gait time, distance, and velocity. Compared to the SACH foot, the single-axis foot had a higher cadence and velocity which indicating a better performance in dynamic condition.

6. Stance and Step Dynamics:

Overall stance, swing and heel contact times reported in table (5-5) of the gait cycle were consistent with previous works with small differences found across conditions. The stance and step dynamics outlined in the gait cycle slight variations in stance time and heel contact time among the foot types, with the multi-axis foot performing more closely to natural gait patterns.

These results indicate that the multi-axis foot significantly improves performance characteristics, which may lead to improved mobility and quality of life for users.

5.3. F-Socket results

The understanding Interaction with Socket is important for optimizing socket design to minimize pressure points and enhance overall user comfort.

The F-socket test was conducted to ascertain the maximum concentrated pressure on the socket. During the test, sensors were placed in four locations: front, behind, left, and right. The highest pressure was observed on the left side of the socket. The test results were recorded while the patient was walking on the floor. Figures (5-10), (5-11), and (5-12) showed the results of the pressure distribution on the socket for SACH foot, single-axis foot, and multi-axis foot, respectively.

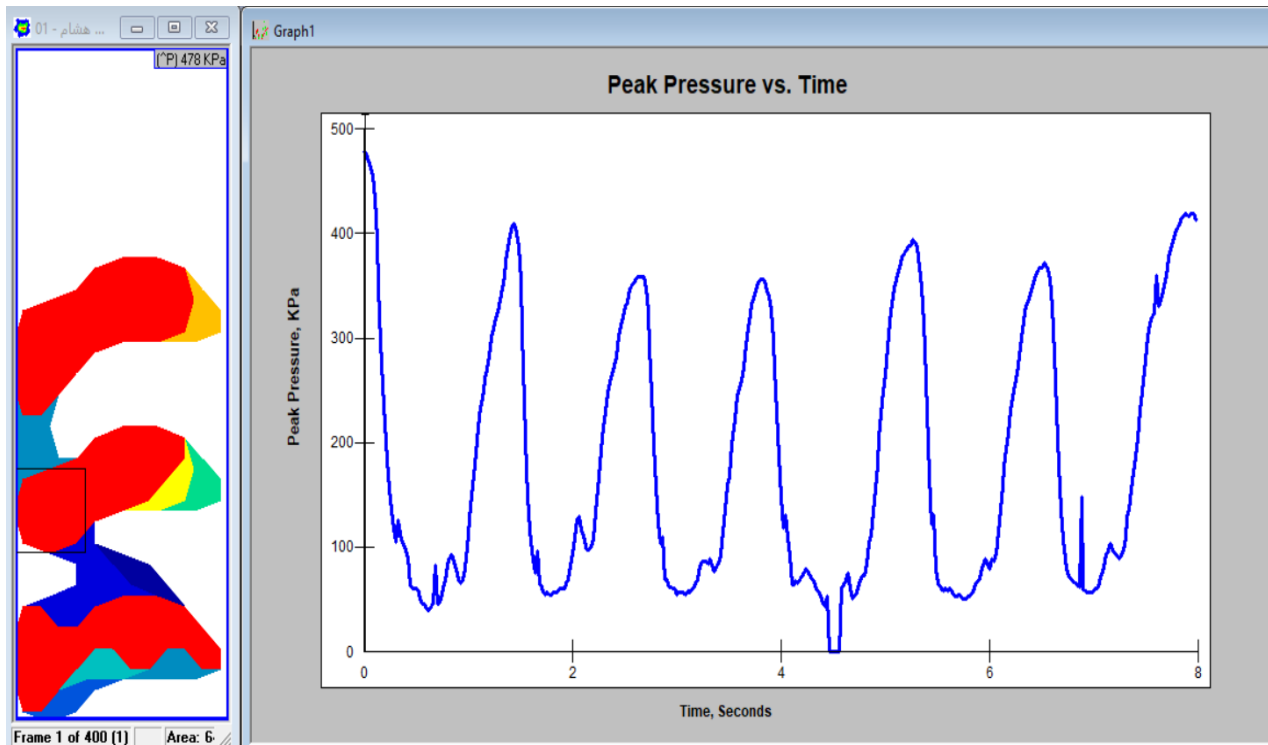


Figure (5-10) pressure distribution with time on the socket for SACH foot.

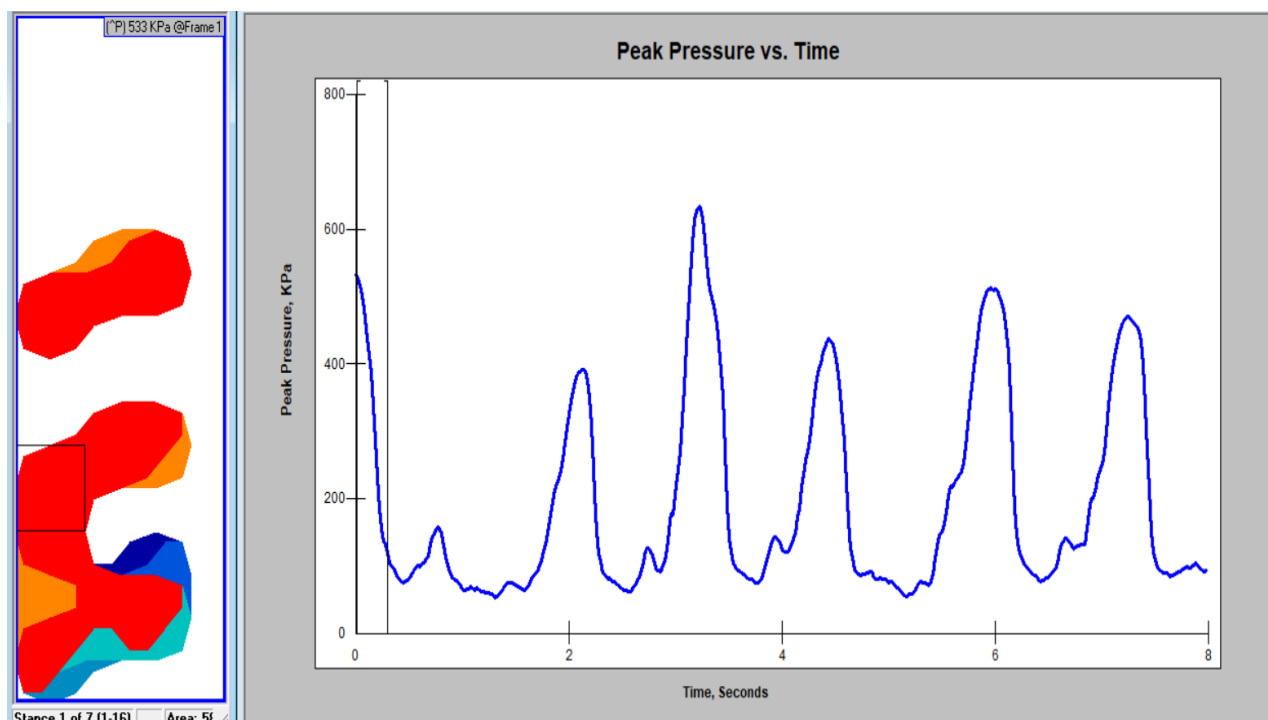


Figure (5-11) pressure distribution with time on the socket for single axis foot

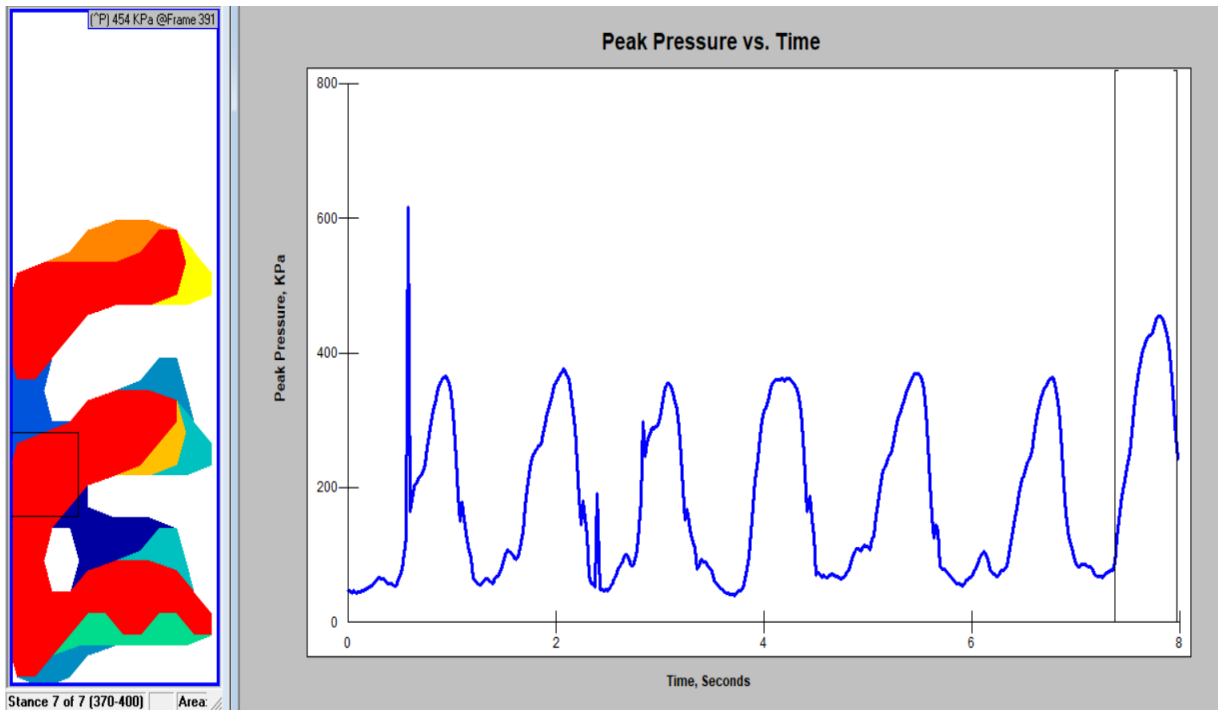


Figure (5-12) pressure distribution with time on the socket for multi axis foot.

The pressure distribution over time based on the data provided in Figures above showed the following:

- **SACH Foot (Figure 5-10):**

The pressure distribution for the SACH foot typically shows a stable pattern, with consistent pressure levels during the gait cycle and lower peak pressures compared to others, indicating that it distributes loads more evenly throughout the walking cycle. However, the lack of adaptability in dynamic situations might limit its effectiveness, especially on uneven surfaces.

- **Single-Axis Foot (Figure 5-11):**

The single-axis foot generally displays higher peak pressures, particularly during specific phases of the gait cycle, such as heel strike and toe-off. This indicates that the foot concentrates forces in certain areas, which can lead to discomfort over time.

The pressure may fluctuate significantly as it reacts to the movement, suggesting that while it provides a natural gait, the concentrated pressures can increase the risk of skin irritation or discomfort.

- Multi-Axis Foot (Figure 5-12):

The multi-axis foot demonstrates a more adaptive pressure distribution pattern. It shows variable pressures that adjust based on the user's movement and the surface being walked on. This adaptability results in better shock absorption, leading to a more comfortable experience for the user. The pressure distribution peaks at different times compared to the other foot types, reflecting its ability to manage dynamic loads effectively.

Additionally, the pressure versus percentage data curves are presented in separate figures (5-13), (5-14), and (5-15) for each type of prosthetic foot which obtained from the device. The peak pressure recorded for the SACH foot was 33 psi (227.53 kPa); for the single-axis foot, it was 40 psi (275.79 kPa); and for the multi-axis foot, it was 35 psi (241.3 kPa).

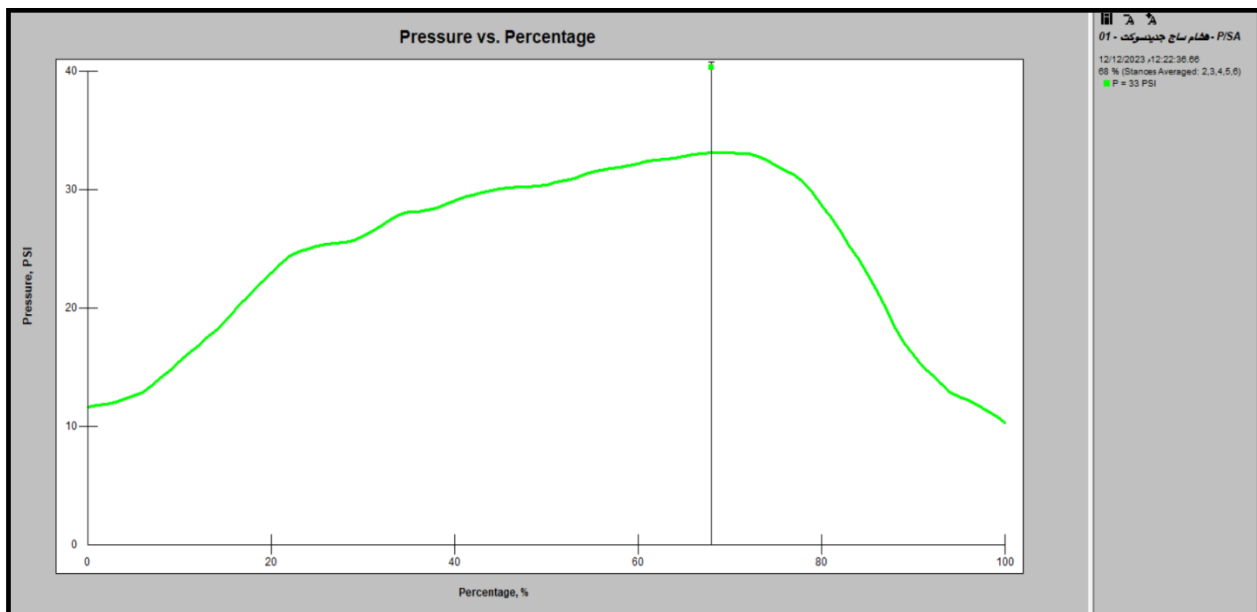


Figure (5-13) the pressure vs. percentage for SACH foot

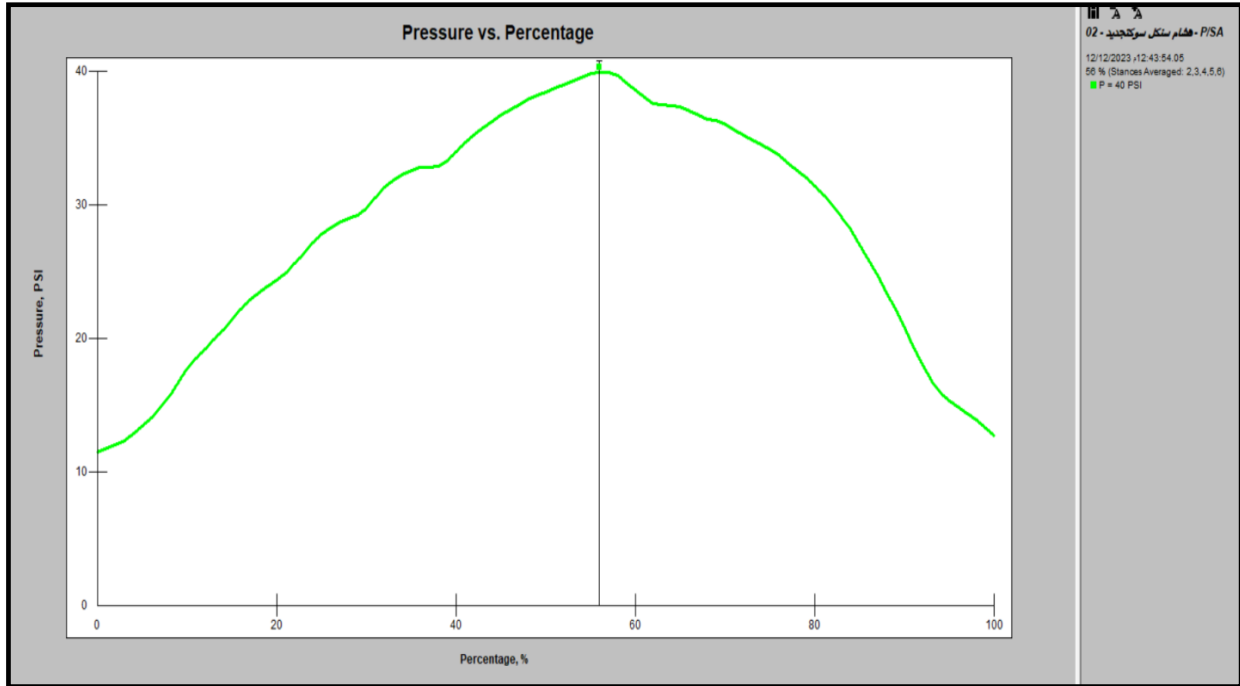


Figure (5-14) the pressure vs. percentage for single axis foot

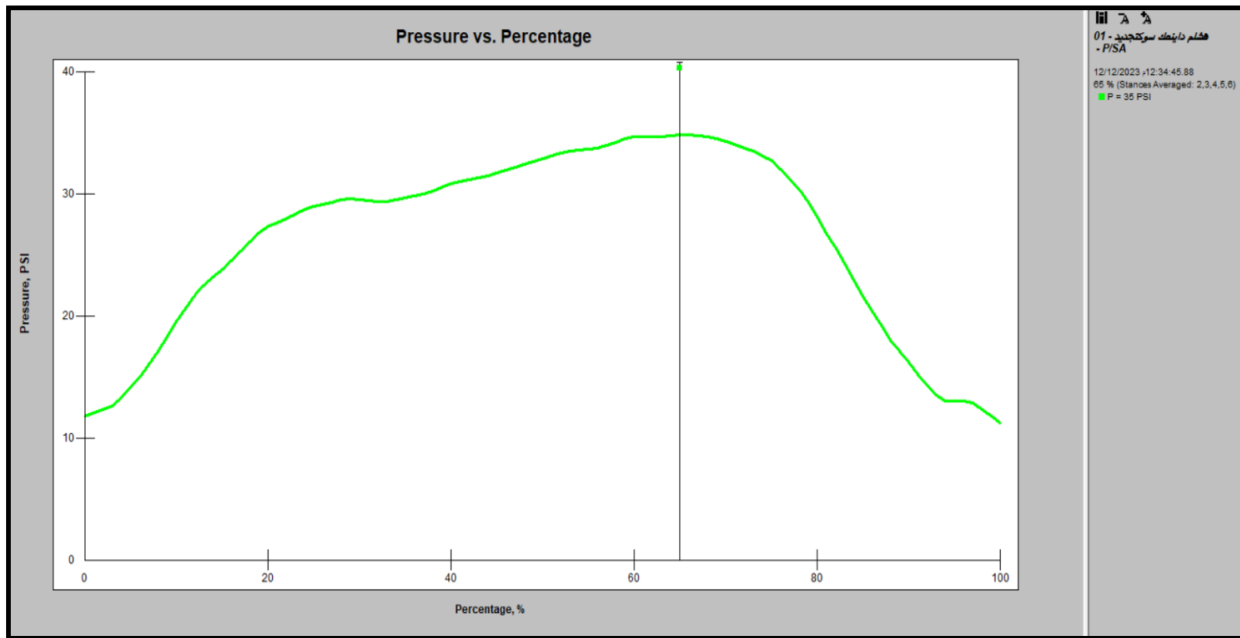


Figure (5-15) the pressure vs. percentage for multi axis foot.

The peak pressure recorded comparison for the three types of prosthetic feet showed the following: SACH foot pressure distribution shows moderate loading,

which may translate to decent comfort. While single-axis foot exhibited the highest peak pressure, indicating potential for discomfort and increased risk for skin issues. On other hand multi-axis foot showed slightly better pressure distribution than the single-axis foot, providing a balance between performance and comfort.

Generally, SACH foot offers stability; however, it lacks adaptive characteristics, which may limit its performance in varied terrains. While single-axis foot provides a more natural gait than the SACH foot but tends to concentrate loads more, as evidenced by the highest peak pressure. Another type is the multi-axis foot, with a design that allows it to conform to different surfaces, leading to improved shock absorption and load distribution, which can either make the user more comfortable while walking or improve overall experience.

Although none of the three types is superior in pressure distribution, dynamic performance, and user comfort, the foot that performed best was the multi-axis foot, making it the most favorable option out of the three. The design-engineered running shoes can potentially adapt better to various surfaces -- a must for the active life.

5.4. EMG Activity of the lower limb Muscles results

This involves the data of the muscle activity through the Electromyography (EMG) test performed on the lower limb muscles (rectus femoris) while using SACH, single-axis and multi-axis prosthetic feet.

The outcome showed no significant difference in muscle activity between the three types of prosthetic feet. This indicates that muscle activation patterns of the rectus femoris were similar regardless of the foot type. This finding is especially interesting because it suggests that the type of prosthetic foot may not

have a substantial impact on muscle performance when walking, at least not with regard to the rectus femoris activity.

The body tends to recruit muscle fibers (The myofibril) in a consistent manner during specific movements, such as walking. The rectus femoris, a key muscle in the quadriceps group, plays a critical role in knee extension and hip flexion. Regardless of the type of prosthetic foot, the underlying biomechanical demands of walking—such as maintaining balance, producing forward motion, and stabilizing the pelvis—remain similar, leading to consistent muscle activation patterns.

Lastly, the reason we did not see large differences in muscle activity in our limb analysis on our various prosthetic feet was likely due to the similar recruitment patterns of muscle as well as gait mechanics and compensatory movement patterns, as well as the functional design of prosthetics, and user adaptation. These factors indicate that the selection of one prosthetic that does not differ significantly from another may not be the main influencing factor of activity in the rectus femoris during gait.

Fatigue and muscle pattern reports for the three types of prosthetics feet are illustrated in Figures (5-16), and (5-17) respectively.

These numbers probably represent how the muscle worked over time and whether any fatigue might progress during longer use of each prosthetic foot. Muscle engagement appears to be similar, regardless of foot type.

Further information regarding for the power spectrum reports shown in Figures (5-18), and (appendix B) for the three types of prosthetic feet provide further insights into the frequency components of the EMG signals. Analyzing this

data can help identify the efficiency and effectiveness of muscle recruitment during walking. The consistency across different foot types could indicate that the muscle's response to load and movement is stable, regardless of the prosthetic design.

Figures (5-19), and (appendix B) the images display present the standard EMG analysis report for the three types of prosthetics feet , which likely summarizes the overall muscle activity metrics. This comprehensive overview reinforces the conclusion that the type of prosthetic foot does not significantly influence the muscle activity of the rectus femoris.

These findings have important implications for the design and selection of prosthetic feet. If muscle activity remains consistent across various foot types, clinicians and patients may focus on other factors, such as comfort, stability, and functional performance, when selecting a prosthetic foot.

In summary, the EMG analysis reveals that muscle activity in the lower limb, particularly in the rectus femoris, is not significantly affected by the type of prosthetic foot used. This consistency may provide a basis for further studies into other aspects of prosthetic design and patient outcomes, emphasizing the need to consider a holistic approach to rehabilitation and prosthetic fitting.

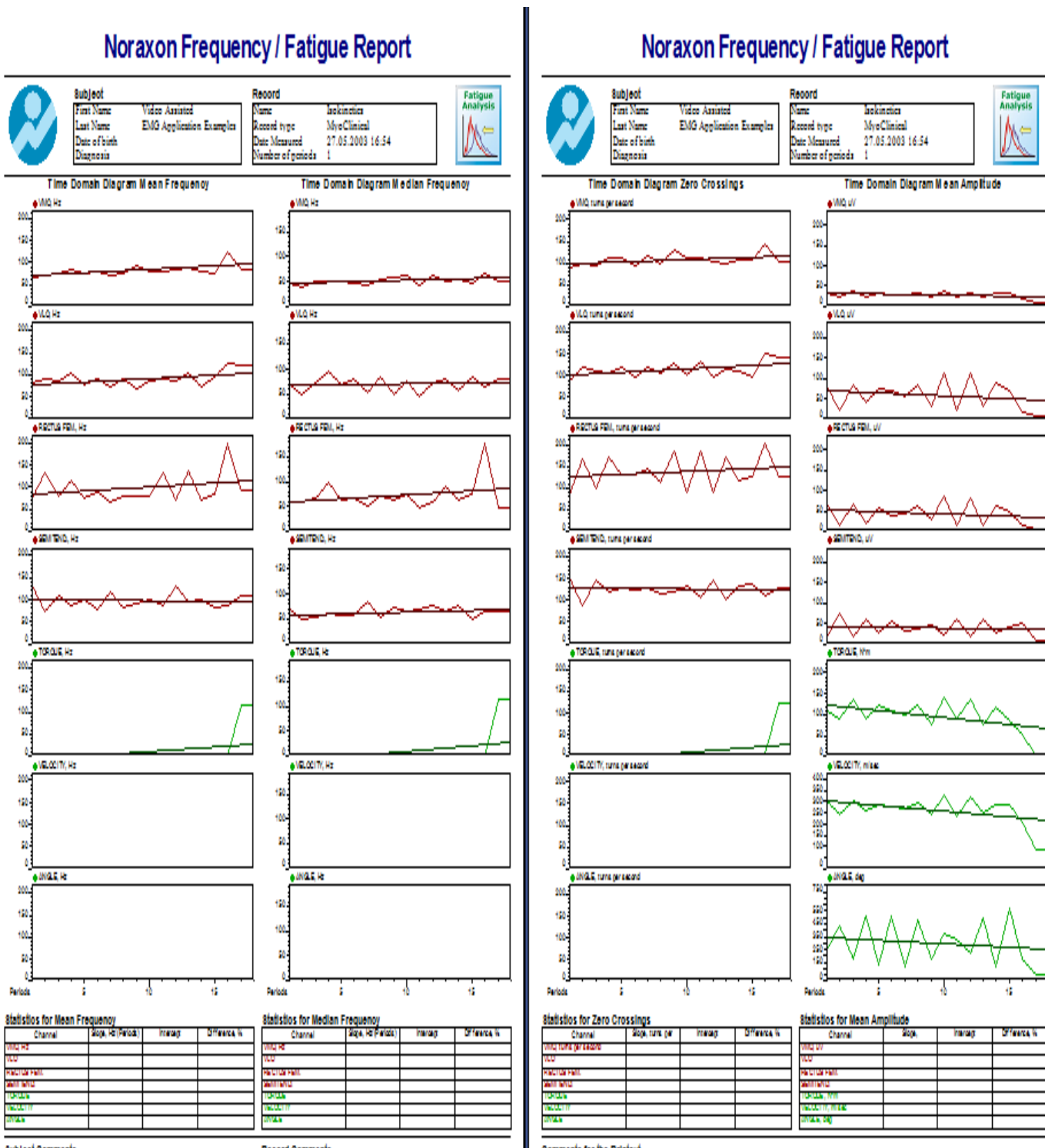


Figure (5-16) the fatigue report for Noraxon EMG test for SACH foot.

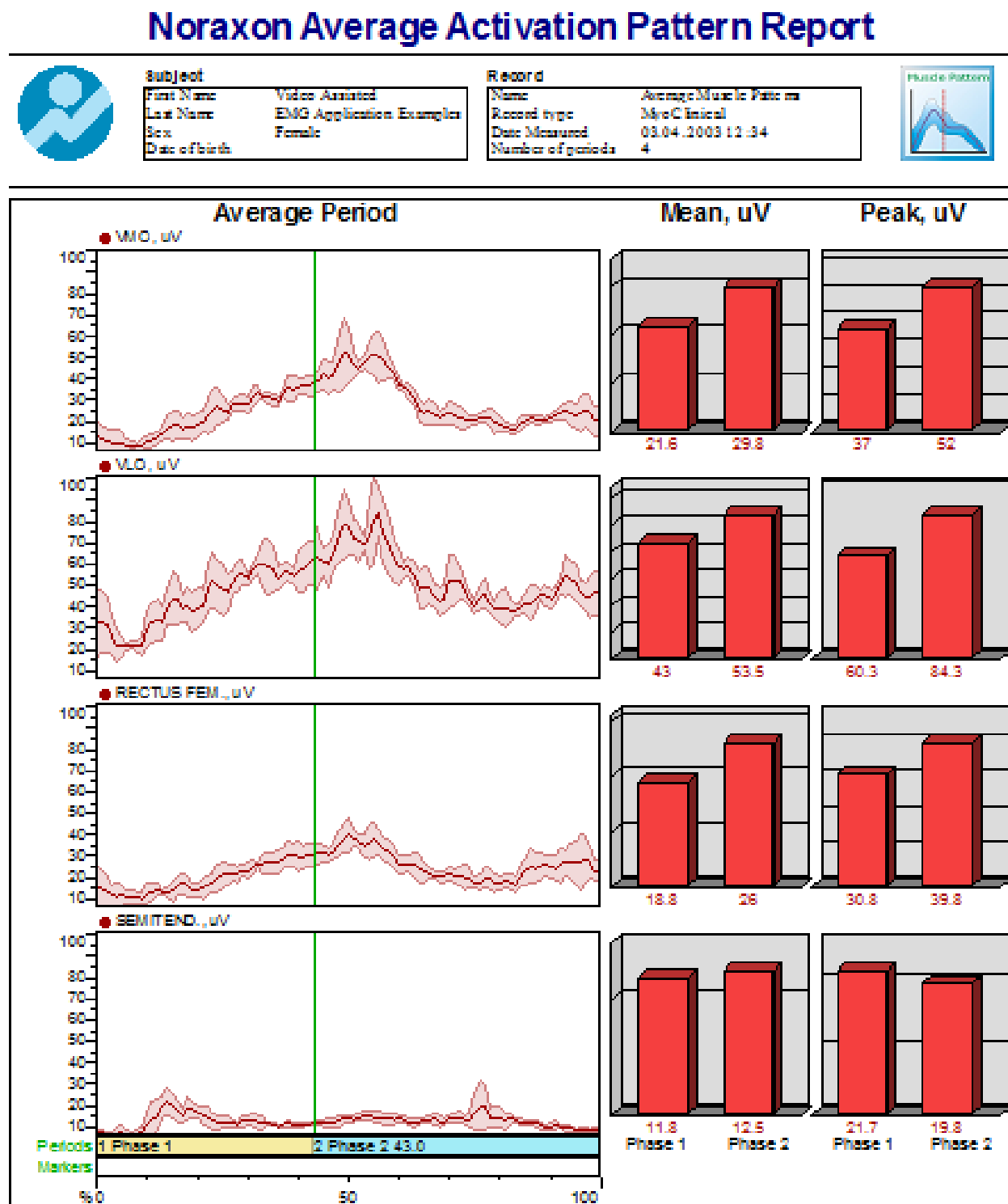


Figure (5-17) the muscle pattern report for the Noraxon EMG test for SACH foot.

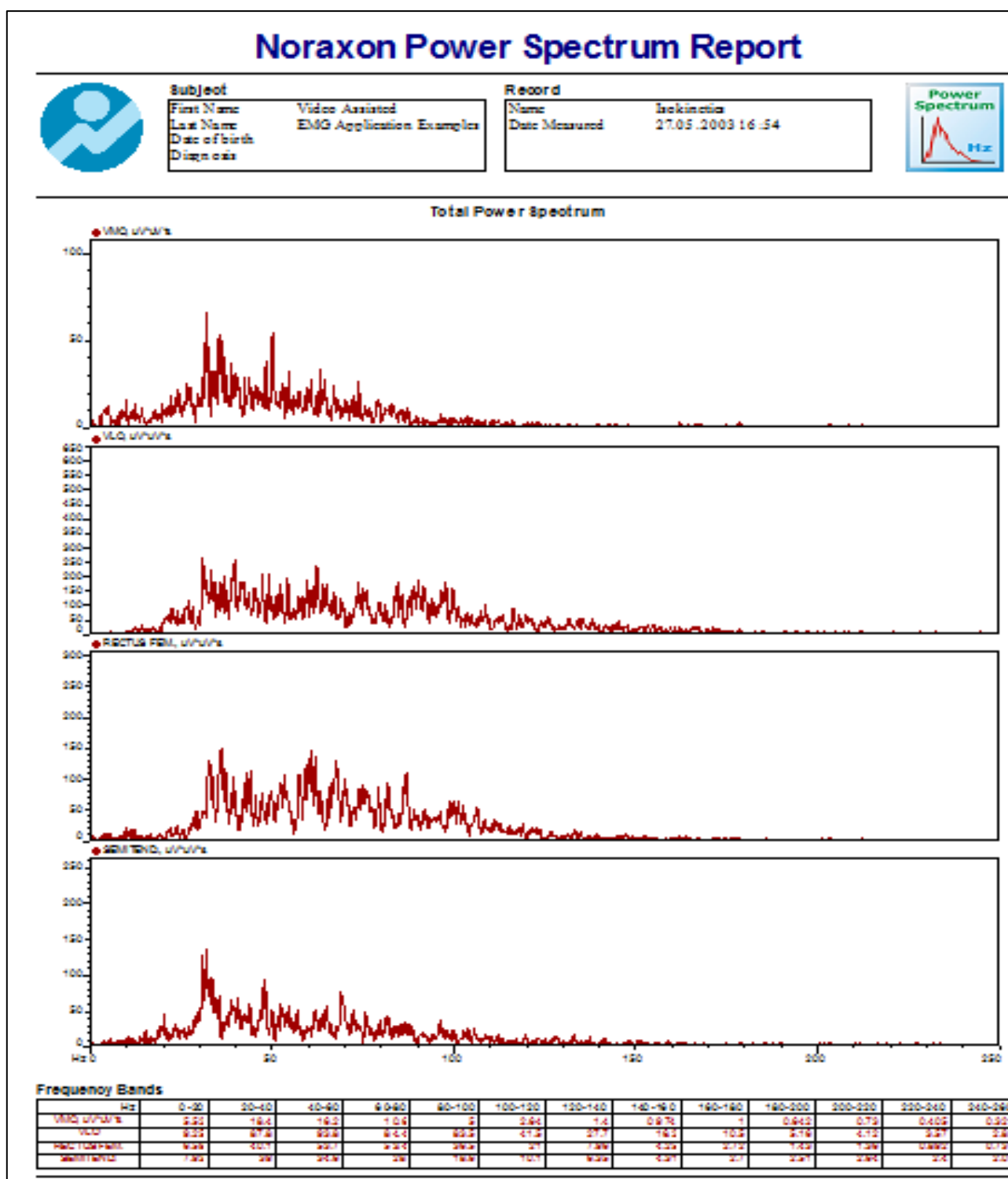


Figure (5-18) the power spectrum report for Noraxon EMG test for SACH foot.

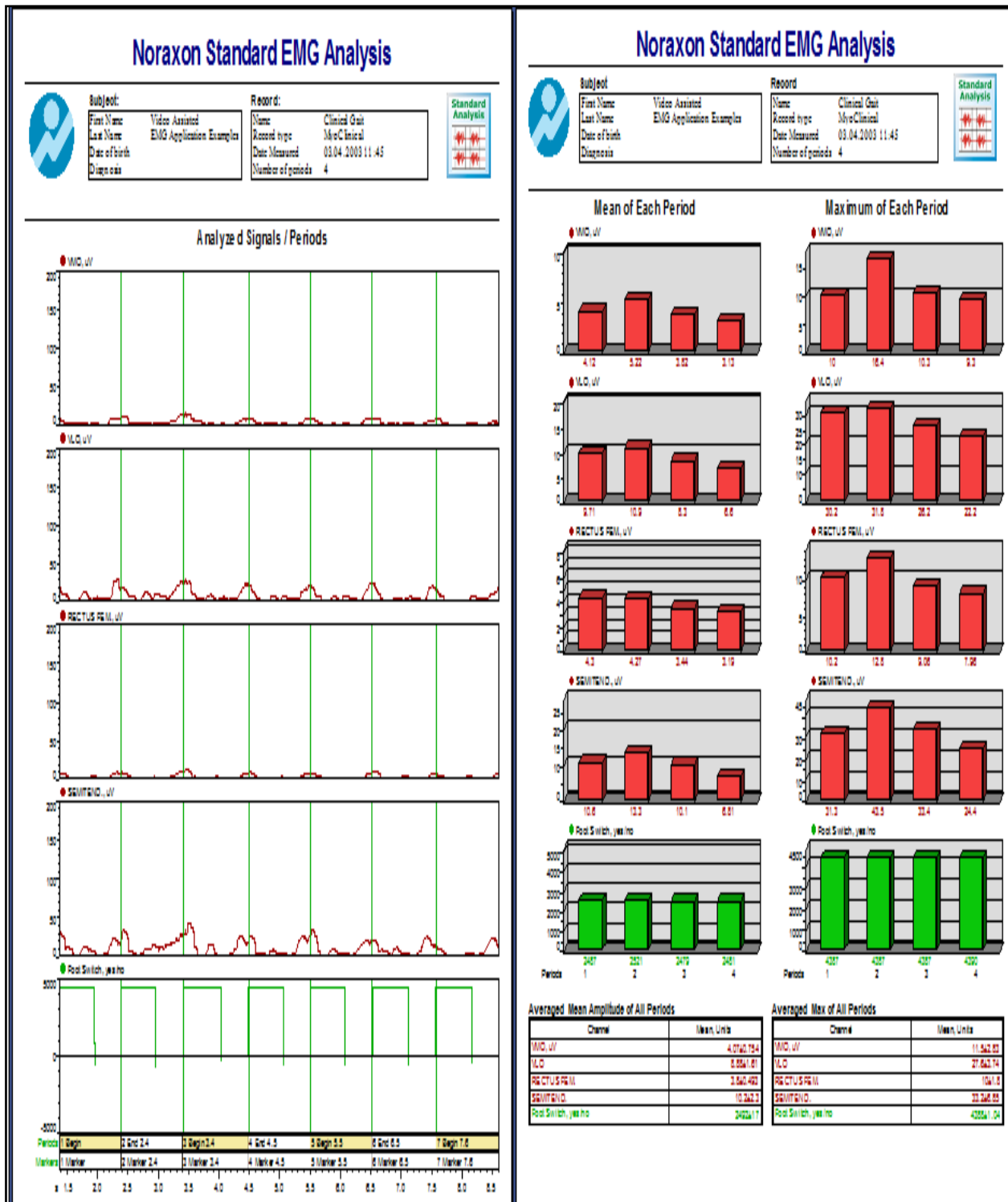


Figure (5-19) show the standard EMG analysis report for the test for SACH foot.

5.5. Acceleration results

The results of acceleration were measured at two sites (knee and hip) using the patient's accelerometer sensor while the patient walked in a bounded circular path, wearing the SACH, single-axis, and multi-axis prosthetic limbs. Each joint was tested three times during the gait cycle with different types of prosthetic feet. The sensor was fixed on the patient's body, and the readings were recorded for each type of foot. The patient walked in a specific circular area for 60 seconds, and the Vernier acceleration sensor device was used to measure acceleration, as shown in Figure (5-20).

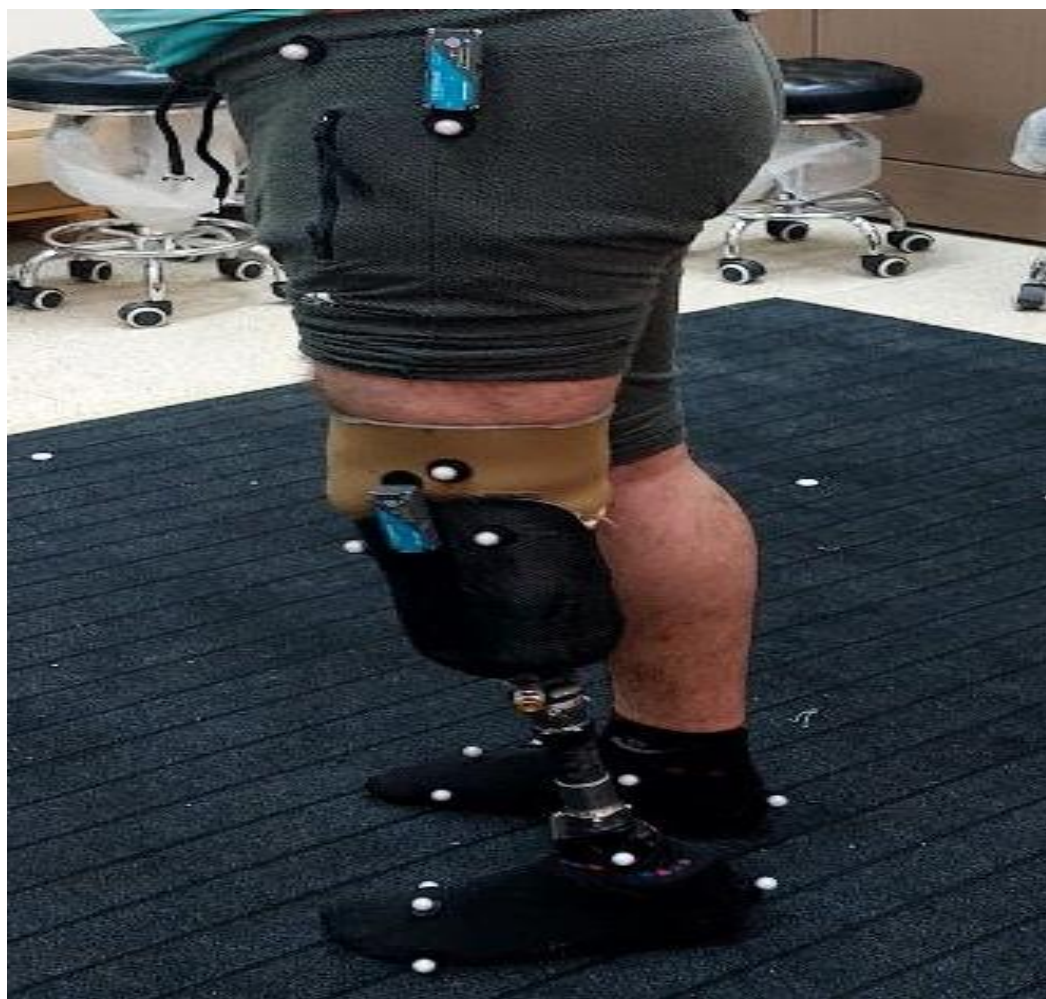


Figure (5-20) show the vernier acceleration sensor on the patient.

The acceleration results for the SACH foot at two locations—the knee and the hip—are shown in Figures (5-21), (5-22), and (5-23) for the X, Y, and Z directions.

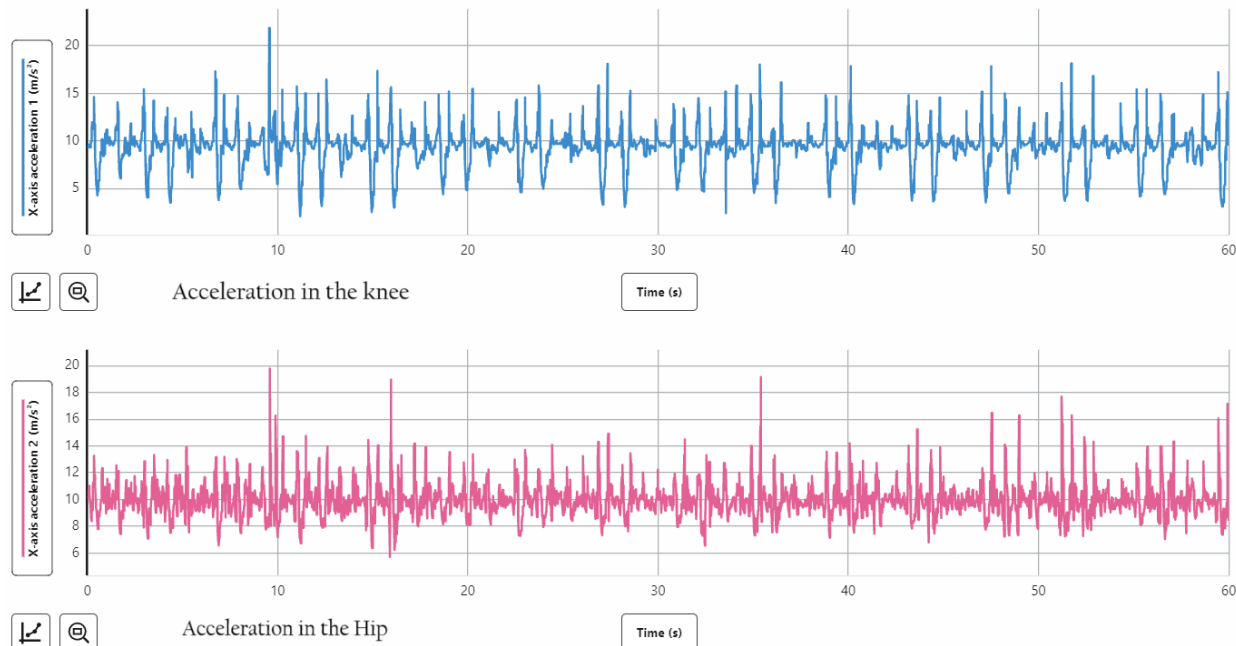


Figure (5-21) acceleration-time for the knee and Hip in X-Direction in SACH foot.

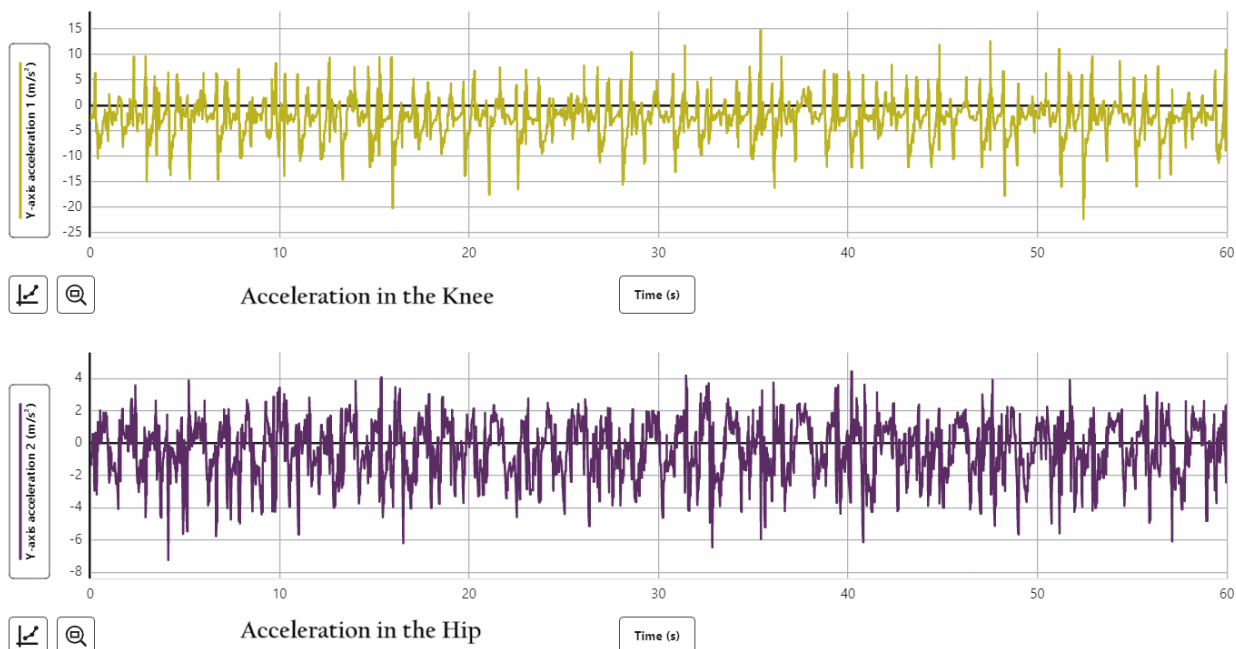


Figure (5-22) acceleration-time for the knee and Hip in Y-Direction in SACH foot.

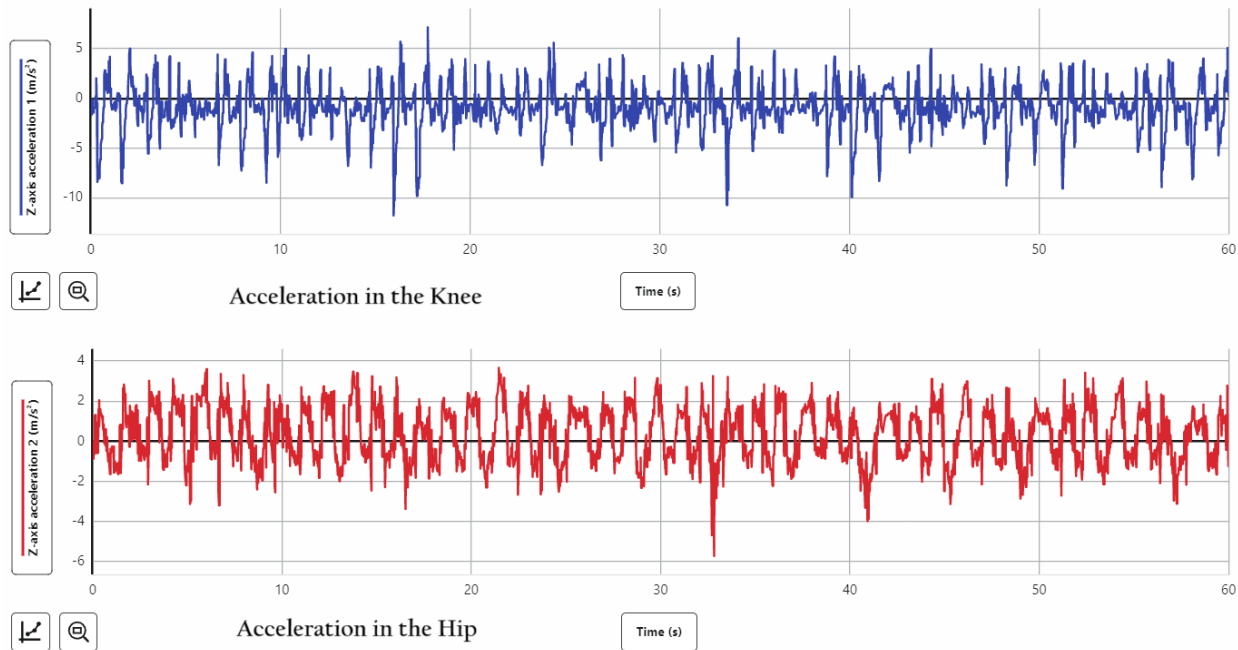


Figure (5-23) acceleration-time for the knee and Hip in Z-Direction in SACH foot.

The acceleration results for the single-axis foot at both locations—the knee and the hip—are shown in Figures (5-24), (5-25), and (5-26) for the X, Y, and Z directions.

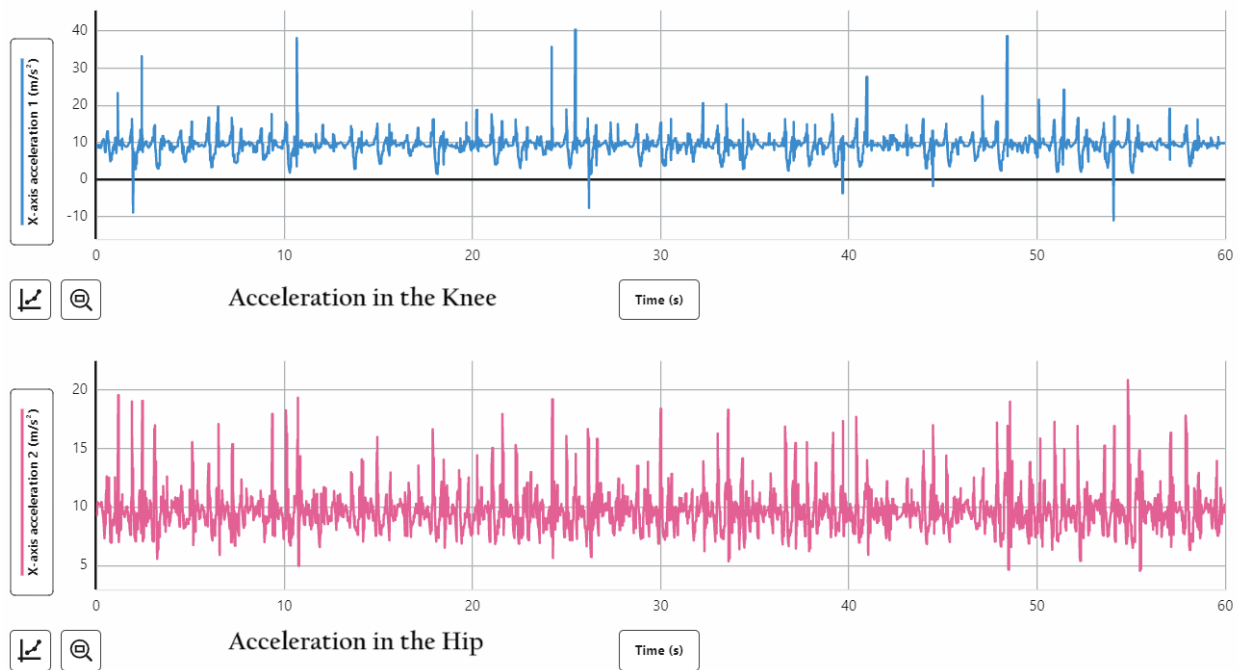


Figure (5-24) acceleration-time for the knee and Hip in X-Direction in Single axis foot.

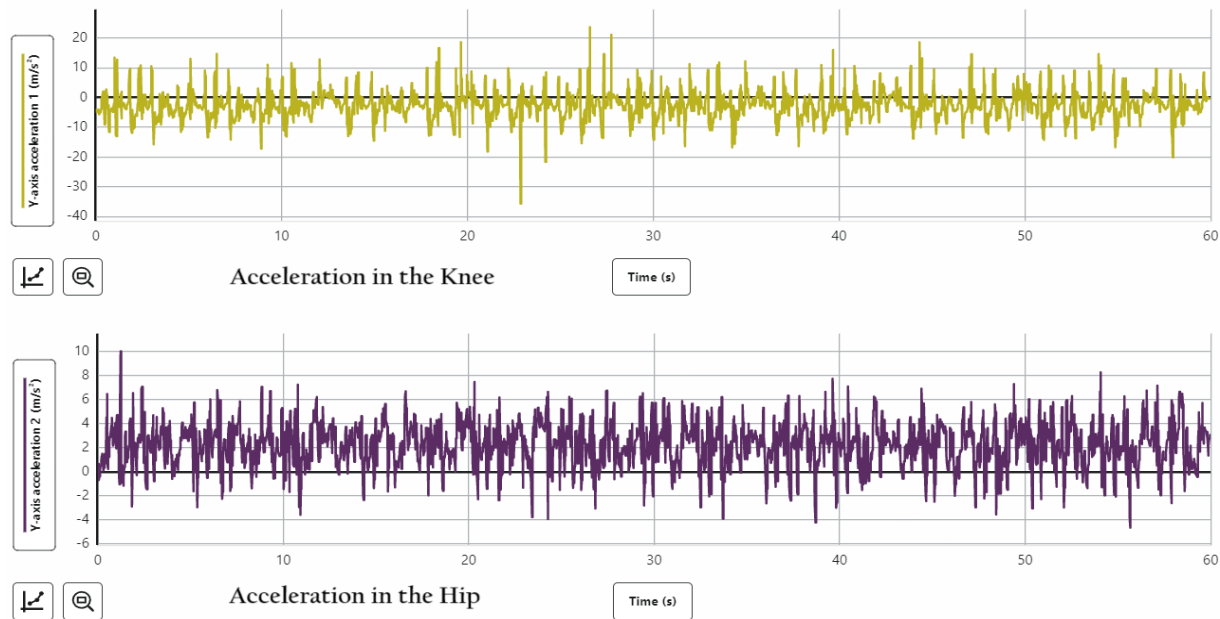


Figure (5-25) acceleration-time for the knee and Hip in Y-Direction in Single axis foot.

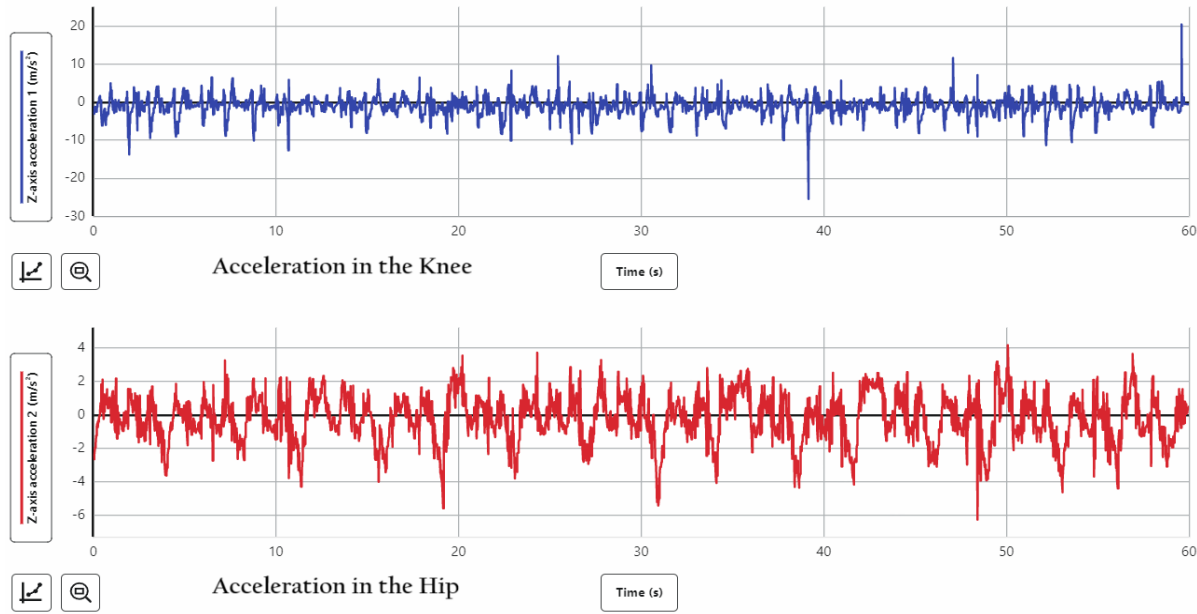


Figure (5-26) acceleration-time for the knee and Hip in Z-Direction in Single axis foot.

The results for the multi-axis foot regarding acceleration at two locations the knee and the hip as shown in Figures (5-27), (5-28), and (5-29) for the X, Y, and Z directions.

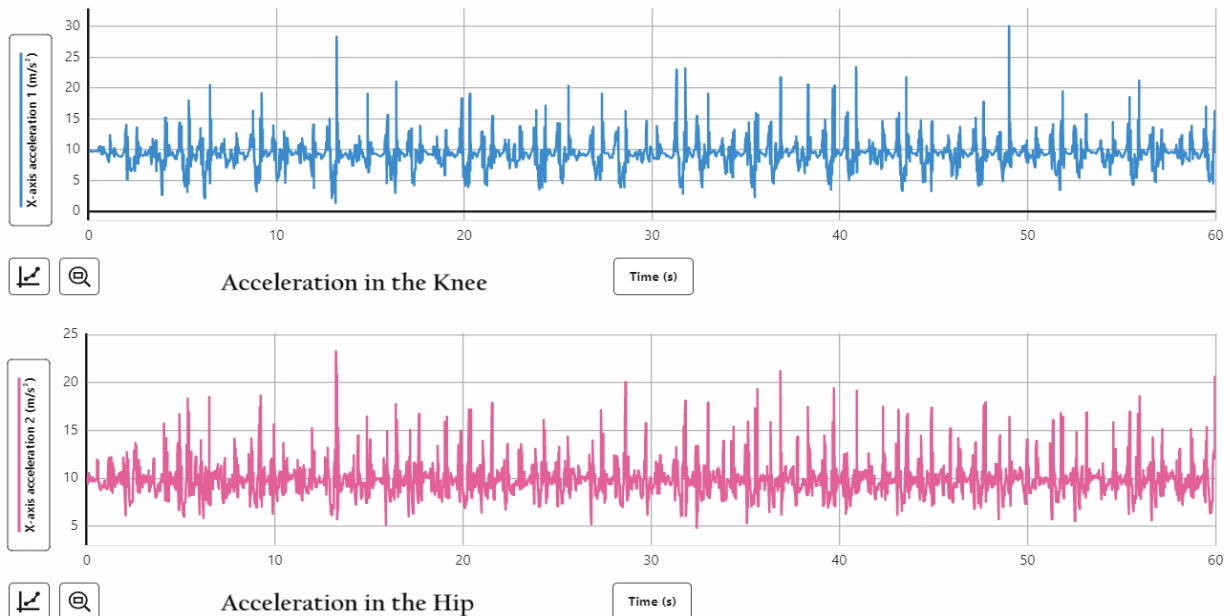


Figure (5-27) acceleration-time for the knee and Hip in X-Direction in multi- axis foot.

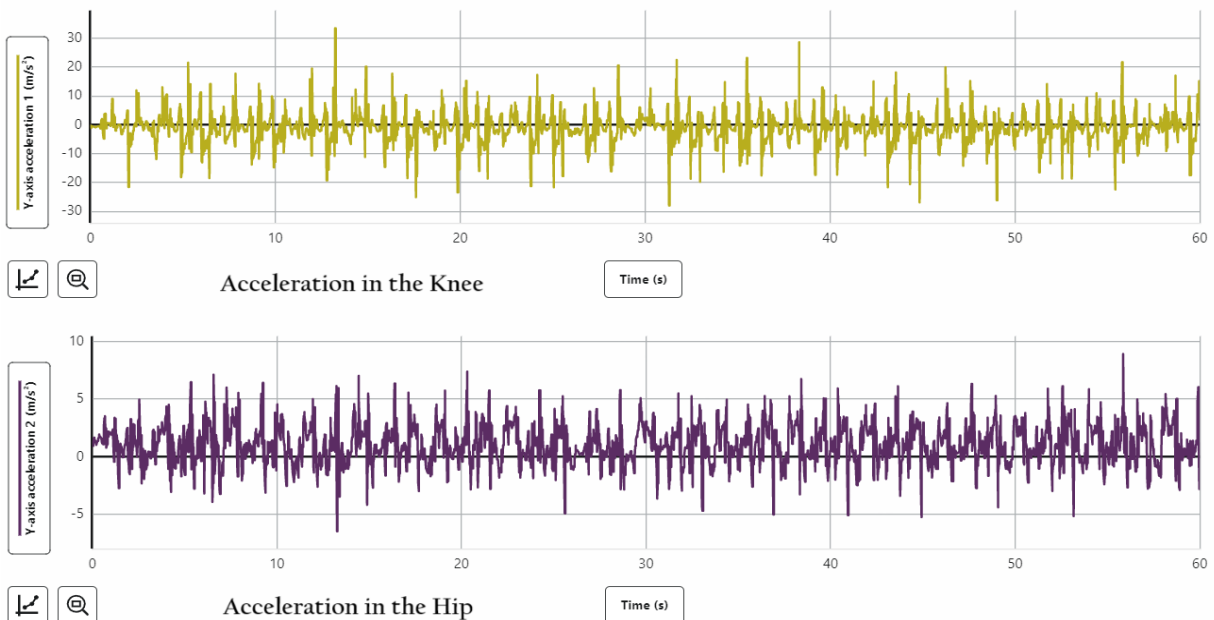


Figure (5-28) acceleration-time for the knee and Hip in Y-Direction in multi- axis foot.

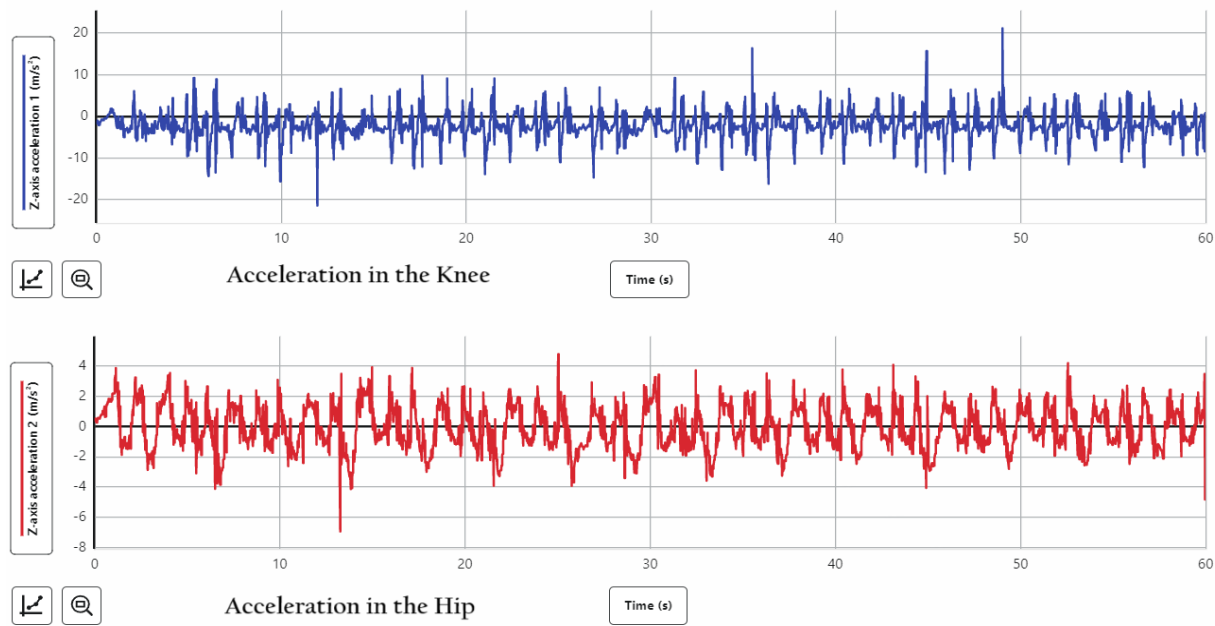


Figure (5-29) acceleration-time for the knee and Hip in Z-Direction in multi- axis foot.

When the sensor is placed on the knee or hip of the patient, the results indicate that increasing the height of the sensor site above the floor leads to a decrease in the recorded acceleration while the patient is walking. This implies that there is a negative correlation between the height of the sensor above the floor and the acceleration data when the sensor is attached to the knee or hip. This relationship may be influenced by factors such as changes in the patient's movement dynamics, alterations in the distribution of forces as the sensor is elevated, or variations in gravitational effects on the sensor at different heights. Other factors, such as muscle, skin, and fat, also contribute to the reduction in acceleration.

The maximum and minimum values of acceleration at the hip and knee for the three types of feet are presented in Table (5-5) below, along with the mean value of acceleration.

Table (5-5) the acceleration value in three types of feet.

Type of foot		Knee acceleration(m/s ²)			Hip acceleration(m/s ²)		
		X	Y	Z	X	Y	Z
SACH foot	max	21.874	40.391	7.158	19.777	4.434	3.664
	Min	2.074	-10.979	-11.785	5.709	-7.241	-5.721
	mean	9.33	9.265	-0.901	9.987	-0.394	0.320
Single foot	max	40.391	23.715	20.474	20.816	8.269	4.181
	Min	-10.979	-35.67	-25.423	4.550	-4.564	-6.267
	mean	9.264	-2.462	-0.972	9.706	2.276	-0.183
Multi foot	max	30.082	33.512	16.351	23.301	8.920	4.789
	Min	1.342	-27.98	-16.186	4.833	-6.465	-6.952
	mean	9.353	-1.033	-2.103	9.928	1.105	-0.046

5.6. Vibration results

The acceleration values were measured at the patient's prosthetic foot for both the knee and hip joints for the three types of feet during the gait cycle. The Vernier Graphical Analysis program was used to convert the acceleration values into vibration values using Fast Fourier Transform (FFT). The results shown in Figures (5-30), (5-31), and (5-32) represent the frequency values for the SACH foot in the X, Y and Z-directions respectively.

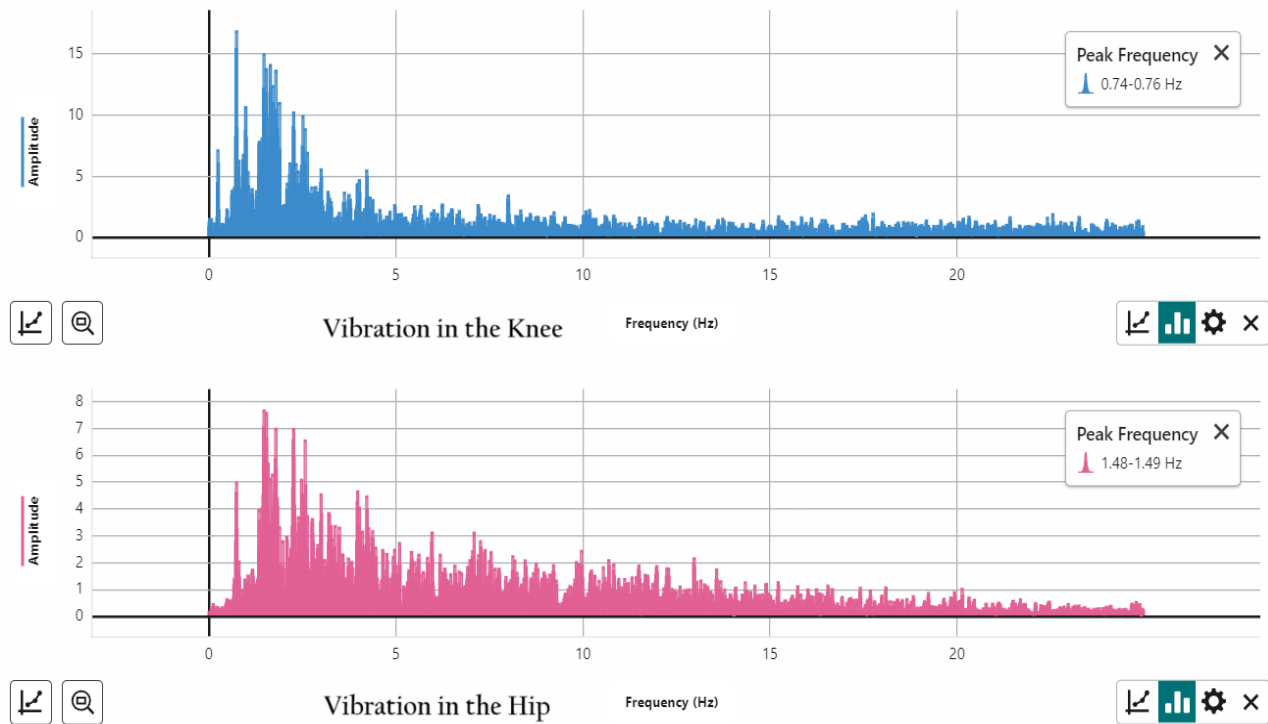


Figure (5-30) vibration at the knee and Hip in X-Direction for SACH foot.

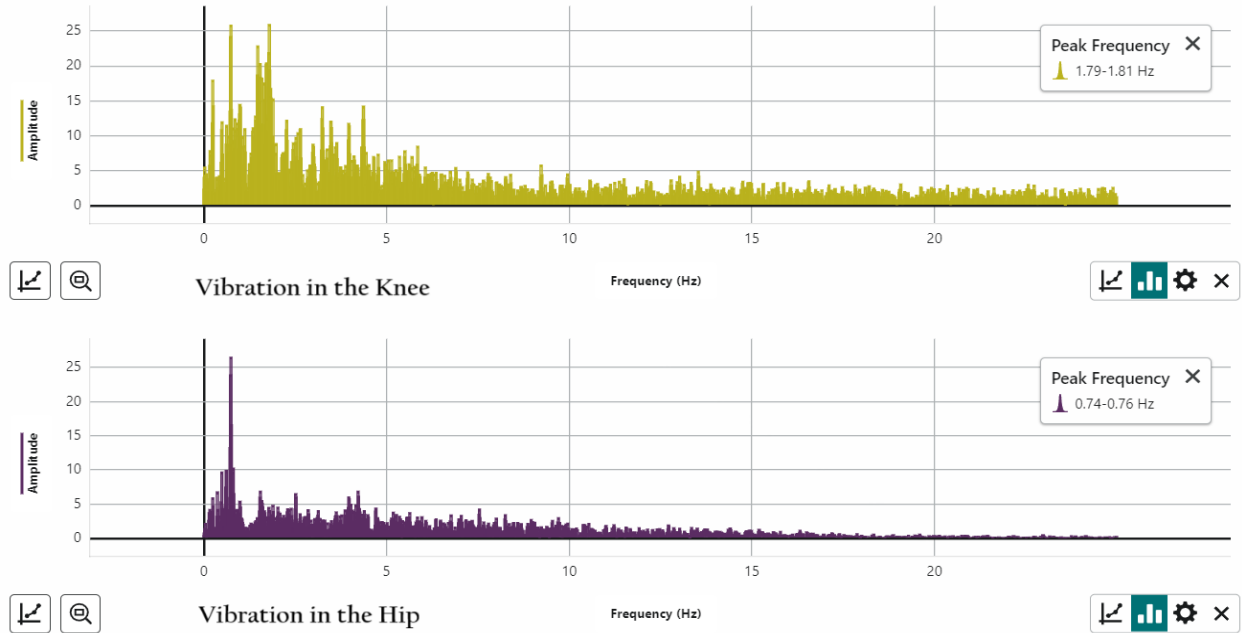


Figure (5-31) vibration at the knee and Hip in Y-Direction for SACH foot.

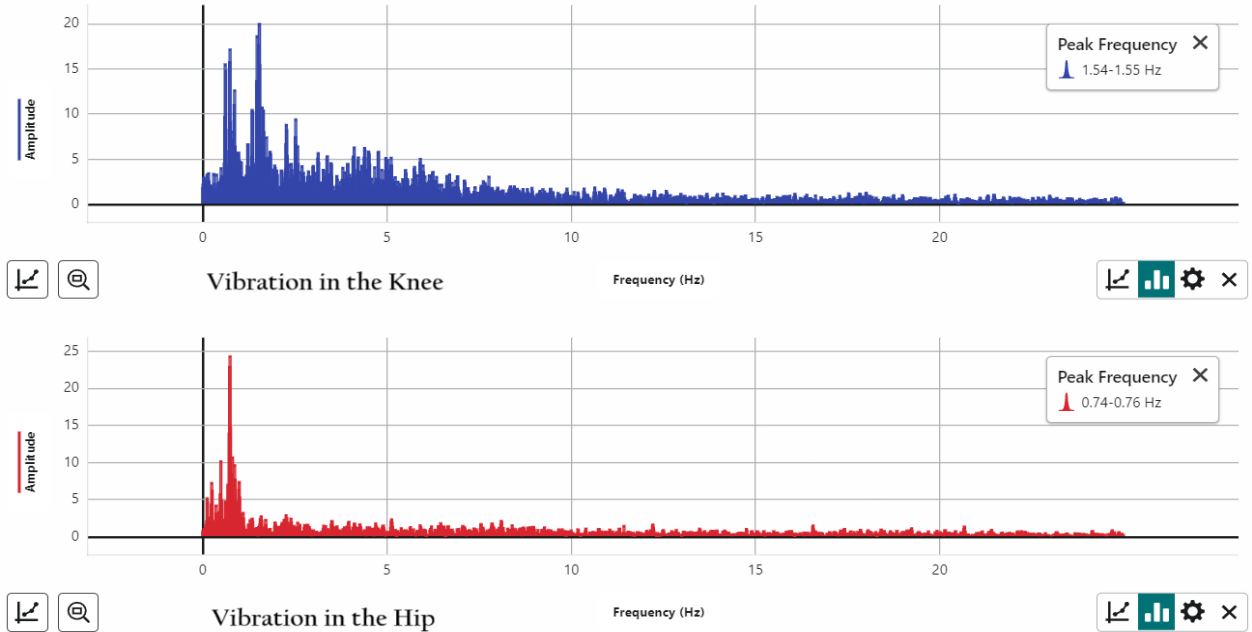


Figure (5-32) vibration at the knee and Hip in Z-Direction for SACH foot.

The results shown in Figures (5-33), (5-34), and (5-35) represent the frequency values for the Single axis foot in the X, Y and Z-directions respectively.

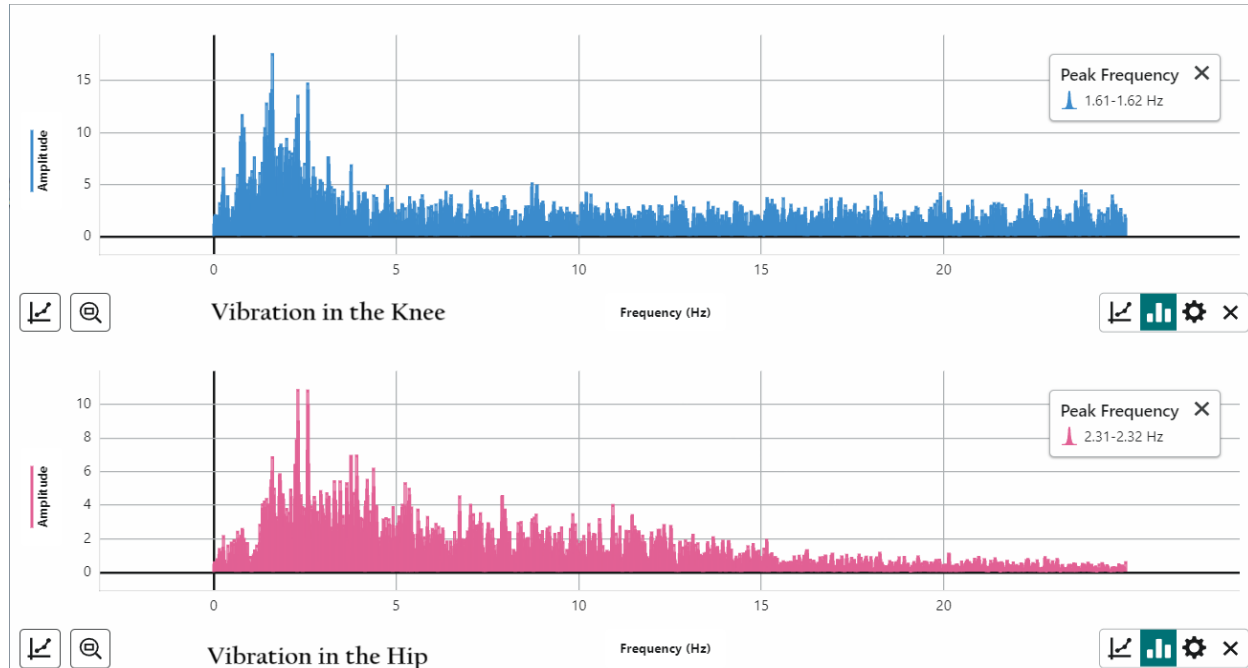


Figure (5-33) vibration at the knee and Hip in X-Direction for single-axis foot.

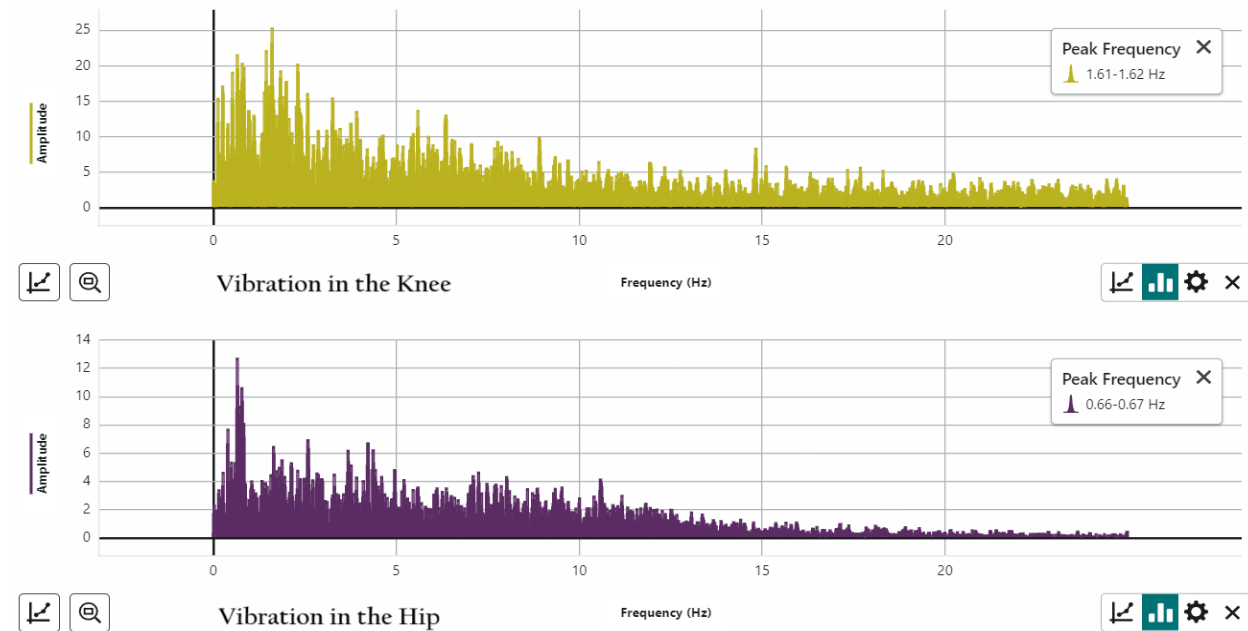


Figure (5-34) vibration at the knee and Hip in Y-Direction for single-axis foot.

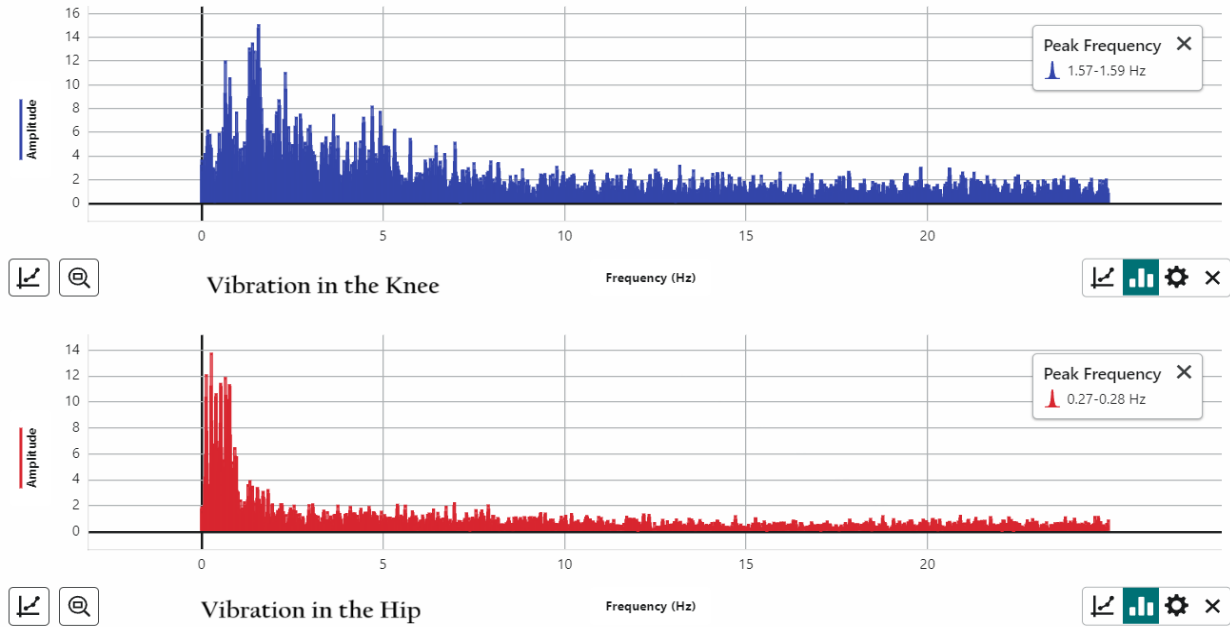


Figure (5-35) vibration at the knee and Hip in Z-Direction for single-axis foot.

The results shown in Figures (5-36), (5-37), and (5-38) represent the frequency values for the Multi axis foot in the X, Y and Z-directions respectively.

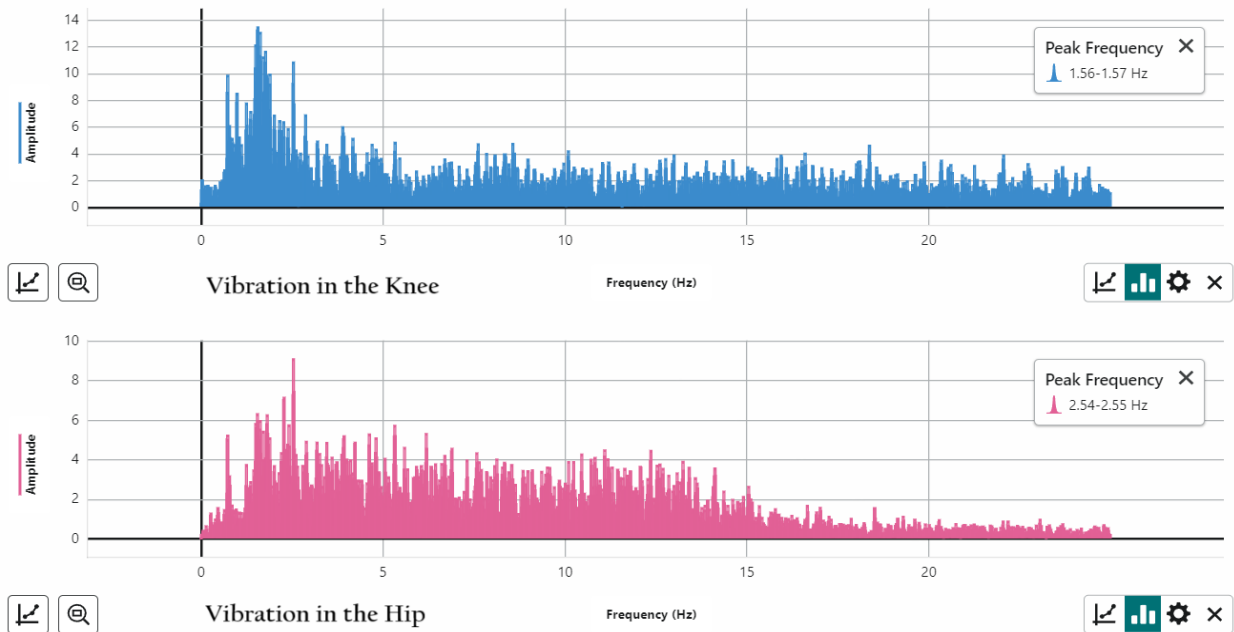


Figure (5-36) vibration at the knee and Hip in X-Direction for multi-axis foot.

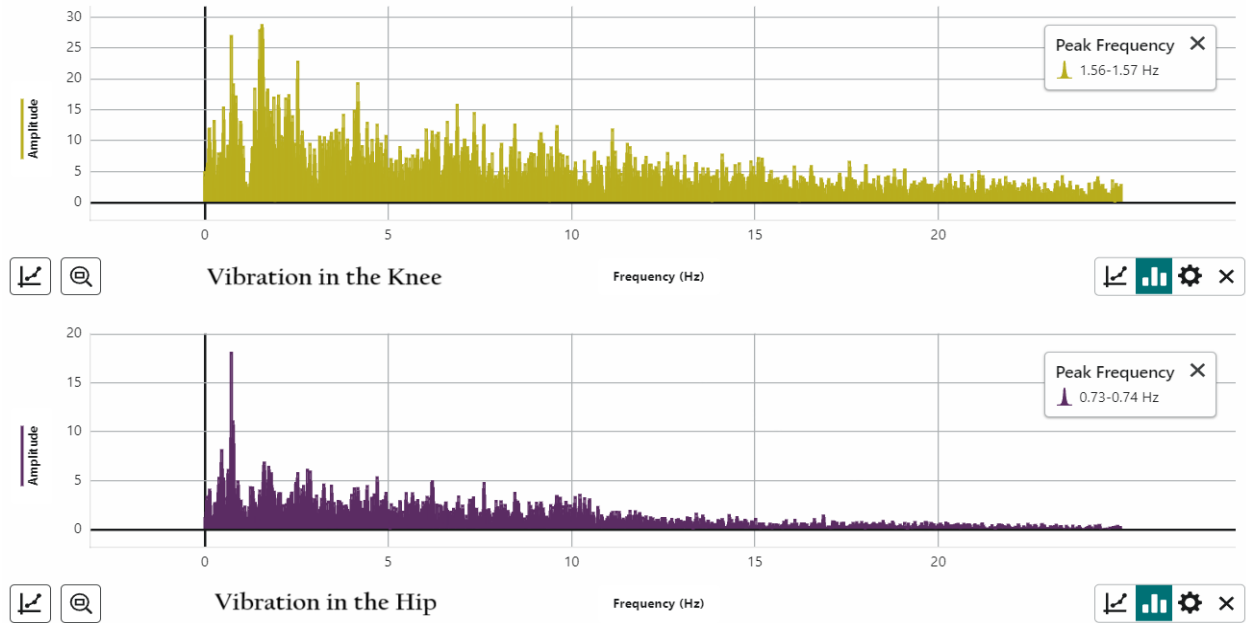


Figure (5-37) vibration at the knee and Hip in Y-Direction for multi-axis foot.

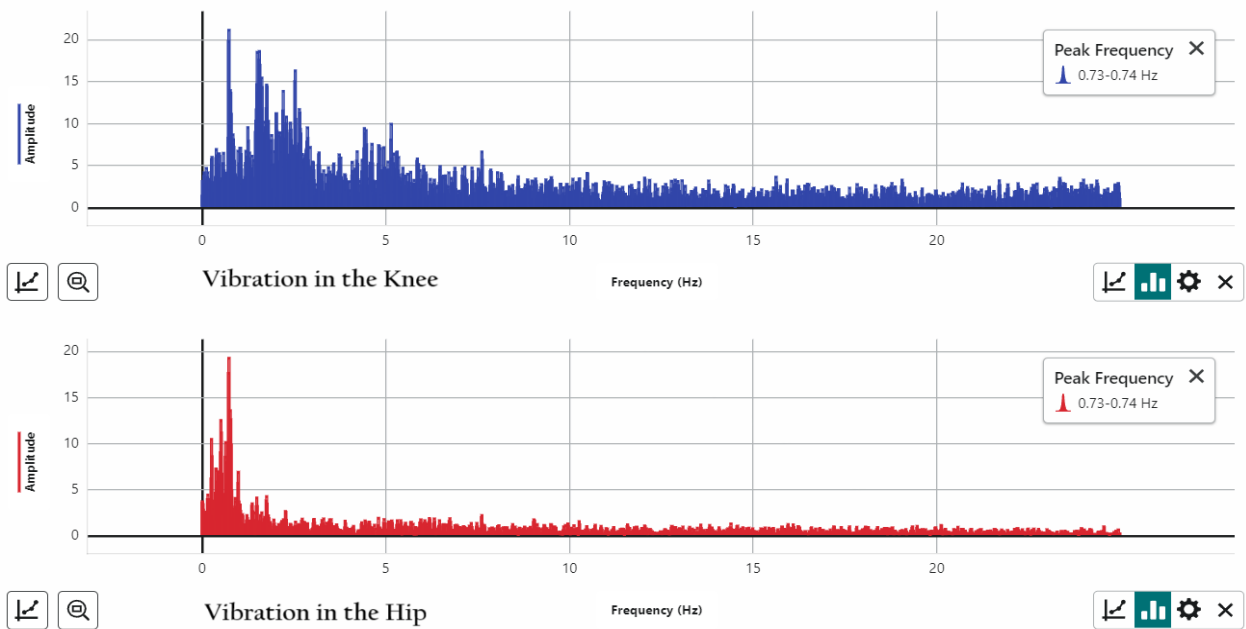


Figure (5-38) vibration at the knee and Hip in Z-Direction for multi-axis foot.

The following table presents a comparative analysis of the foot types (SACH foot, single-axis foot, and multi-axis foot) for walking, based on RMS values and key considerations such as vibration absorption, stability and comfort, and weight distribution. The root mean square (RMS) values of vibration at the knee and hip for the three types of feet are shown in Table (5-6) below. These values were calculated using MATLAB software as shown in (appendix A), which converted acceleration values into vibration values through Fast Fourier Transform (FFT) and then computed the RMS.

Table (5-6) the RMS value in three types of feet.

Type of Foot	Knee RMS(m/s ²)			Hip RMS(m/s ²)		
	X	Y	Z	X	Y	Z
SACH foot	0.25	0.15	0.08	0.26	0.07	0.05
Single foot	0.26	0.18	0.09	0.26	0.09	0.05
Multi foot	0.25	0.19	0.13	0.26	0.07	0.05

The SACH foot has several advantages, including reasonable performance in the X-axis (0.25 m/s²), indicating good vibration absorption during forward motion. Additionally, it boasts the lowest RMS values in both the Y (0.15 m/s²) and Z axes (0.08 m/s²), demonstrating effective management of lateral and vertical vibrations.

However, it does have some drawbacks, particularly in lateral stability, as it performs slightly worse than the Single foot in the Y-axis.

In contrast, the Single foot excels with the highest performance in the X-axis (0.26 m/s^2) and shows lower RMS values in the Y (0.18 m/s^2) and Z (0.09 m/s^2) axes, indicating superior vibration absorption and increased stability. Nonetheless, it has higher RMS in the Y-axis compared to the Multi foot, which may lead to some lateral instability.

The Multi foot also shows competitive performance in the X-axis (0.25 m/s^2) and provides good stability in the Y-axis (0.19 m/s^2). However, it has the highest RMS in the Z-axis (0.13 m/s^2) among the three types, suggesting less effective vertical vibration management, which could result in discomfort over longer distances.

In conclusion the SACH foot is the most favorable option among the three types for minimizing excessive motion and providing stability, particularly in lateral and vertical directions. Its lower RMS values in the Y and Z axes indicate better overall performance compared to the Single and Multi-feet. The Single foot, while advantageous in the X-axis, does not surpass the SACH foot in overall stability. The best choice ultimately depends on individual needs and walking conditions, but the SACH foot stands out as the superior option for stability and comfort.

5.7. 3DMA Rizzoli Gait Analysis

Three-dimensional analysis of gait (3DMA) provides several results, including pelvic, hip, knee, ankle, and foot angles for both the right and left legs, along with the range of motion for these joints while the patient walks in a bounded circular path wearing the SACH, single-axis, and multi-axis prosthetic limbs. The results of the OptiTrack gait analysis were measured at three sites (hip, knee, and ankle) using the patient's Motive sensor with an artificial prosthetic foot, as shown in Figure (5.39).



Figure (5-39) show the sensor on the patient and the position of test.

The test was conducted at Al-Khwarizmi College of Engineering, Department of Biomedical Engineering. The results were obtained as shown in the following.

5.7.1 Gait cycle analysis

The results of the gait analysis are shown in Figures (5-40), (5-41), and (5-42) for the SACH, single-axis, and multi-axis feet.

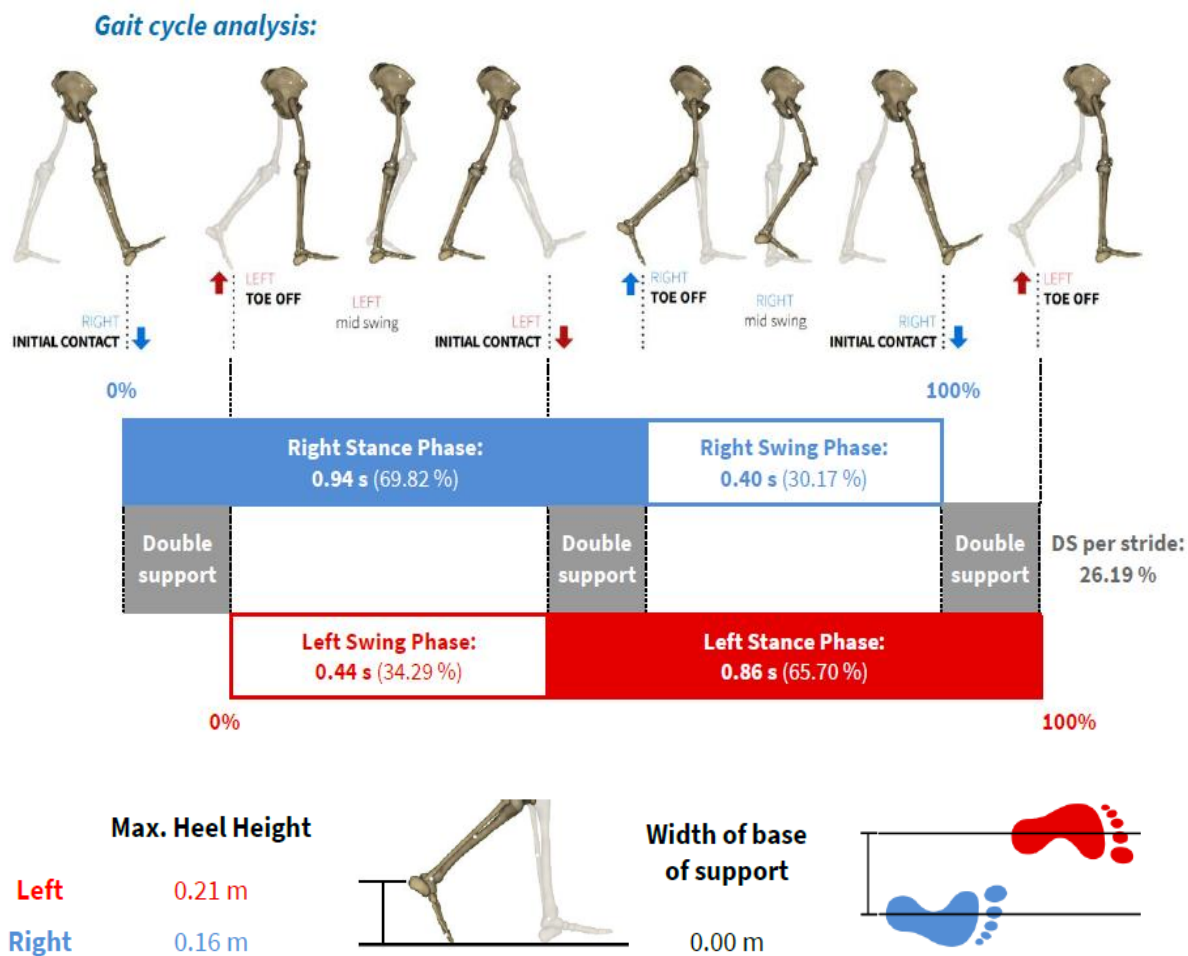


Figure (5-40) Gait Analysis for SACH foot.

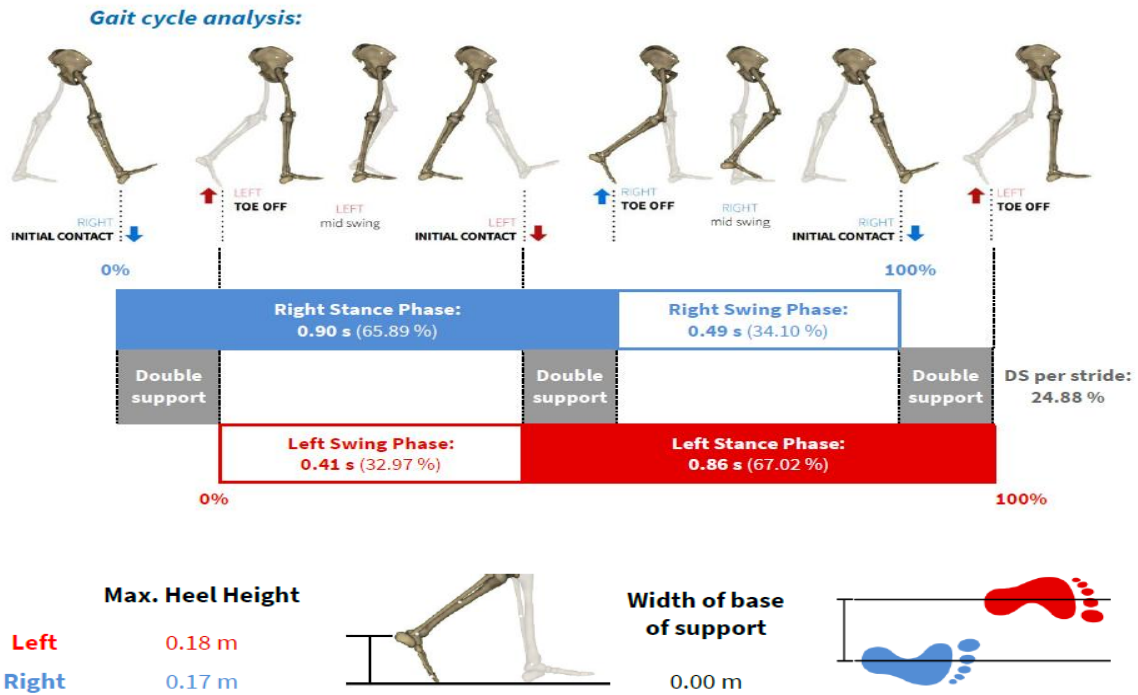


Figure (5-41) Gait Analysis for single axis foot.

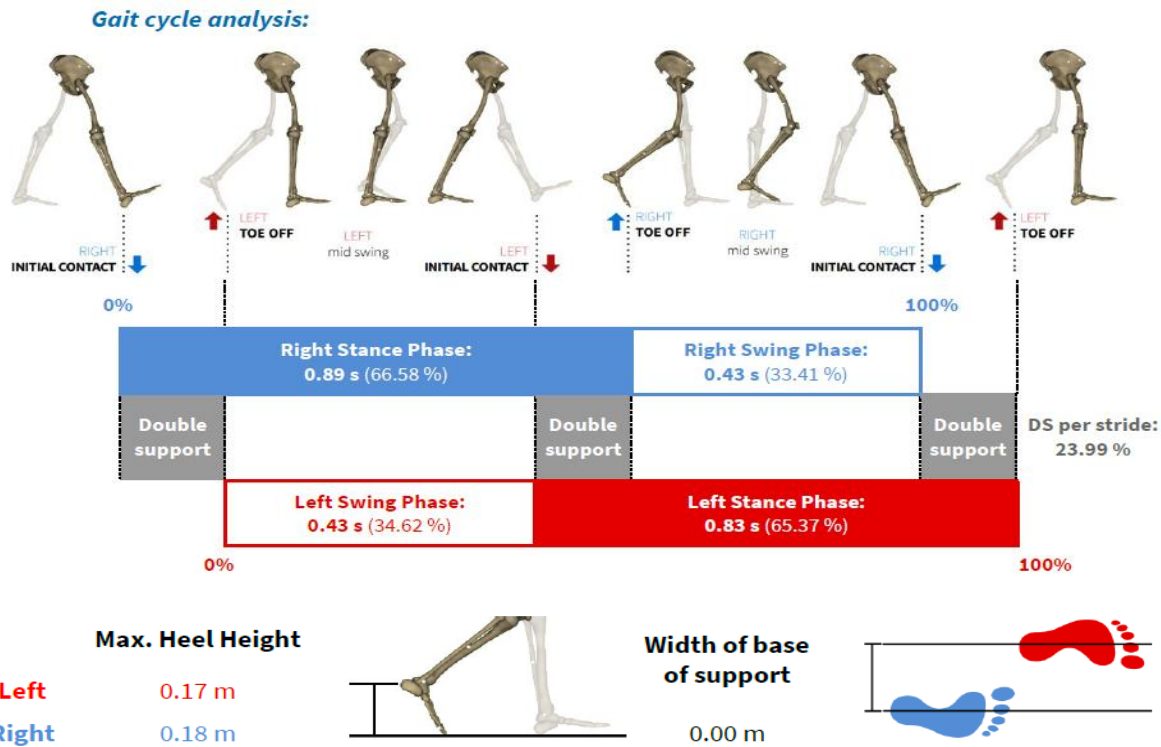


Figure (5-42) Gait Analysis for multi axis foot.

Gait analysis for multi axis was expectable and there is a good compatibility between the results of the right and left leg, stance phase results was (66.58 % _ 65.37%) left-right foot respectively and for swing phase recorded (34.62% _33.41%) left-right foot, total number of strides was (44_42) left-right foot and cadence was (92.28 steps/min) with speed (0.57 m/s) this results due to the patient walking in close steps at a slow speed through a bounded area in circle path .

As for the single foot, there was a little difference from the normal range of results, but also recorded a good compatibility between the results of the right and left leg. stance phase results were (65.89 % _ 67.02%) left-right foot respectively and for swing phase recorded (32.97% _34.10%) left-right foot, total number of strides was (45_40) left-right foot and cadence was (89.94 steps/min) with speed (0.55 m/s).

For the SACH foot, there was a more difference from the multi and single foot in the range of results, but also recorded a good compatibility between the results of the right and left leg. stance phase results were (69.82 % _ 65.70%) left-right foot respectively and for swing phase recorded (34.29% _30.17%) left-right foot, total number of strides was (44_44) left-right foot and cadence was (90.44 steps/min) with speed (0.51 m/s).

5.7.2 Pelvis Angle Results

The result for pelvis angle given in three planes: pelvic tilt (anterior and posterior), pelvic obliquity (superior, inferior), and pelvic rotation (internal/external) for three cases with three types of feet. This analysis aims to assess the compatibility between the three types and to evaluate the extent of improvement achieved. Figures (5-43), (5-44), and (5-45) show the results of the pelvic angle for the SACH, single-axis, and multi-axis feet, respectively.

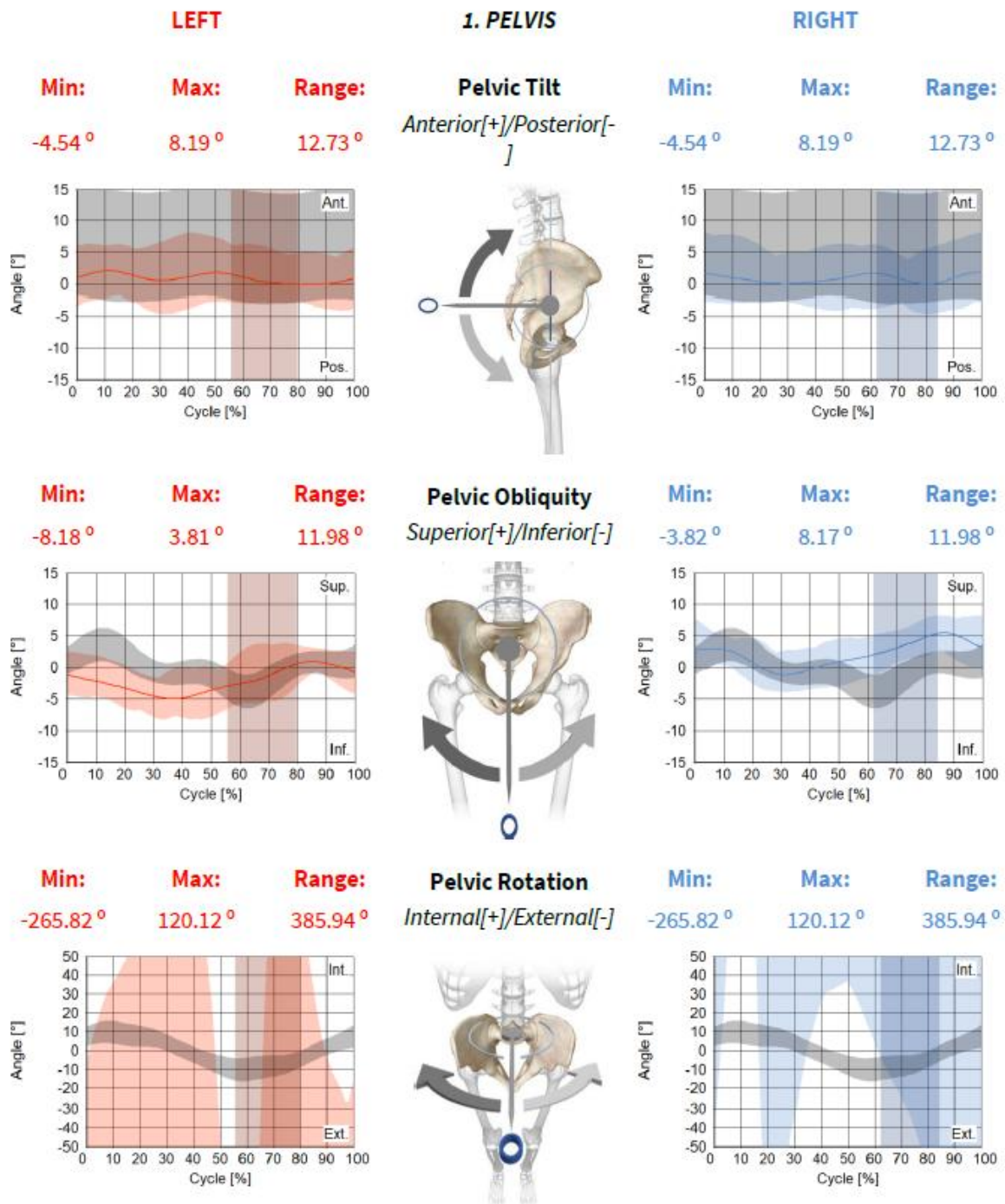


Figure (5- 43) pelvic tilt, obliquity& rotation angle for SACH foot.

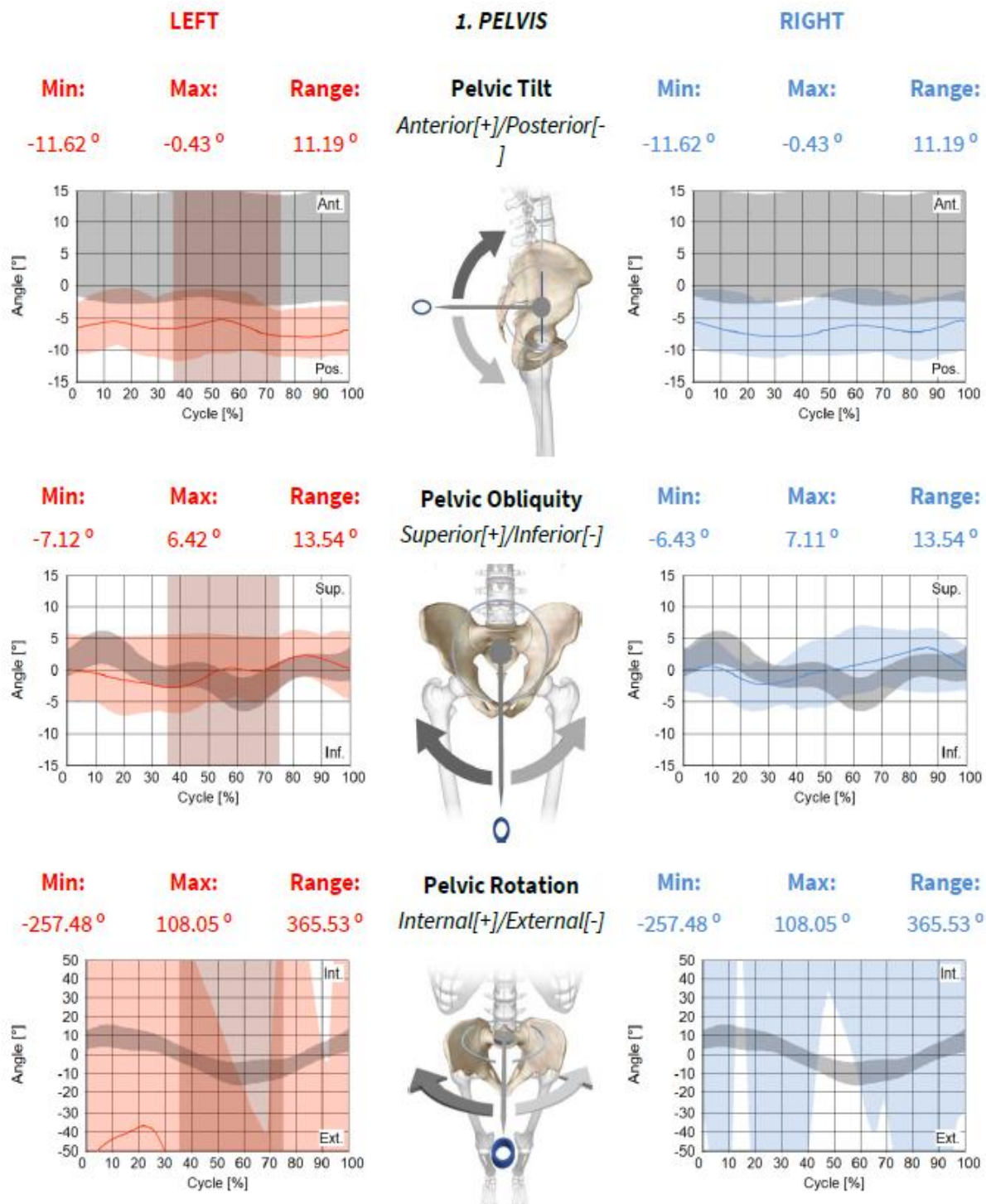


Figure (5-44) pelvic tilt, obliquity& rotation angle for single axis foot.

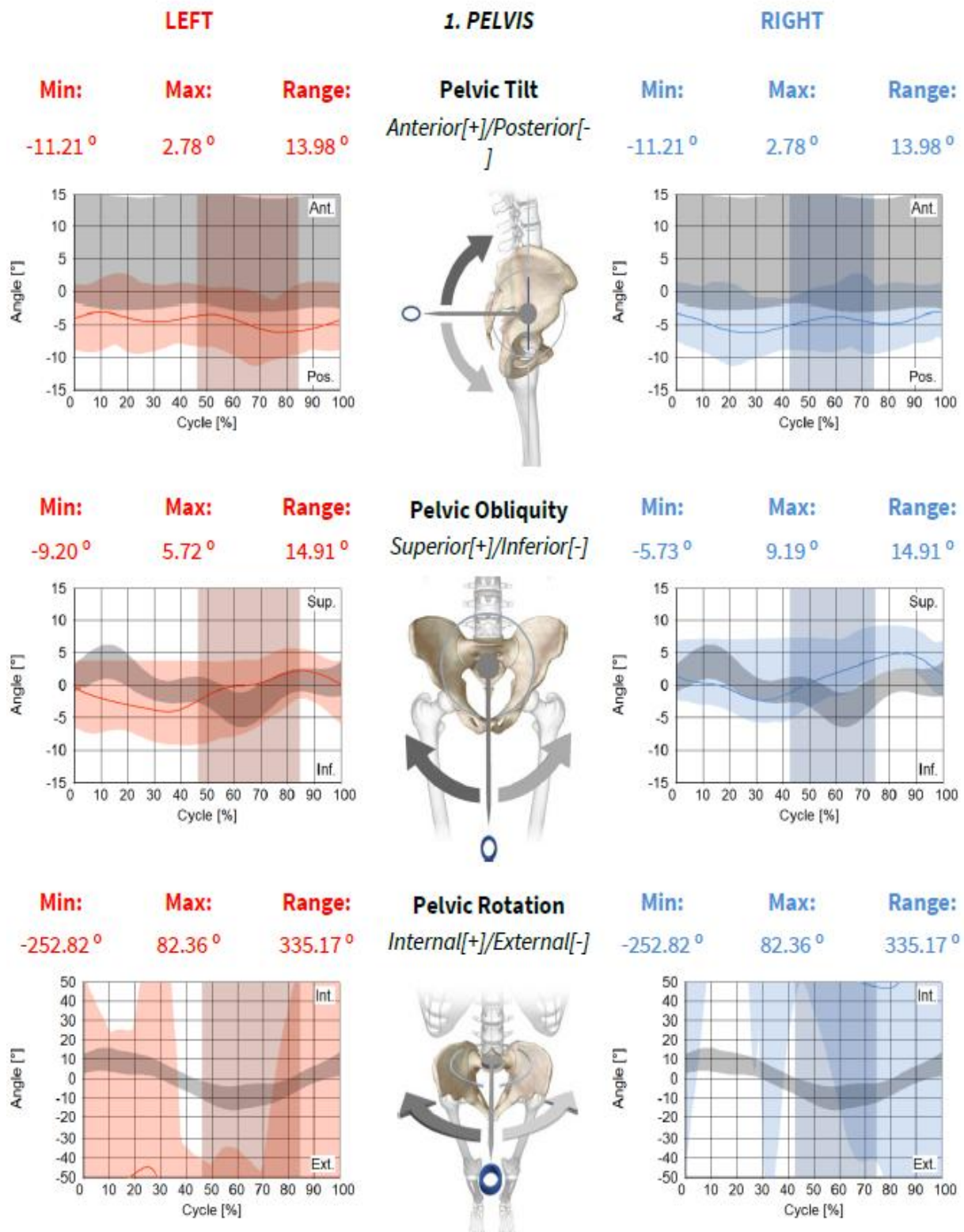


Figure (5 - 45) pelvic tilt, obliquity& rotation angle for multi axis foot.

The Figure (5-43) shown results of pelvic tilt for SACH foot (Anterior [+]/Posterior [-]) plane the (left-right) legs angle was (-4.54°, -4.54°) minimum and (8.19°, 8.19°) maximum it's within the normal range ,while pelvic obliquity (Superior [+]/Inferior [-]) plane angle (-8.18°, -3.82°) minimum (left-right) legs angle and (3.81°, 8.17°) maximum (left-right) legs angle, and for pelvic rotation internal [+]/ external [-] plane angle (-265.82°) minimum (left-right) legs angle and (120.12°) maximum (left-right) legs angle.

Figure (5-44) shown the results for single axis foot for pelvic tilt (Anterior [+]/Posterior [-]) plane the (left-right) legs angle was (-11.62°, -11.62°) minimum and (-0.43°, -0.43°) maximum it's within the normal range ,while pelvic obliquity (Superior [+]/Inferior [-]) plane angle (-7.12°, -6.43°) minimum (left-right) legs angle and (6.42°, 7.11°) maximum (left-right) legs angle, and for pelvic rotation internal [+]/ external [-] plane angle (-257.48°) minimum (left-right) legs angle and (108.05°) maximum (left-right) legs angle.

The figure (5-45) shown the pelvic angle for multi axis foot in transtibial prosthesis limb, in pelvic tilt (Anterior [+]/Posterior [-]) plane the (left-right) legs angle was (-11.21°, -11.21°) minimum and (2.78 °, 2.78°) maximum it's within the normal range ,while pelvic obliquity (Superior [+]/Inferior [-]) plane angle (-9.20°, -5.73°) minimum (left-right) legs angle and (5.72°, 9.91°) maximum (left-right) legs angle, and for pelvic rotation (internal [+]/ external [-]) plane angle (-252.82°) minimum (left-right) legs angle and (82.36°) maximum (left-right) legs angle .

The results of the pelvic angle showed there was more than a slight difference between the right and left leg for the SACH foot in the pelvic tilt, pelvic obliquity and pelvic rotation.

The results of the pelvic angle showed a convergence between the angles of the right leg and the left leg, and it was within the normal range for the single axis foot.

As for the multi axis foot, there was a slight difference between the right and left leg, but it was acceptable and within normal ranges. Also, the results were almost similar between both multi & single axis. Especially in case of pelvic rotation angles the results was compatible.

5.7.3 Hips Angle Results

For hip angle three planes' results recorded. Hip flexion (flexion [+]/ extension [-]), hip abduction (adduction [+]/ abduction [-]), hip rotation (internal [+]/ external [-]) figure (5-46), (5-47) and (5-48) shown the result of hip angle for SACH, single and multi-axis feet respectively.

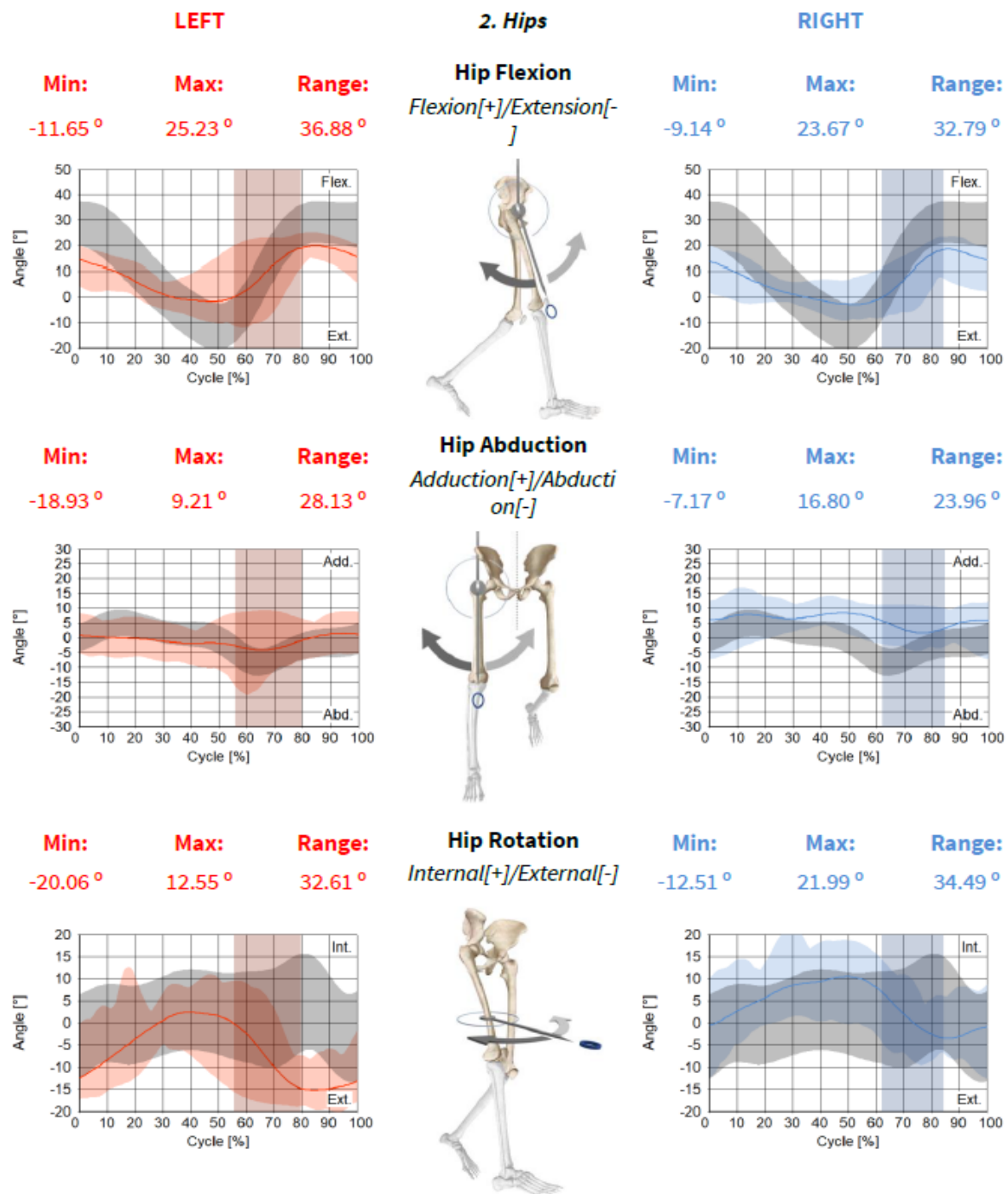


Figure (5-46) Hip Flection, Abduction& Rotation angle for SACH foot.

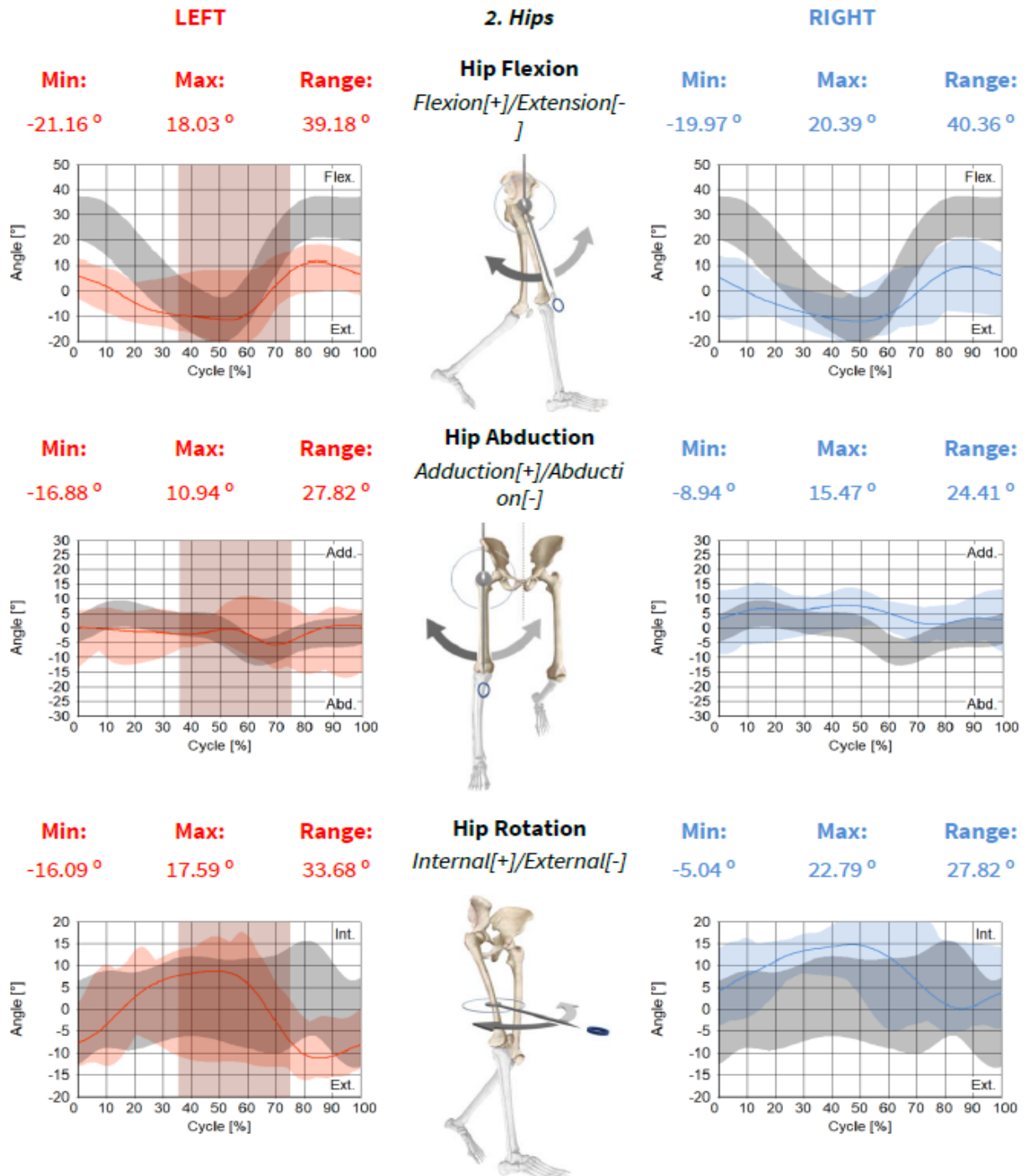


Figure (5-47) Hip Flection, Abduction& Rotation angle for Single axis foot.

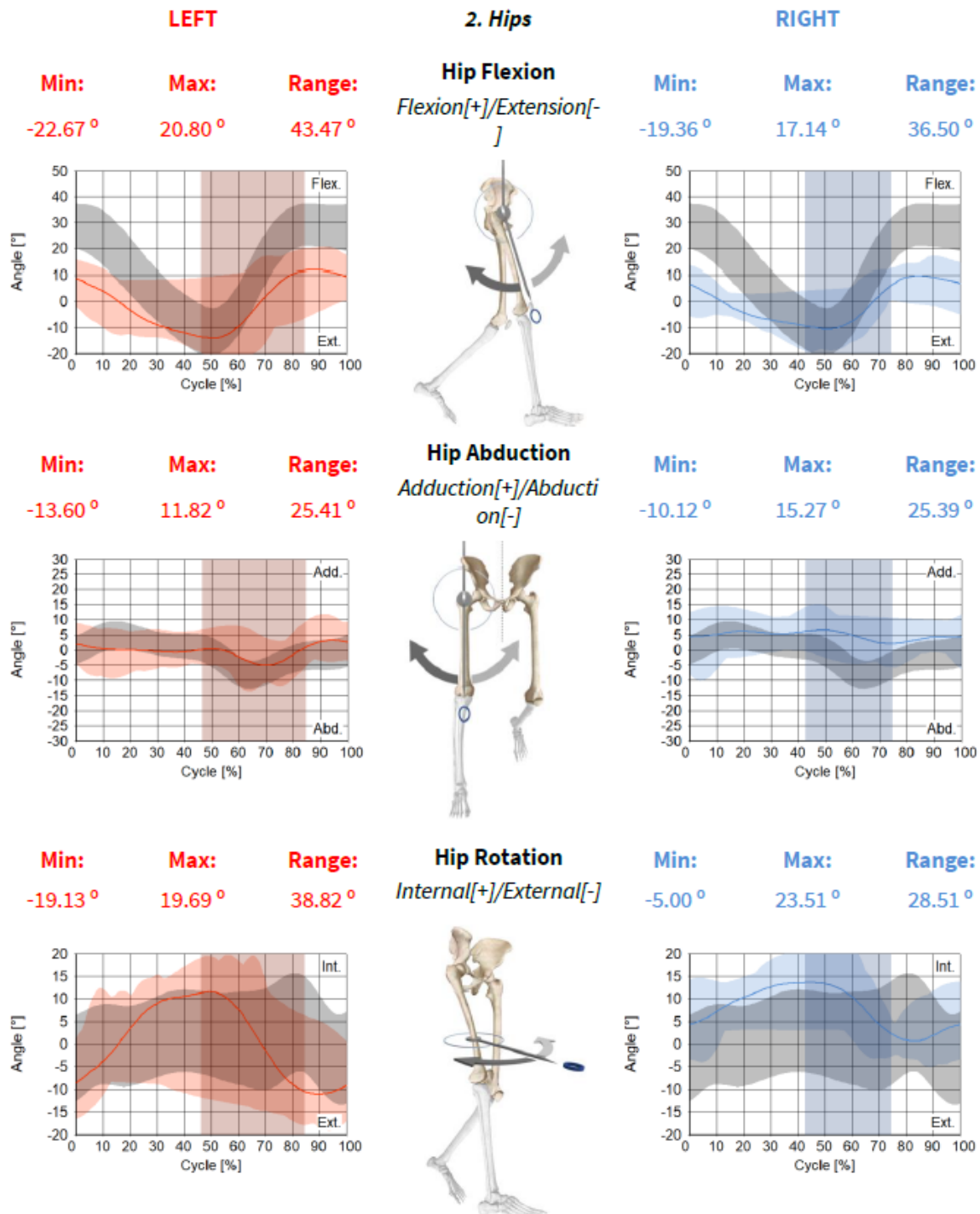


Figure (5-48) Hip Flection, Abduction& Rotation angle for Multi-axis foot.

The results in figure (5-46) shown the Hip angle for SACH foot, in hip (flexion ,extension) the (left-right) minimum extension angle was(-11.65°,-9.14°) while the (left-right) maximum flexion angle was (25.23°,23.67°) respectively .for hip (Adduction, Abduction) angle the (left-right) minimum abduction angle was (-18.93°,-7.17°),while the (left-right) maximum Adduction hip angle was (9.21°, 16.80°) respectively and for hip rotation the results minimum external hip rotation angle was (-20.09°,-12.51°) and maximum internal hip rotation angle was (12.55°,21.99°) respectively.

While the results in figure (5-47) shown the Hip angle for single axis foot, in hip(flexion ,extension) the (left-right) minimum extension angle was(-21.16°,-19.97°) while the (left-right) maximum flexion angle was (18.03°,20.39°) respectively .for hip (Adduction, Abduction) angle the (left-right) minimum abduction angle was(-16.88°,-8.94°),while the (left-right) maximum Adduction hip angle was (10.94°, 15.47°) respectively and for hip rotation the results was (-16.09°,-5.04°) minimum external hip rotation angle and maximum internal hip rotation angle was (17.59°,22.79°) respectively .

The results in figure (5-48) shown the Hip angle for multi axis foot, in hip (flexion ,extension) the (left-right) minimum extension angle was(-22.68°,-19.36°) while the (left-right) maximum angle was(20.80°,17.14°) respectively .for hip (Adduction, Abduction) angle the (left-right) minimum abduction angle was (-13.60°,-10.12°),while the (left-right) maximum Adduction hip angle was (11.82°, 15.27°) respectively and for hip rotation the results was (-19.13°,-5.00°) minimum external hip rotation angle and maximum internal hip rotation angle was (19.69°,23.82°) respectively .

The results of the hip angle showed a convergence between the angles of the right leg and the left leg, and it was within the normal range for three types of prosthetic feet. As for the multi axis foot and the single axis foot,

there was a slight difference between the right and left leg, but it was acceptable and within normal ranges. There was more than a slight difference between the right and left leg for the SACH foot in the hip flexion, hip abduction and hip rotation.

5.7.4. Knee Angle Results

The result for knee angle given in three case knee flexion, knee abduction and knee rotation these results display in figure (5-49), (5-50) and (5-51) for SACH, single axis and multi axis feet respectively.

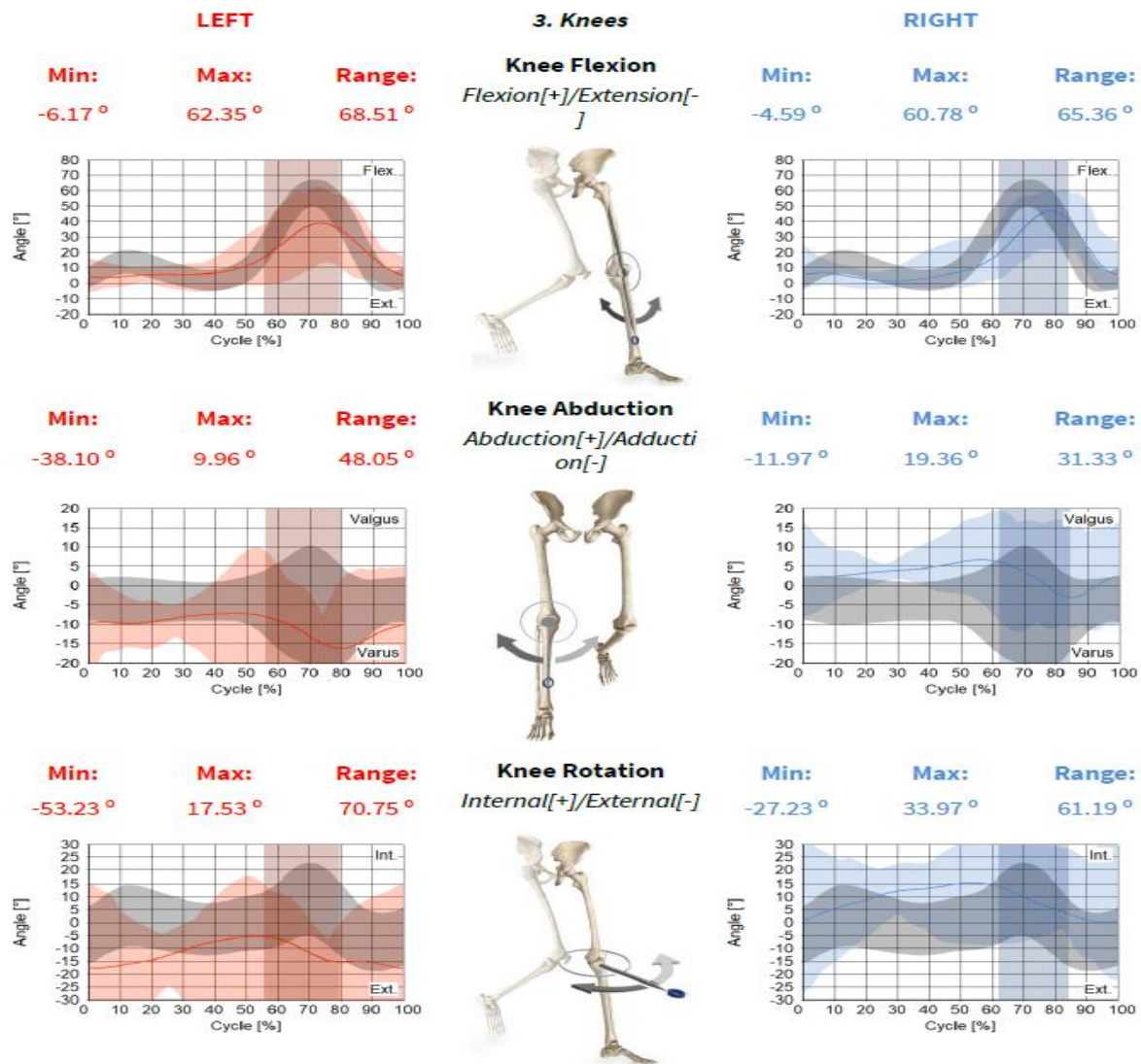


Figure (5-49) Knee flexion, Knee abduction, Knee rotation for SACH foot.

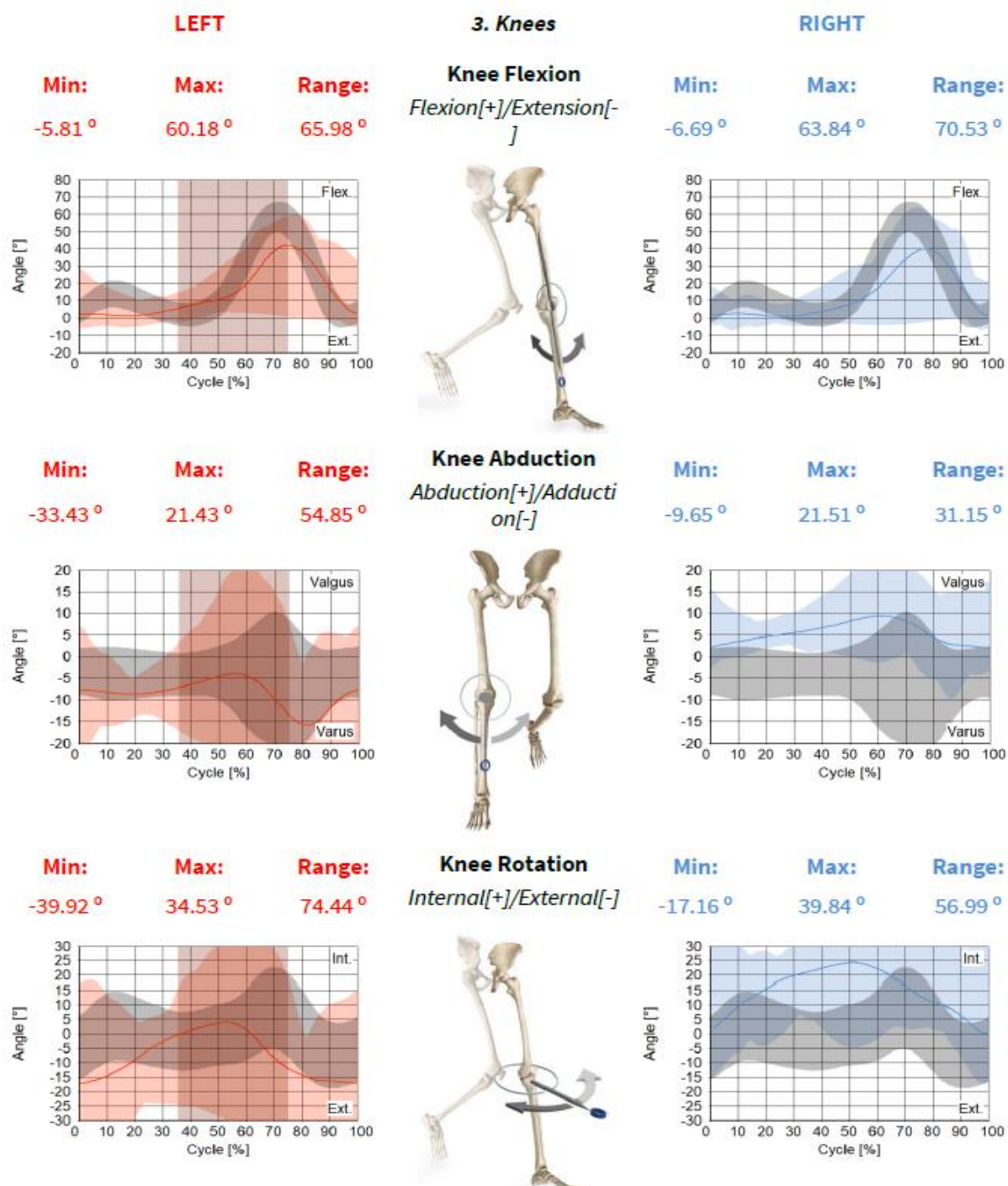


Figure (5-50) Knee flexion, Knee abduction, Knee rotation for Single axis foot.

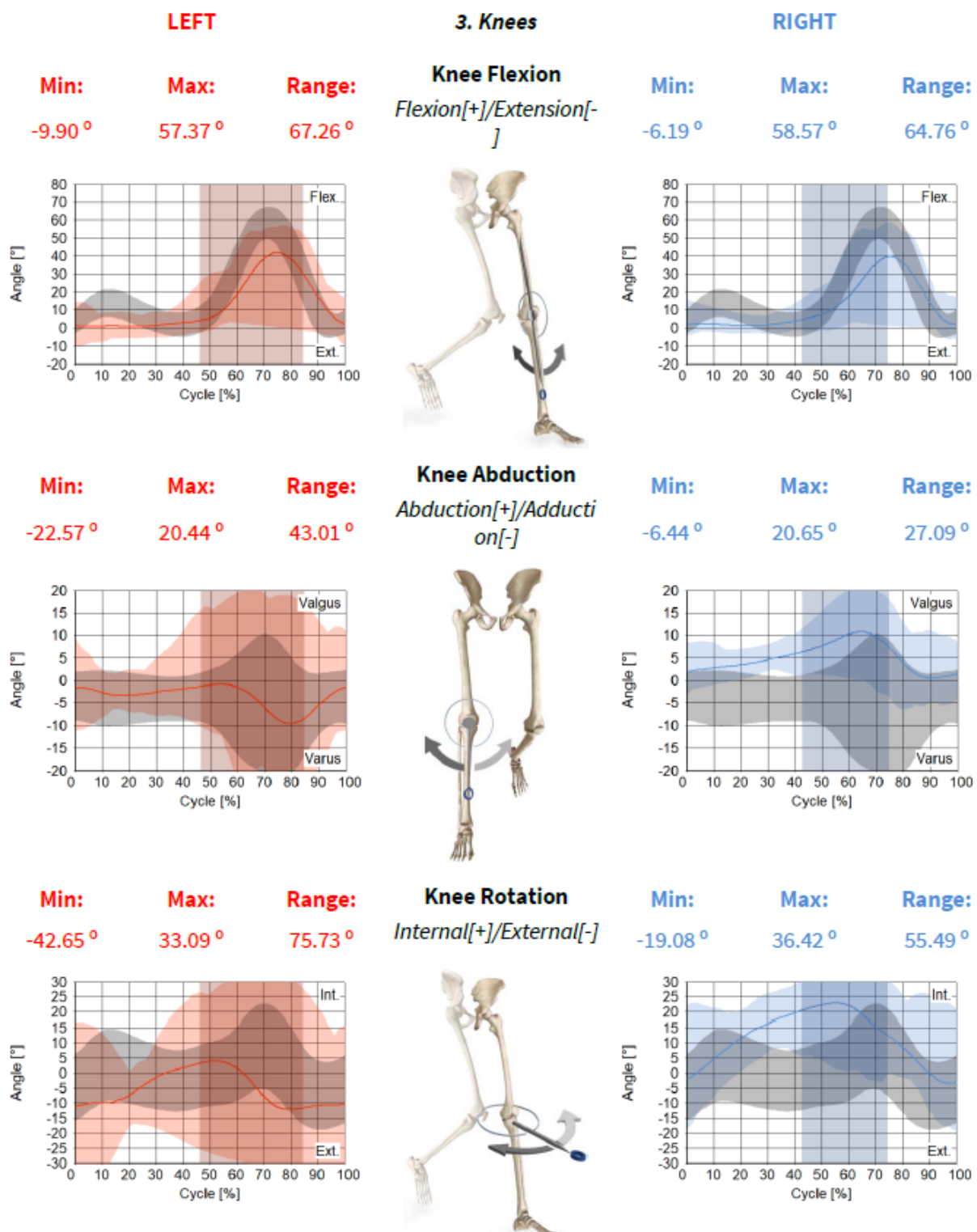


Figure (5-51) Knee flexion, Knee abduction, Knee rotation for Multi axis foot.

The results in figure (5-49) shown the knee angle for SACH foot, in knee (flexion ,extension) the (left-right) minimum extension angle was $(-6.17^\circ, -4.59^\circ)$ and the (left-right) maximum flexion angle was $(62.35^\circ, 60.78^\circ)$ respectively .while the knee (Adduction, Abduction) angle recorded the (left-right) minimum Abduction angle $(-38.10^\circ, -11.97^\circ)$ and maximum Adduction angle $(9.96^\circ, 19.36^\circ)$.The analysis of knee (Internal, External) rotation angle recorded the (left-right) minimum External angle $(-53.23^\circ, -27.23^\circ)$, with the (left-right) maximum Internal angle $(17.53^\circ, 33.97^\circ)$ respectively.

The results in figure (5-50) shown the knee angle for single axis foot, in knee (flexion ,extension) the (left-right) minimum extension angle was $(-5.381^\circ, -6.69^\circ)$ and the (left-right) maximum flexion angle was $(60.81^\circ, 63.84^\circ)$ respectively .while the knee (Adduction, Abduction) angle recorded the (left-right) minimum Abduction angle $(-33.43^\circ, -9.65^\circ)$ and maximum Adduction angle $(21.43^\circ, 21.51^\circ)$.For the knee (Internal, External) rotation angle recorded the (left-right) minimum External angle $(-39.92^\circ, -17.16^\circ)$, with the (left-right) maximum Internal angle $(34.53^\circ, 39.84^\circ)$ respectively.

The results in figure (5-51) shown the knee angle for multi axis foot, in knee (flexion ,extension) the (left-right) minimum extension angle was $(-9.90^\circ, -6.19^\circ)$ and the (left-right) maximum flexion angle was $(57.37^\circ, 581.57^\circ)$ respectively .while the knee (Adduction, Abduction) angle recorded the (left-right) minimum Adduction angle $(-22.57^\circ, -6.44^\circ)$ and maximum Abduction angle $(20.44^\circ, 20.65^\circ)$.finally the knee (Internal, External) rotation angle recorded the (left-right) minimum External angle $(-42.65^\circ, -19.08^\circ)$, with the (left-right) maximum Internal angle $(33.09^\circ, 36.42^\circ)$ respectively.

The results of the knee joint angles were very consistent in the case of extension and flexion with the normal ranges and within the normal behavior of three types of feet. For the knee flexion the three types of feet are very closely in the result. While the knee Abduction angle and the knee rotation there was a slight difference between the right and left leg for the SACH foot.

5.7.5. Ankle Flexion Angle Results

The results for ankle flexion angles, including ankle (dorsal, plantar) flexion, ankle (inversion, eversion) abduction, and ankle (internal, external) rotation, are shown in Figures (5-52), (5-53), and (5-54) for the SACH, single-axis, and multi-axis feet, respectively.

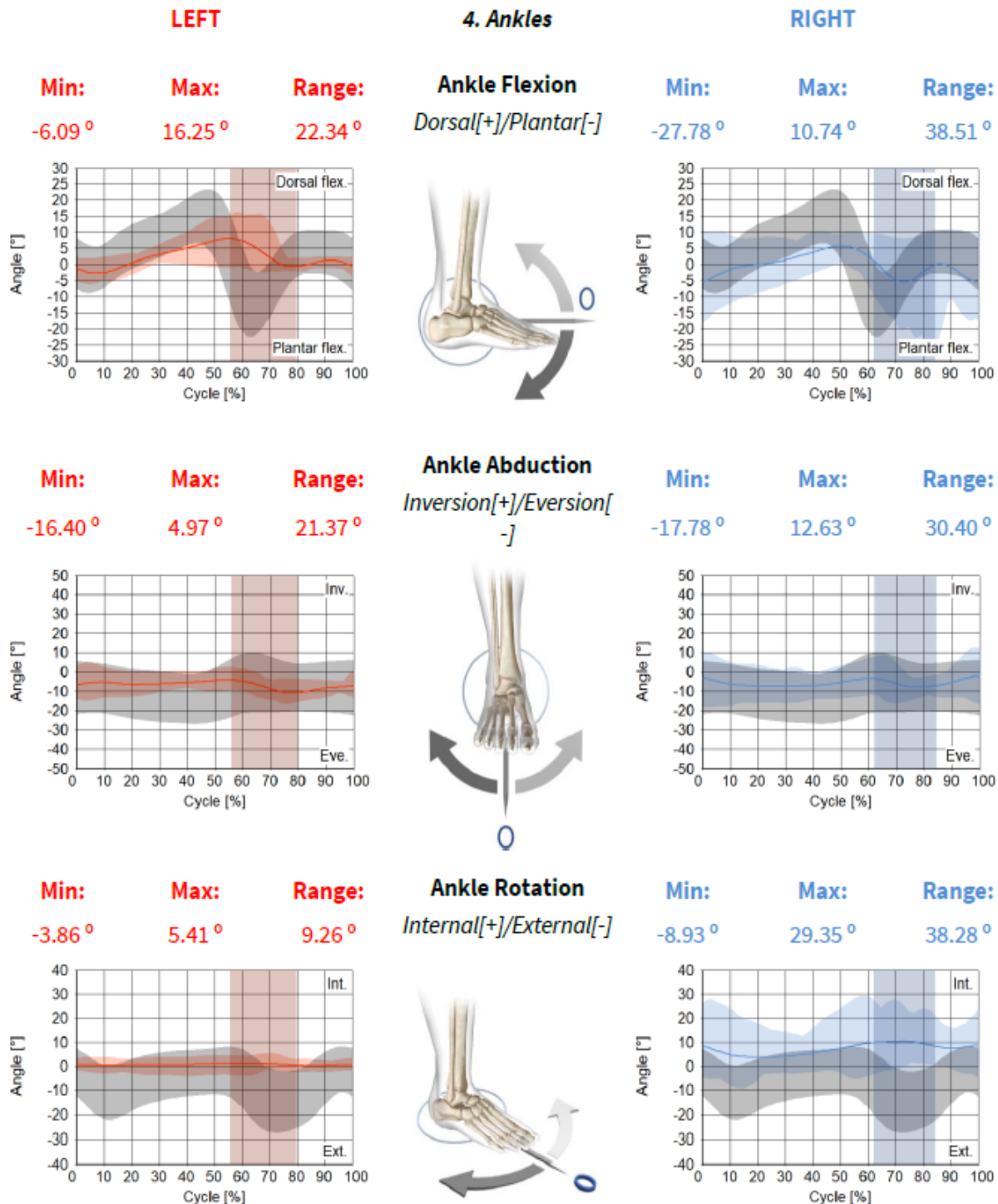


Figure (5-52) ankle (flexion, Abduction, rotation) angle for SACH foot.

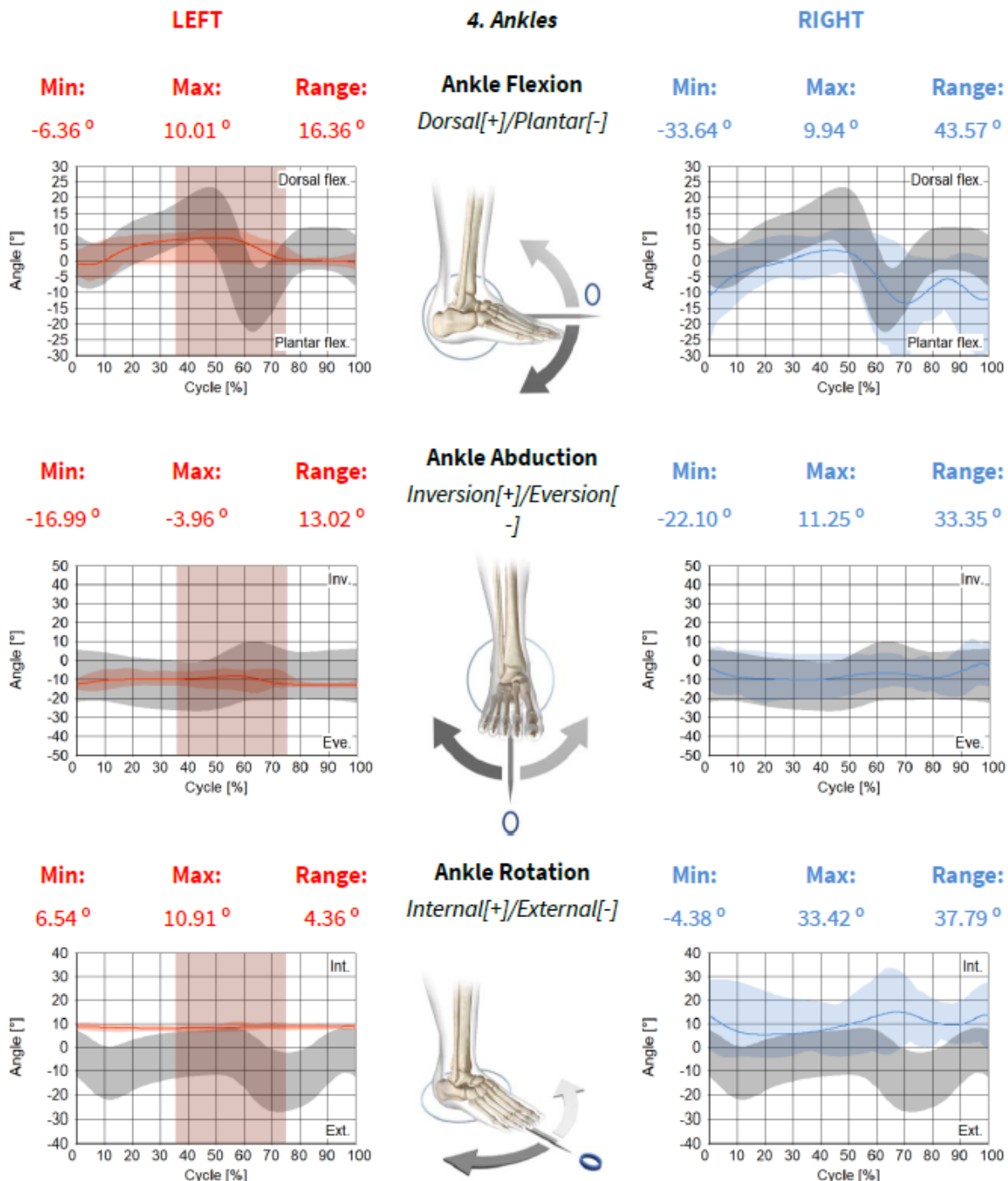


Figure (5-53) ankle (flexion, Abduction, rotation) angle for Single axis foot.

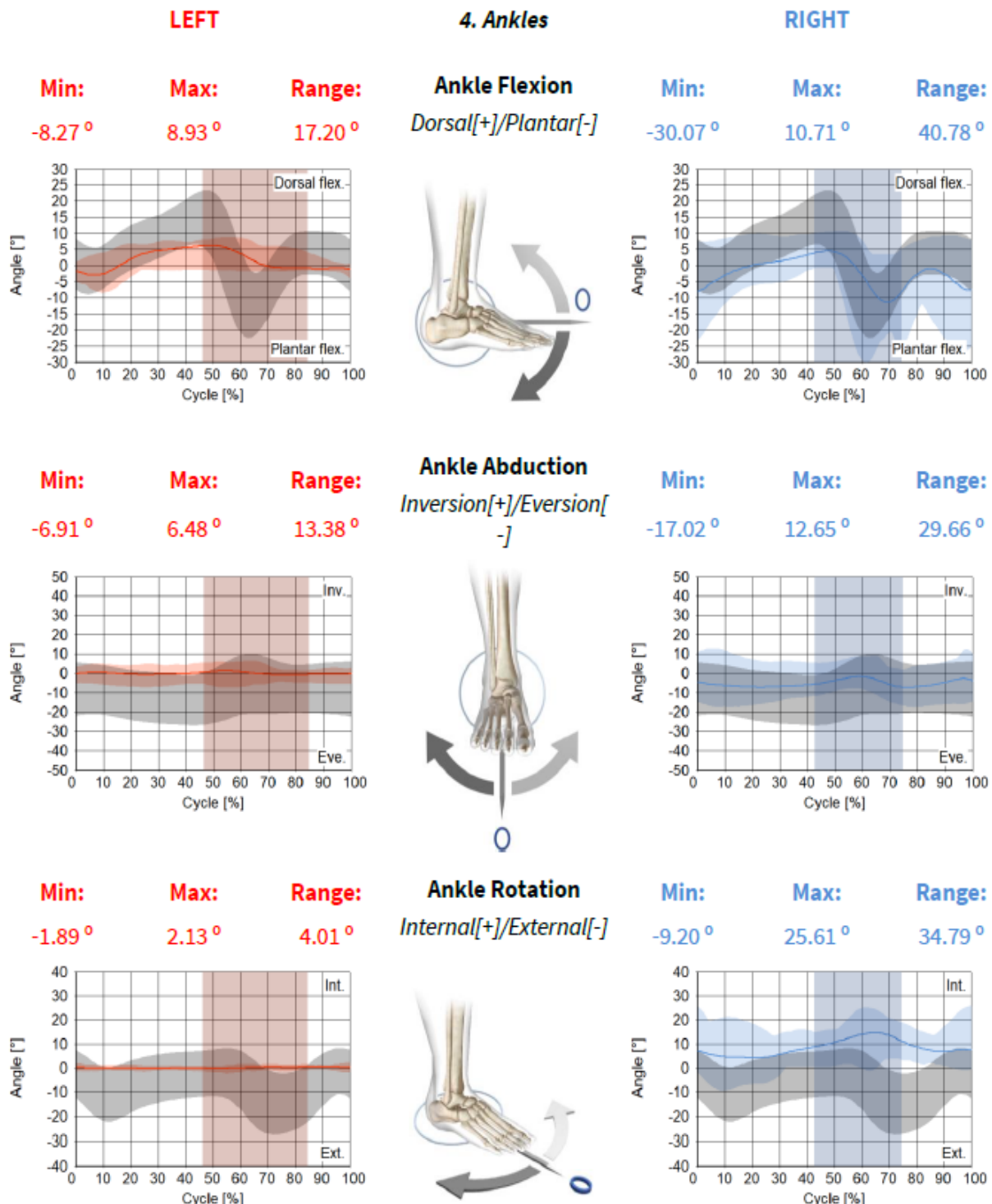


Figure (5-54) ankle (flexion, Abduction, rotation) angle for Multi axis foot.

The result for SACH foot as shown in figure (5-52) recorded for (left-right) ankle flexion angle was $(-6.06^\circ, -27.78^\circ)$ minimum and $(16.25^\circ, 10.74^\circ)$ maximum, while for (left-right) ankle abduction angle recorded $(-16.40^\circ, -17.78^\circ)$ minimum with $(4.97^\circ, 12.63^\circ)$ maximum, finally (left-right) ankle rotation angle recorded $(-3.86^\circ, -8.93^\circ)$ minimum with $(5.41^\circ, 29.35^\circ)$ maximum rotation angle.

While the result for single axis foot as shown in figure (5-53) recorded for (left-right) ankle flexion angle was $(-6.36^\circ, -33.64^\circ)$ minimum and $(10.01^\circ, 9.94^\circ)$ maximum, while for (left-right) ankle abduction angle recorded $(-16.99^\circ, -22.10^\circ)$ minimum with $(-3.96^\circ, 11.25^\circ)$ maximum, finally (left-right) ankle rotation angle recorded $(6.54^\circ, -4.36^\circ)$ minimum with $(10.91^\circ, 33.42^\circ)$ maximum rotation angle.

The results of multi axis foot as shown in figure (5-54) recorded for (left-right) ankle flexion angle was $(-8.27^\circ, -30.07^\circ)$ minimum and $(8.93^\circ, 10.71^\circ)$ maximum, while for (left-right) ankle abduction angle recorded $(-6.091^\circ, -17.02^\circ)$ minimum with $(6.48^\circ, 12.65^\circ)$ maximum, finally (left-right) ankle rotation angle recorded $(-1.89^\circ, -9.20^\circ)$ minimum with $(2.13^\circ, 25.61^\circ)$ maximum rotation angle.

The results for the ankle flexion angle were The Single Axis Foot generally demonstrates the widest ranges of motion in ankle flexion, abduction, and rotation angles compared to the SACH Foot and Multi Axis Foot. In terms of flexibility and adaptability, the Single Axis Foot offers a broader range of ankle angles for various movements. The Multi Axis Foot shows competitive ranges, especially in ankle abduction and rotation angles, indicating good support for these movements. The SACH Foot, while providing moderate ranges, may offer a balance between motion and stability.

5.7.6. Foot Direction Angle Results

The results for foot direction angles, including (internal, external) foot direction, are shown in Figures (5-55), (5-56), and (5-57) for the SACH, single-axis, and multi-axis feet, respectively.

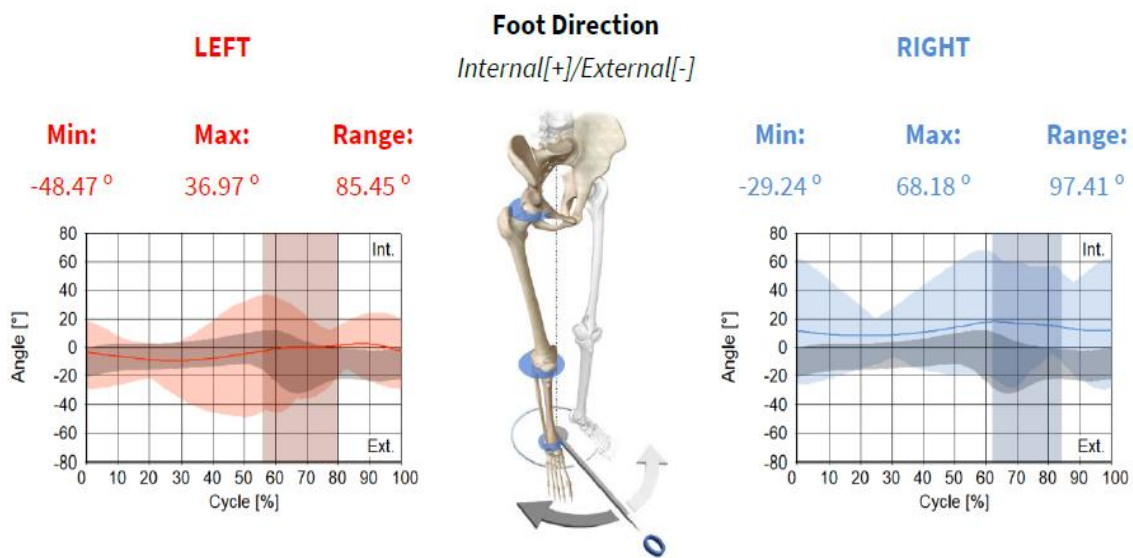


Figure (5-55) foot (Internal, External) direction angle for SACH foot.

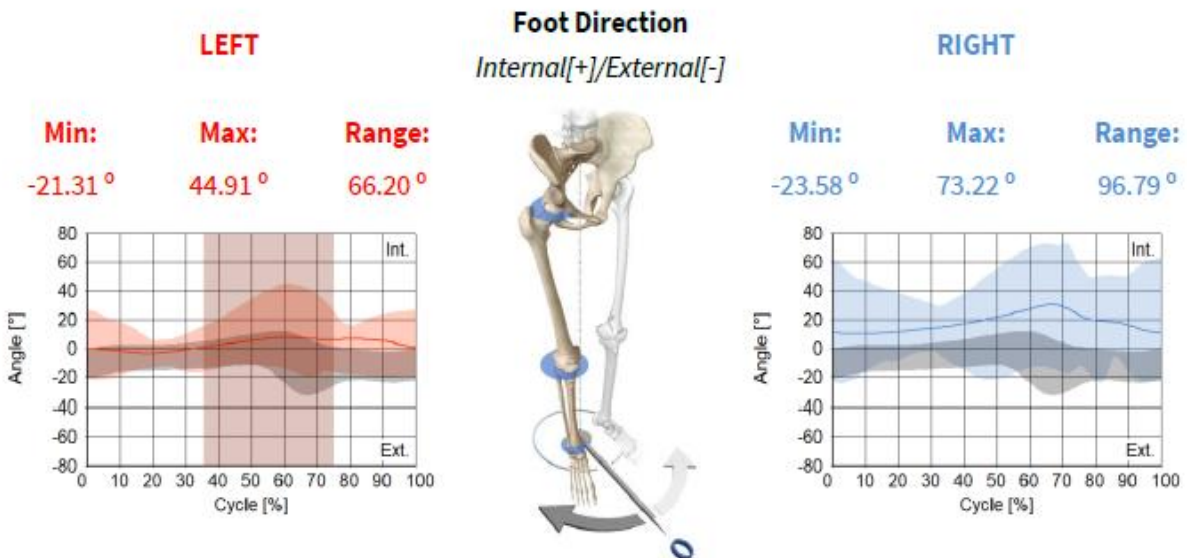


Figure (5-56) foot (Internal, External) direction angle for single axis foot.

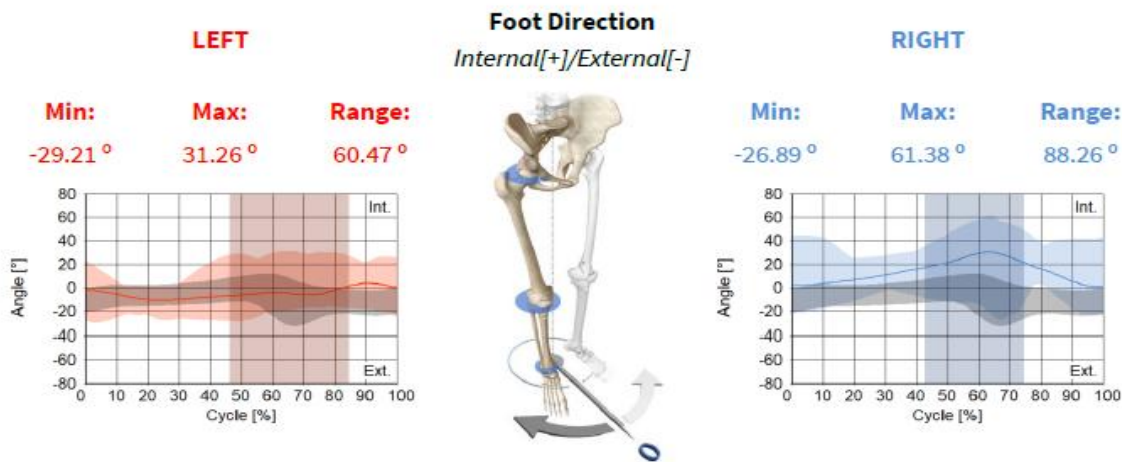


Figure (5-57) foot (Internal, External) direction angle for multi axis foot.

The figure (5-55) shown that the foot direction angle for SACH foot recorded (-48.47°, -29.24°) for (left, right) minimum external foot direction angle, with (36.97°, 68.18°) maximum internal direction angle respectively.

While figure (5-56) shown that the foot direction angle for single axis foot recorded (-21.31°, -23.58°) for (left, right) minimum external foot direction angle, with (44.91°, 73.22°) maximum internal direction angle respectively. Figure (5-57) shown that the foot direction angle for multi axis foot recorded (-29.21°, -26.89°) for (left, right) minimum external foot direction angle, with (31.26°, 61.38°) maximum internal direction angle respectively. These results were acceptable within the normal range. Considering the ranges of external foot direction angles the greater variability and flexibility in foot positioning are desired, the SACH Foot preferred. For more controlled and predictable foot direction angles, the Single Axis Foot a suitable choice. The Multi Axis Foot offers a balance between the two, providing moderate ranges of foot direction angles.

5.8. Simulation and results analysis

5.8.1. Introduction

Prosthetic sockets play a critical role in ensuring both structural integrity and user comfort in prosthetic limb systems. This study employs finite element analysis (FEA) to investigate the stress distribution and safety factors of a prosthetic socket under different loading conditions. A three-dimensional (3D) model of the socket was developed, and simulations were performed to analyze the mechanical behavior under SACH, single-axis and multi-axis combined loading scenarios. The study focuses on assessing stress behavior along the principal orthogonal axes (X, Y, and Z), evaluating safety factors, and identifying potential structural weaknesses. The results provide key insights into the performance of the prosthetic socket, aiding in the development of improved, durable, and more efficient designs.

Prosthetic sockets serve as the primary interface between an amputee's residual limb and the prosthetic limb system. They must balance structural strength with user comfort, ensuring both biomechanical stability and long-term durability. Due to prolonged cyclic loading and varying external forces, these components are susceptible to stress concentrations, leading to potential failures, discomfort, or reduced performance over time. Therefore, an in-depth understanding of the stress distribution within the socket is crucial for improving its design and longevity. This research aims to:

1. Utilize finite element analysis (FEA) to evaluate stress distribution within the prosthetic socket under different loading conditions.
2. Determine safety factors for each loading scenario and assess their implications.

3. Analyze stress variations along the X, Y, and Z axes to identify potential weak points.
4. Provide recommendations for enhancing the socket's structural efficiency and user comfort.

- Material Yield Strength: 25 MPa

The external pressure is assumed to originate from a zero-reference point ($x = 0.2625$, $y = 0.1365$, $z = 0.0892$) and progressively increase outward. Composites would be better suited for future prosthetics considering the present HDPE material has performed well under the simulated conditions. Such materials are high strength at lower weights and will probably further reduce stress concentrations increasing the upper prosthetic foot durability.

5.8.2. Finite Element Model

5.8.2.1. Model geometry

The prosthetic socket was modeled as a three-dimensional (3D) structure, through SimScale Software, using precise geometric parameters to replicate real-world conditions. The geometry consists of a hollow, load-bearing shell with a height of 0.3 m, a width of 0.2 m, and a uniform wall thickness of 7 mm. The structural shape is designed to accommodate pressure variations and ensure even stress distribution.

The model geometry was developed using computer-aided design (CAD) software and later imported into the finite element analysis (FEA) environment. The final prosthetic socket geometry accurately represents a functional socket structure subjected to external loading conditions.

5.8.2.2. Mesh generation

To ensure computational accuracy and convergence, a structured finite element tetrahedral mesh was generated. The mesh was refined in regions experiencing high-stress gradients, particularly around load application points and transition zones.

The mesh quality was assessed based on the element aspect ratio, skewness, and Jacobian determinant to maintain numerical stability. The final model consisted of approximately 250,000 finite elements, balancing computational efficiency with accuracy.

The meshed model provides an optimized structure for performing stress and deflection analyses while ensuring the reliability of the simulation results.

5.8.3. Model Development

A detailed 3D model of the prosthetic socket was created using finite element modeling techniques, as shown in Figure (5-58).

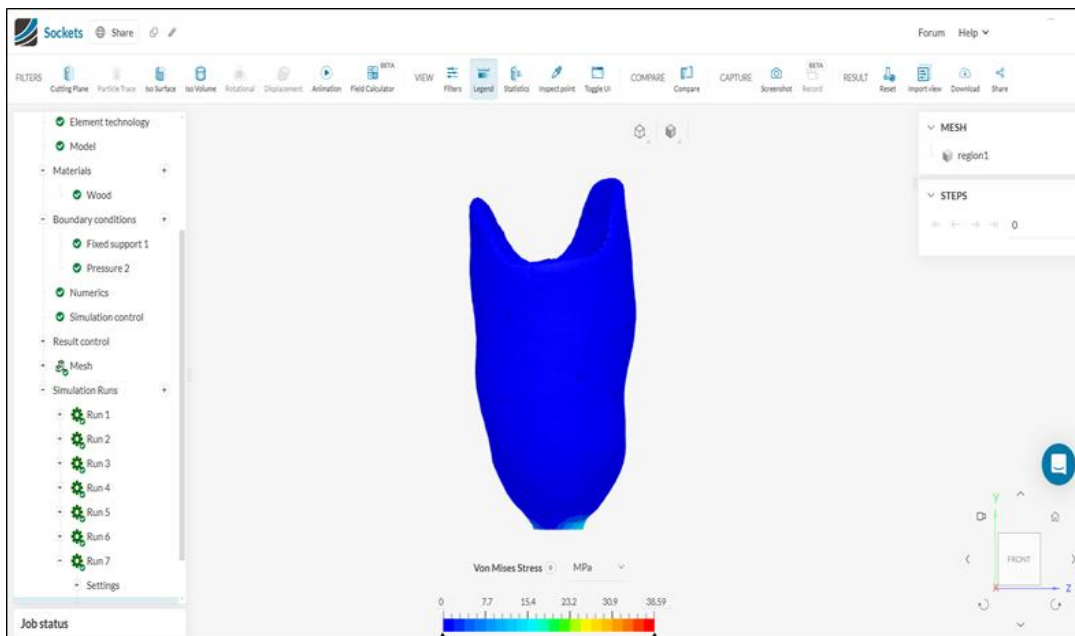


Figure (5-58) 3D FE model.

5.8.4. Boundary Condition Impact

The fixed support at the bottom of the prosthetic foot was one of the factors that influenced the global stress distribution. By restricting the base, it is found that most of the stress has been conveyed to the foot's upper region. This aligns with the objective of the design, which is to reduce stresses at the bonding area.

5.8.5. Loading Conditions

Three distinct pressure-loading scenarios were considered in the analysis:

- SACH foot loading: 227.53 kPa
- Multi-axis foot loading: 241.3 kPa
- Single- axis foot loading: 275.79 kPa

Each loading condition was applied progressively outward from the defined reference point, simulating realistic pressure distributions experienced by prosthetic users. The reference point for stress and deflection analysis was defined at (x = 0.2625, y = 0.1365, z = 0.0892).

5.8.6. Computational Analysis

The analysis involved the following key computational aspects:

- Stress Distribution Evaluation: Stress variation was assessed based on the vertex distance from the zero-reference point.

- Safety Factor Calculation: The ratio between the material yield strength (25 MPa) and the computed maximum stress was determined.
- Statistical Analysis: The mean, standard deviation, and peak stress were computed for each axis (X, Y, Z) under all loading conditions.

To enhance the understanding of stress concentration areas, interactive 3D visualizations were generated. These provide a clearer representation of high-stress zones, aiding in design optimization efforts.

5.8.7. Results and Discussion

The stress analysis was conducted for three different pressure conditions: 227.53 kPa, 241.3 kPa, and 275.79 kPa. The results indicate a direct correlation between the applied pressure and the maximum stress and deflection (displacement) experienced within the structure, as presented in Fig. (5.59). As expected, higher pressure levels resulted in increased stress values, which consequently affected the safety factor, as shown in Table (5-7).

Table (5-7): Stress analysis under impact pressures.

Pressure (kPa)	Max Stress (MPa)	Safety Factor
227.53	12.5	2
241.3	14.2	1.76
275.79	18.9	1.32

The results show that under the highest-pressure condition for Single- axis foot (275.79 kPa), the maximum stress approaches critical levels, resulting in a reduced safety factor. This suggests that prolonged exposure to such pressures could lead to structural failure if appropriate design reinforcements are not implemented.

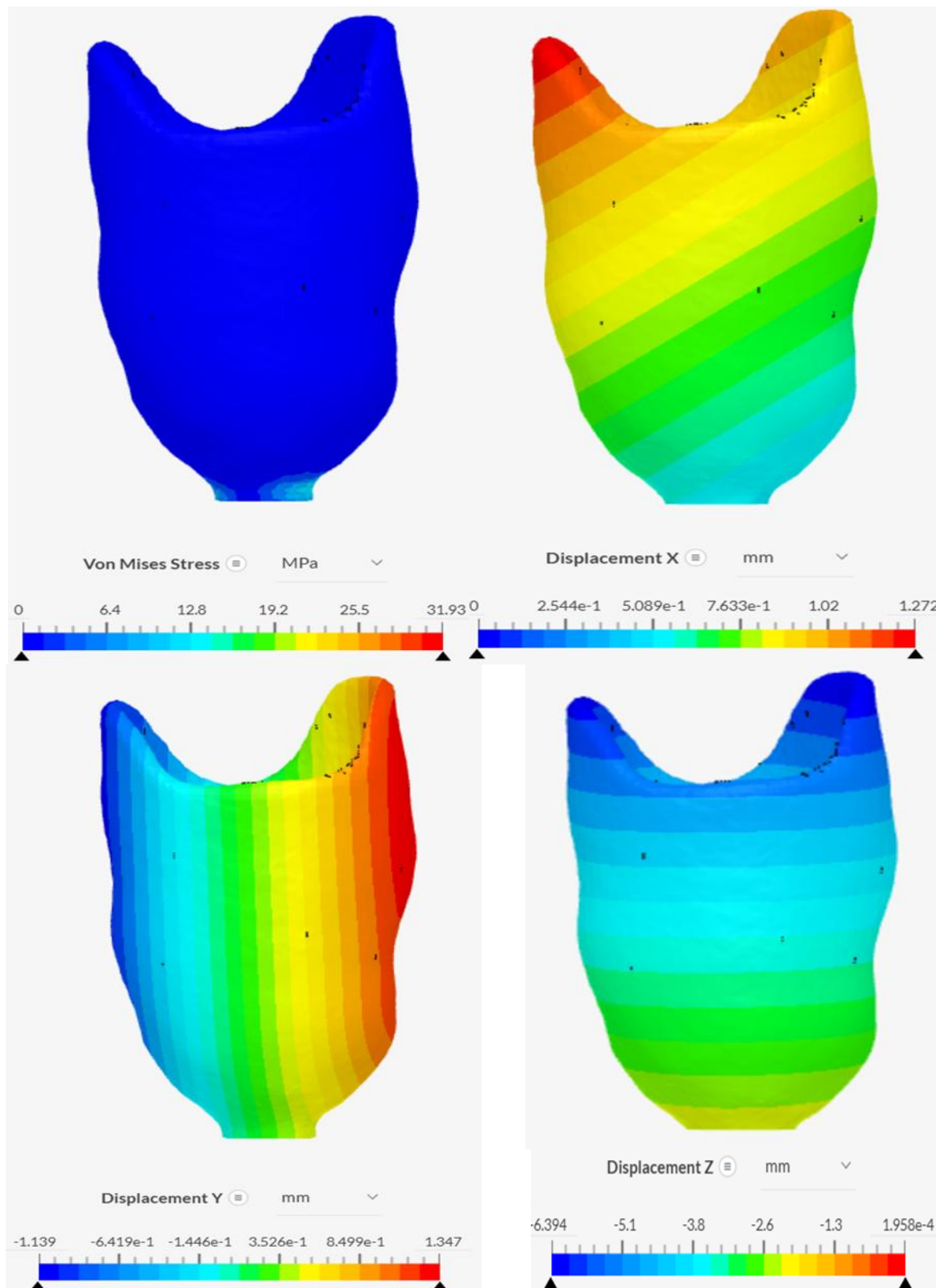


Figure (5-59) Analysis results..

5.8.7.1. Detailed Stress Analysis

Stress distribution patterns were examined along three principal axes (X, Y, and Z) to assess variations in response to different pressure loads, as presented in Tables (5-8) , (5-9) and (5-10).

Table (5-8) Stress Distribution for SACH foot pressure (227.53 kPa.)

Axis	Min Stress (MPa)	Max Stress (MPa)	Mean Stress (MPa)	Standard Deviation (MPa)
X	2.1	9.8	6.3	2.4
Y	1.7	11.2	6.8	2.9
Z	2.5	12.5	7.1	3.1

Table (5-9) Stress Distribution for Multi axis foot pressure (241.3 kPa.)

Axis	Min Stress (MPa)	Max Stress (MPa)	Mean Stress (MPa)	Standard Deviation (MPa)
X	2.5	11.1	7.4	2.8
Y	1.9	12.7	7.9	3.2
Z	2.9	14.2	8.3	3.5

Table (5-10) Stress Distribution for Single axis foot pressure (275.79 kPa.)

Axis	Min Stress (MPa)	Max Stress (MPa)	Mean Stress (MPa)	Standard Deviation (MPa)
X	3	14.6	9.3	3.5
Y	2.5	16.4	10.1	3.9
Z	3.6	18.9	11.2	4.2

From the analysis, the highest stress values are recorded along the Z-axis, which suggests that this axis experiences the most significant load-induced deformations. This is consistent with the expected behavior in pressure-loaded structures, where vertical and transverse stress components dominate the overall response.

5.8.7.2. Deflection (Displacement) Analysis

The structural deflection of the prosthetic socket under different loading conditions is a crucial factor in ensuring user comfort, safety, and performance reliability. Excessive deflection may lead to discomfort, instability, or material failure. The built FE model was used to compute the maximum and mean deflections under three pressure conditions (227.53 kPa, 241.3 kPa, and 275.79 kPa).

The deflection distribution was analyzed along the ($x = 0.2625$, $y = 0.1365$, $z = 0.0892$) axes to determine deformation trends and identify high-displacement zones. The results indicate that:

- The maximum deflection occurred at the upper rim of the socket, where the structure is less constrained.
- The minimum deflection was observed near the base, where the structure is more rigid.
- The deflection increased with applied pressure, demonstrating a proportional relationship between loading magnitude and structural deformation.

The calculated deflections for each loading condition are summarized in Table (5-11) below.

Table (5-11). Deflection analysis under different pressure conditions.

Pressure (kPa)	Min Deflection (mm)	Max Deflection (mm)	Mean Deflection (mm)	Standard Deviation (mm)
SACH foot	0.12	1.85	0.79	0.45
Multi axis foot	0.14	2.03	0.91	0.5
Single axis foot	0.17	2.42	1.08	0.57

The obtained deflection values are within acceptable limits, ensuring the prosthetic socket remains functional and comfortable under standard operating conditions.

The maximum deflection (2.42 mm at Single axis foot) remains below critical deformation thresholds, indicating that material selection and design parameters provide adequate stiffness and durability.

A higher safety margin is maintained under normal loading conditions (SACH foot, Multi axis foot), but further testing at extreme loads is recommended to validate long-term structural performance.

Optimizing the wall thickness or reinforcing high-stress regions could further enhance load-bearing capacity while minimizing excessive deformation.

5.8.7.3. Safety Factor Assessment

The safety factor was evaluated at critical stress points to determine structural stability under each pressure condition. Ensuring that the minimum safety factor remains above 1.5 for all operational conditions is crucial for long-term reliability. The tables (5-12), (5-13) and (5-14) present the safety factors at different vertices:

Table (5-12) Safety Factor Evaluation for SACH foot (227.53 kPa).

Vertex Index	Stress (MPa)	Safety Factor
V1	5.3	4.72
V2	7.6	3.29
V3	10.1	2.47

Table (5-13) Safety Factor Evaluation for Multi axis foot (241.3 kPa).

Vertex Index	Stress (MPa)	Safety Factor
V1	6.2	4.03
V2	9.3	2.69
V3	12.8	1.95

Table (5-14) Safety Factor Evaluation for Single axis foot (275.79 kPa).

Vertex Index	Stress (MPa)	Safety Factor
V1	7.8	3.21
V2	12.5	2
V3	18.9	1.32

The safety factor values highlight potential failure points under extreme loading conditions. Notably, at Single axis foot, the minimum safety factor drops to 1.32, indicating that the structure is approaching its failure threshold. This underscores the need for design optimizations, such as reinforcement in high-stress regions or material selection with higher yield strength.

The stress variations observed in the X, Y, and Z directions further indicate that load distribution is non-uniform, with the highest deformations occurring in the Z-axis. This behavior suggests that structural modifications such as redistributing material mass or incorporating stress-relief features may be necessary to improve overall load-bearing capacity.

Furthermore, the observed standard deviations in stress values indicate the degree of variability in different regions of the structure. Higher standard deviations, as noted at Single axis foot, signify increased localized stress concentrations that could lead to material fatigue over time. Addressing these variations through optimized design approaches can enhance long-term structural integrity.

Chapter six

Conclusions and

Recommendations

Chapter Six

Conclusions and Recommendations

6.1 Conclusions

This study consisted of two main parts. The first part involved a biomechanical analysis of three types of prosthetic feet (SACH, single-axis, and multi-axis), focusing on their performance during daily activities for below-knee amputees. The second part analyzed the stress distribution on prosthetic foot component (socket) using Abaqus 6.5 simulation software, with an emphasis on the upper part where forces were applied.

The findings of this study indicate to the following:

1. The GRF results demonstrated that the multi-axis foot provides enhanced performance, with the highest GRF (703.024 N) and lift force (585.85 N), potentially improving mobility and quality of life for users. In comparison, the SACH foot recorded the lowest GRF (663.116 N), followed by the single-axis foot (674.182 N).
2. The F-socket test measured peak pressures on the socket: 33 psi (227.53 kPa) for the SACH foot, 40 psi (275.79 kPa) for the single-axis foot, and 35 psi (241.3 kPa) for the multi-axis foot. The SACH foot offers stability but lacks adaptability for varied terrains. The single-axis foot provides a more natural gait but concentrates loads more, as shown by the highest pressure. The multi-axis foot adapts to different surfaces, offering better shock absorption and load distribution, enhancing the user's walking experience.
3. The EMG test on the rectus femoris showed no significant differences in muscle activity among the three types of prosthetic feet.

4. Acceleration results were collected at knee and hip locations using the patient's accelerometer sensor during walking trials with different prosthetic limbs. Findings revealed that higher sensor placement height corresponds to reduced acceleration while walking, influenced by increased distance from the floor and other factors like muscle, skin, and fat.
5. The Vernier Graphical Analysis program was used to convert the acceleration values into vibration values using Fast Fourier Transform (FFT). The root mean square (RMS) values of vibration at the knee and hip for the three types of feet were calculated using MATLAB software.
6. The SACH foot is the most favorable option among the three types for minimizing excessive motion and providing stability, particularly in lateral and vertical directions. Its lower RMS values in the Y and Z axes indicate better overall performance compared to the Single and Multi-feet. The Single foot, while advantageous in the X-axis, does not surpass the SACH foot in overall stability. The best choice ultimately depends on individual needs and walking conditions, but the SACH foot stands out as the superior option for stability and comfort.
7. Three-dimensional gait analysis (3DMA) yields various joint angles including pelvic, hip, knee, ankle, and foot angles for each leg during walking with different prosthetic limbs. The multi-axis foot demonstrated greater mobility and was closer to natural foot movement, while the results for the single-axis feet were very close in terms of movement. For the SACH foot, there was a more difference from the multi and single foot in the range of results.
8. The simulation reveals that the Multi-Axis Foot distributes stress moderately (11.1, 12.7, 14.2 MPa across X, Y, Z axes) but lacks shock absorption compared to the SACH and Single-Axis Feet. The Single-Axis Foot exhibits

the highest stress (275.79 kPa), nearing critical levels with a low safety factor (1.32), and risking structural failure under prolonged use.

9. The simulation also reveals that for active users, the Multi-Axis Foot offers balanced stress distribution. While for stability-focused users, the SACH Foot is safer but less dynamic. The Single-Axis Foot requires reinforcements to mitigate high-stress zones and enhance longevity.
10. Design improvements should prioritize Z-axis reinforcement and material selection to ensure long-term reliability.

Conclusion: The Multi-Axis Foot emerges as the best option overall due to its superior performance in GRF, adaptability, pressure distribution, and reduced vibrations. While the SACH foot excels in stability, its limitations in terrain adaptability and lower GRF make it less favorable compared to the Multi-Axis foot. The Single-Axis foot, although it has some benefits, does not match the overall performance and comfort of the Multi-Axis foot. Ultimately, the choice should consider individual activity levels and specific user needs.

6.2 Recommendations

Depending on interest, existing work can be further extended in multiple directions. The following recommendations and suggestions are for further works:

1. Analyze the application of novel materials (e.g., composites or smart materials) in prosthetic feet to study their effects on vibration damping and stress distribution.
2. Create comprehensive biomechanical models that can emulate a multitude of foot activities (running, climbing) and examine how different foot types perform under different conditions.

3. Look at how researchers are creating multifunctional prosthetic feet that can automatically adjust to different activities or terrains, possibly using smart technology to make adjustments in real time.
4. Investigate the influence of environment (such as temperature, humidity, terrain type) on the performance of various types of prosthetic foot, as well as the vibration and stress experienced.
5. Prosthetic foot types effects in terms of pediatric population

References

- [1] Ayyer, Lavanya R., and Asmita C. Moharkar. "Co-relation of functional mobility with anxiety in traumatic below knee amputees." *Int J Physiother Res* 9.5 (2021): 4013-18.
- [2] Chambers, A. "Physiotherapy for amputees." *Tidy's Physiotherapy. 13th ed. London: Butterworth-Heinemann* (2003).
- [3] O'Sullivan at.al, Physical Rehabilitation, Chapter 22 "Amputation". Edition 6
- [4] Murray, Craig D., and Jezz Fox. "Body image and prosthesis satisfaction in the lower limb amputee." *Disability and rehabilitation* 24.17 (2002): 925-931.
- [5] Norton, Kim. "A brief history of prosthetics." *InMotion* 17.7 (2007): 11-3.
- [6] Ismawan, Ade Reza, et al. "A review of existing transtibial bionic prosthesis: mechanical design, actuators and power transmission." *Journal of Biomedical Science and Bioengineering* 1.2 (2022): 65-72.
- [7] Dougherty, Paul J. "Research and future developments in upper and lower limb prostheses." *Current Orthopaedic Practice* 24.2 (2013): 149-152.
- [8] Trent, Lauren, et al. "A narrative review: current upper limb prosthetic options and design." *Disability and Rehabilitation: Assistive Technology* (2020).
- [9] McGimpsey, Grant, and Terry C. Bradford. "Limb prosthetics services and devices." *Bioengineering Institute Center for Neuroprosthetics Worcester Polytechnic Institution* (2008): 1-35.
- [10] Orr, J. F., W. V. James, and A. S. Bahrani. "The history and development of artificial limbs." *Engineering in Medicine* 11.4 (1982): 155-161.

[11] Hussain, Samreen, Sarmad Shams, and Saad Jawaid Khan. "Impact of medical advancement: Prostheses." *Computer Architecture in Industrial, Biomechanical and Biomedical Engineering* (2019): 9.

[12] Chui, Kevin K., et al. Orthotics and Prosthetics in Rehabilitation E-Book: Orthotics and Prosthetics in Rehabilitation E-Book. Elsevier Health Sciences, 2019.

[13] Selvam, P. Senthil, et al. "Prosthetics for lower limb amputation." *Prosthetics and Orthotics*. IntechOpen, 2021.

[14] Kelly. *Mechanical vibrations: theory and applications*. Cengage learning, 2012.

[15] Hägström, Eva, et al. "Vibrotactile evaluation: osseointegrated versus socket-suspended transfemoral prostheses." *Journal of Rehabilitation Research & Development* 50.10 (2013).

[16] Jimenez, Meghan C., and Jeremy A. Fishel. "Evaluation of force, vibration and thermal tactile feedback in prosthetic limbs." 2014 Ieee Haptics Symposium (Haptics). IEEE, 2014.

[17] Andrysek, Jan. "Lower-limb prosthetic technologies in the developing world: A review of literature from 1994–2010." *Prosthetics and orthotics international* 34.4 (2010): 378-398.

[18] Voinescu, M., et al. "Estimation of the forces generated by the thigh muscles for transtibial amputee gait." *Journal of biomechanics* 45.6 (2012): 972-977.

[19] Ferreira, César, Luis Paulo Reis, and Cristina P. Santos. "Review of control strategies for lower limb prostheses." *Robot 2015: Second Iberian Robotics Conference: Advances in Robotics, Volume 2*. Springer International Publishing, 2016.

[20] Windrich, Michael, et al. "Active lower limb prosthetics: a systematic review of design issues and solutions." *Biomedical engineering online* 15 (2016): 5-19.

[21] Lechler, Knut, et al. "Motorized biomechatronic upper and lower limb prostheses—clinically relevant outcomes." *PM&R* 10.9 (2018): S207-S219.

[22] Asif, Muhammad, et al. "Advancements, trends and future prospects of lower limb prosthesis." *IEEE Access* 9 (2021): 85956-85977.

[23] Manz, Sabina, et al. "A review of user needs to drive the development of lower limb prostheses." *Journal of neuroengineering and rehabilitation* 19.1 (2022): 119.

[24] Kendell, C., et al. "Indicators of dynamic stability in transtibial prosthesis users." *Gait & posture* 31.3 (2010): 375-379.

[25] Gholizadeh, H., et al. "Transtibial prosthesis suspension systems: systematic review of literature." *Clinical biomechanics* 29.1 (2014): 87-97.

[26] Arifin, Nooranida, et al. "Postural stability characteristics of transtibial amputees wearing different prosthetic foot types when standing on various support surfaces." *The scientific world journal* 2014.1 (2014): 856279.

[27] Paradisi, Francesco, et al. "The Conventional Non-Articulated SACH or a Multiaxial Prosthetic Foot for Hypomobile Transtibial Amputees? A Clinical Comparison on Mobility, Balance, and Quality of Life." *The Scientific World Journal* 2015.1 (2015): 261801.

[28] Safari, Reza, and Margrit Regula Meier. "Systematic review of effects of current transtibial prosthetic socket designs—Part 1: Qualitative outcomes." *Journal of Rehabilitation Research and Development* (2015).

[29] Al-Fakih, Ebrahim A., Noor Azuan Abu Osman, and Faisal Rafiq Mahmad Adikan. "Techniques for interface stress measurements within prosthetic sockets of

transtibial amputees: A review of the past 50 years of research." *Sensors* 16.7 (2016): 1119.

[30] Chatterjee, Subhomoy, et al. "Problems with use of trans-tibial prosthesis." *Journal of Medical Imaging and Health Informatics* 6.2 (2016): 269-284.

[31] Davenport, Philip, et al. "Systematic review of studies examining transtibial prosthetic socket pressures with changes in device alignment." *Journal of Medical and Biological Engineering* 37 (2017): 1-17.

[32] Liu, Jingjing, et al. "Classification and comparison of mechanical design of powered ankle-foot prostheses for transtibial amputees developed in the 21st century: a systematic review." *Journal of Medical Devices* 15.1 (2021): 010801.

[33] Abbod, Esraa A., and Kadhim K. Resan. "Review on the Interface Pressure Measurement for Below Knee Prosthetic Socket." IOP Conference Series: Materials Science and Engineering. Vol. 1094. No. 1. IOP Publishing, 2021.

[34] Goh, J. C. H., et al. "Biomechanical evaluation of SACH and uniaxial feet." *Prosthetics and orthotics international* 8.3 (1984): 147-154.

[35] Huang, Kuo-Feng, et al. "Kinematics properties and energy cost of below-knee amputees." *Biomedical Engineering: Applications, Basis and Communications* 13.02 (2001): 99-107.

[36] Powelson, Thomas, and James Yang. "Literature review of prosthetics for transtibial amputees." *International Journal of Biomechatronics and Biomedical Robotics* 2.1 (2012): 50-64.

[37] Pirouzi, Gh, et al. "Review of the socket design and interface pressure measurement for transtibial prosthesis." *The scientific World journal* 2014.1 (2014): 849073.

[38] Resan, K. K., E. A. Abbod, and T. K. Al-Hamdi. "Prosthetic feet: A systematic review of types, design, and characteristics." *AIP Conference Proceedings*. Vol. 2806. No. 1. AIP Publishing, 2023.

[39] Puers, R., et al. "A telemetry system for the detection of hip prosthesis loosening by vibration analysis." *Sensors and Actuators A: Physical* 85.1-3 (2000): 42-47.

[40] Bedaiwi, Bashar A., and Jumaa S. Chiad. "Vibration Analysis and Measurement in the Below Knee Prosthetic Limb: Part I—Experimental Work." *ASME International Mechanical Engineering Congress and Exposition*. Vol. 45189. American Society of Mechanical Engineers, 2012.

[41] Jweeg, Mohsin Juber, and Jana S. Jaffar. "Vibration Analysis of Prosthesis for the through knee Amputation." *Al-Nahrain Journal for Engineering Sciences* 19.1 (2016): 46-55.

[42] Farahmand, F. "Kinematic and dynamic analysis of the gait cycle of above-knee amputees." *Scientia Iranica* 13.3 (2006).

[43] Vom Fachbereich, "Design and Active Foot for Smart Prosthetic Leg", Ph.D. Thesis, University Darmstadt, December 2007.

[44] Takhakh, Ayad M., Fahad M. Kadhim, and Jumaa S. Chiad. "Vibration Analysis and Measurement in Knee Ankle Foot Orthosis for Both Metal and Plastic KAFO Type." *ASME International Mechanical Engineering Congress and Exposition*. Vol. 56222. American Society of Mechanical Engineers, 2013..

[45] Jweeg, Muhsin J., Kadhim K. Resan, and Muhanad N. Mohammed. "Design and manufacturing of a new prosthetic low cost pylon for amputee." *Journal of Engineering and Sustainable Development* 14.4 (2010): 119-131.

[46] Winiarski, Sławomir, and Alicja Rutkowska-Kucharska. "Estimated ground reaction force in normal and pathological gait." *Acta of Bioengineering & Biomechanics* 11.1 (2009).

[47] Rincon Alvarez, Javier. *Understanding gait analysis: variability of data collected with a pressure sensitive walkway*. Diss. University of Glasgow, 2021.

[48] Al-Fakih, Ebrahim A., Noor Azuan Abu Osman, and Faisal Rafiq Mahmad Adikan. "Techniques for interface stress measurements within prosthetic sockets of transtibial amputees: A review of the past 50 years of research." *Sensors* 16.7 (2016): 1119.

[49] Kiran, K., and K. Uma Rani. "Analysis of EMG signal to evaluate muscle strength and classification." *International Research Journal of Engineering and Technology (IRJET)* 4.7 (2017): 177-182.

[50] Gupta, Ashutosh, et al. "EMG signal analysis of healthy and neuropathic individuals." *IOP Conference Series: Materials Science and Engineering*. Vol. 225. No. 1. IOP Publishing, 2017.

[51] Cimolin, Veronica, and Manuela Galli. "Summary measures for clinical gait analysis: A literature review." *Gait & posture* 39.4 (2014): 1005-1010.

List of Publications

[1] Comfort Ability of a Transtibial Amputee According to a Biomechanical Comparison Between SACH, Single – Axis and Muti – Axis Feet Using GRF and Interface Pressure Tests.



رسالة قبول

عنوان البحث :

Comfort ability of A Transtibial Amputee According to A Biomechanical Comparison between SACH, Single-axis and Multi-axis Feet Using GRF and Interface Pressure Tests

السادة الباحثين : خider رحيم معيد, جمعة سلمان جيد, حسين ابراهيم خلف المحترمين

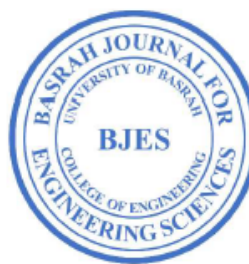
تحية طيبة ...

يسر هيئة التحرير اعلامكم بقبول بحثكم اعلاه للنشر في مجلة البصرة للعلوم الهندسية وسيتم نشره في عدد سوف يحدد لاحقاً مع التقدير.

أ.د. امين احمد نصار

محرر المجلة

<http://bjes.edu.iq>



Appendix A: MATLAB Code

This appendix includes the MATLAB code used to read acceleration data from an Excel file and calculate the root mean square (RMS) of the vibration data. This code is integral to the analysis presented in this thesis.

```
function run_acceleration_to_rms()

% Main script to read acceleration data and calculate RMS

% Define the path to the Excel file on the Desktop

filename = 'C:\Users\DELL 3541\OneDrive\سطح المكتب\acceleration_data.xlsx';

% Read acceleration data from Excel file

try

% Read the data from the first sheet

acceleration_data = readtable(filename); % Read data as a table

% Convert the table to an array (assuming the data is in the first column)

acceleration_data = acceleration_data{:, 1}; % Adjust if your data is in a different
column

% Display the first few elements of the data to verify

disp('Acceleration Data (first 5 samples):');

disp(acceleration_data(1:min(5, end))); % Display first few rows (up to 5)

% Define the sampling frequency (replace with your actual value)

fs = 100; % Sample frequency in Hz
```

```
% Calculate and display the RMS of the vibration data

rms_vibration = calculate_rms_vibration(acceleration_data, fs);

catch ME

fprintf('Error: %s\n', ME.message);

end

end

function rms_vibration = calculate_rms_vibration(acceleration_data, fs)

% Calculate the RMS of the vibration data obtained from FFT

% Input:

% acceleration_data - a vector of acceleration values (m/s2)

% fs - sampling frequency in Hz

% Output:

% rms_vibration - the RMS value of the vibration data

% Step 1: Perform FFT on the acceleration data

N = length(acceleration_data); % Number of samples

Y = fft(acceleration_data); % Compute the FFT

P2 = abs(Y / N); % Two-sided spectrum

P1 = P2(1:floor(N/2)+1); % Single-sided spectrum (ensure integer indexing)

P1(2:end-1) = 2 * P1(2:end-1); % Multiply by 2 for single-sided spectrum
```

```
% Step 2: Calculate RMS of the vibration data

rms_vibration = sqrt(mean(P1.^2)); % RMS of the FFT output

% Display the first five vibration values

disp('First 5 Vibration Values:');

disp(P1(1:min(5, end))); % Display first 5 vibration values

% Display the RMS value

fprintf('The RMS value of the vibration data is: %.2f m/s^2\n', rms_vibration);

end
```

Description

This code performs the following functions:

- Read acceleration data from an Excel file.
- Calculate the RMS of the vibration data using Fast Fourier Transform (FFT).
- Display the first few samples of the acceleration data and the calculated RMS value.

This code is essential for analyzing the vibration data, as detailed in the main body of the thesis.

Appendix B: EMG Activity of the lower limb Muscles results

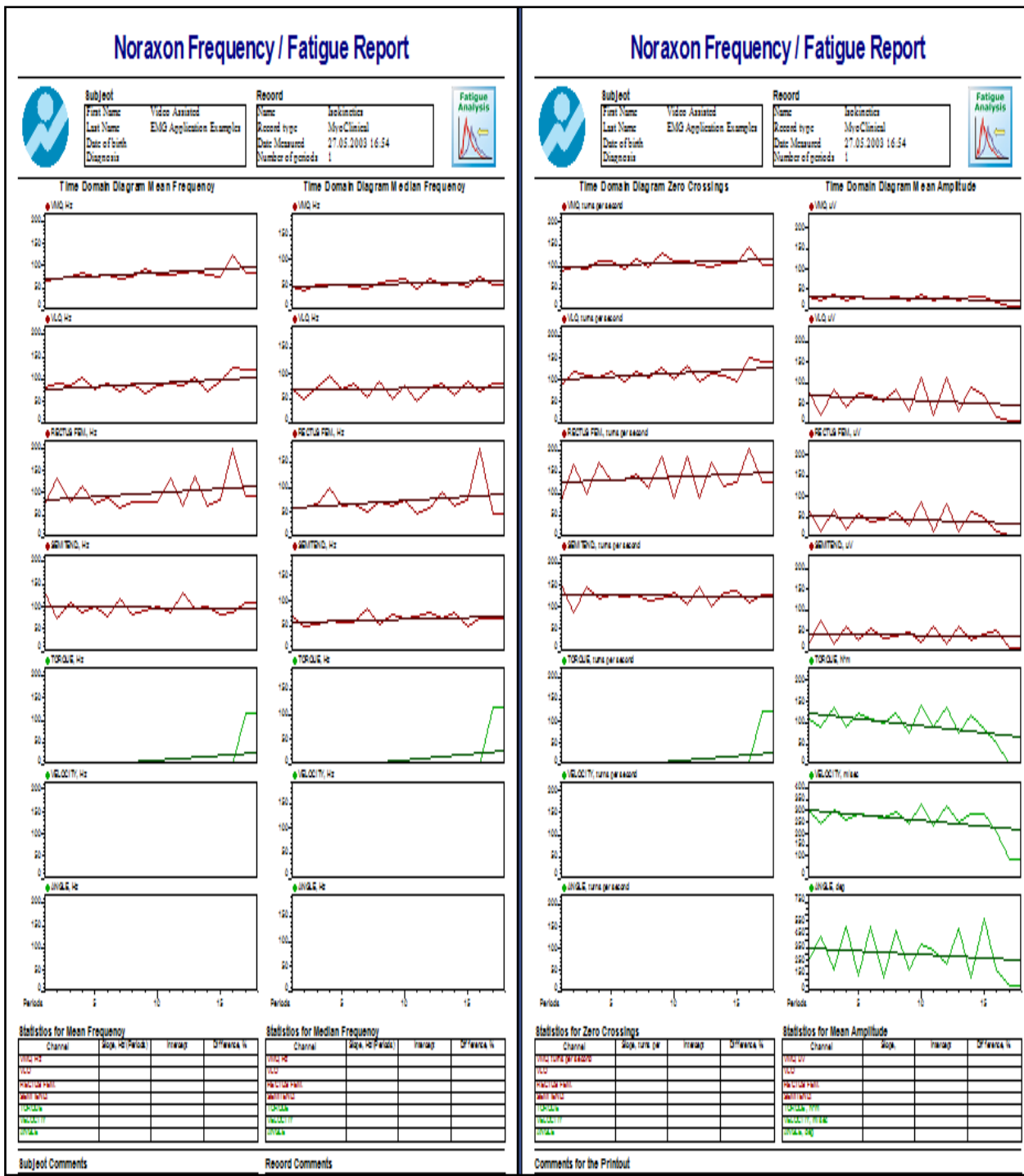


Figure (B-1) the fatigue report for Noraxon EMG test for Single axis foot.

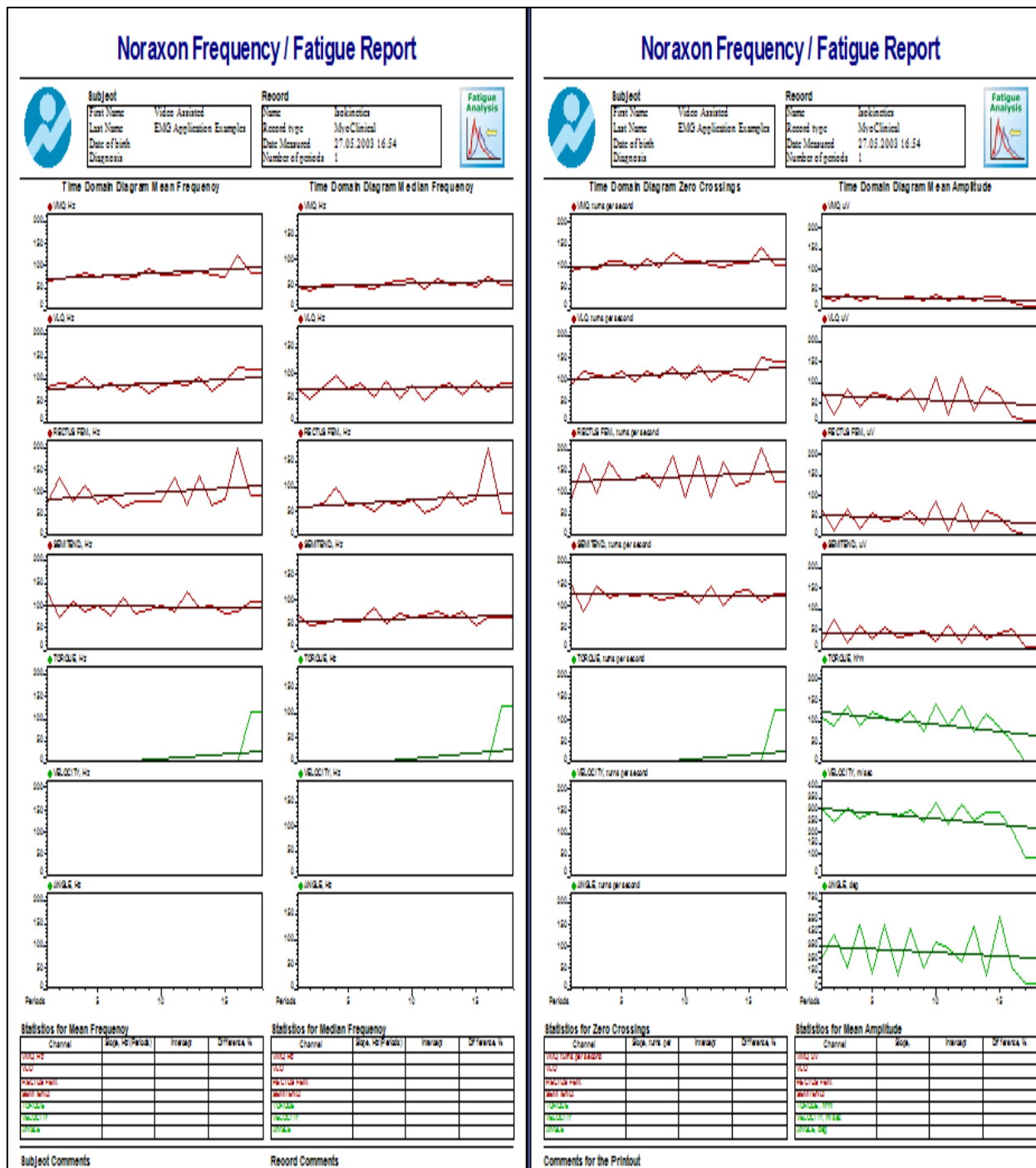


Figure (B-2) the fatigue report for Noraxon EMG test for Multi axis foot.

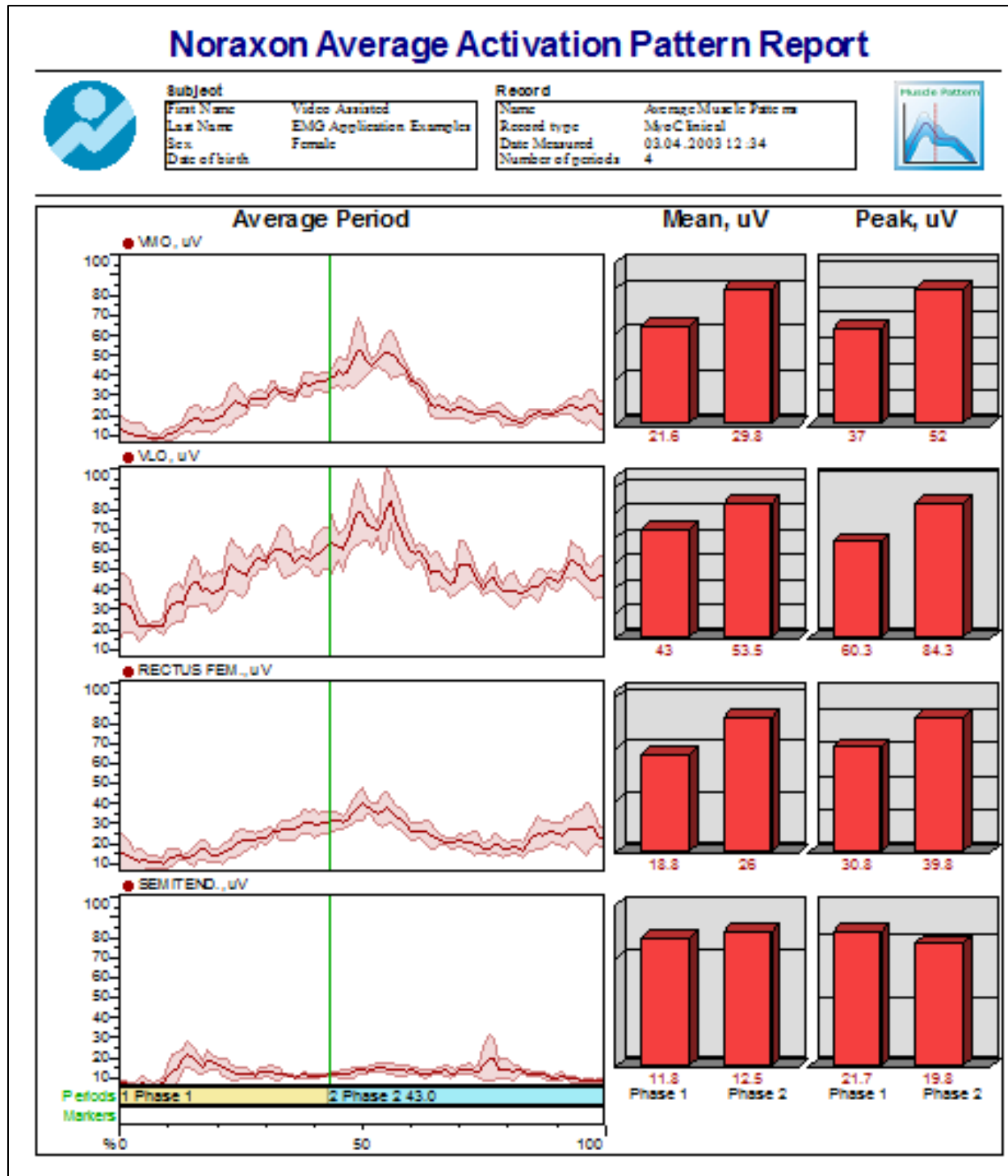


Figure (B-3) the muscle pattern report for the Noraxon EMG test for Single axis foot.

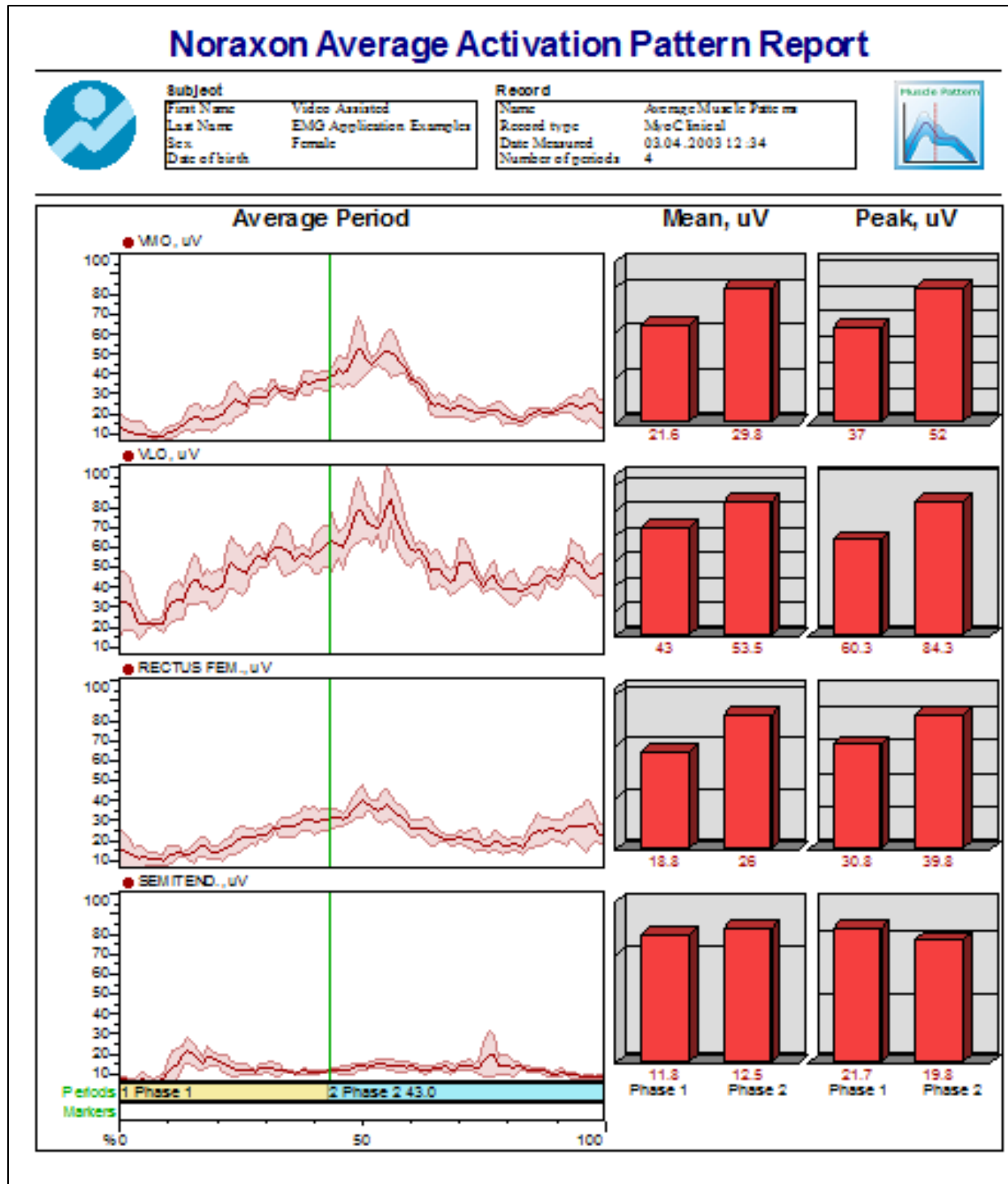


Figure (B-4) the muscle pattern report for the Noraxon EMG test for Multi axis foot.

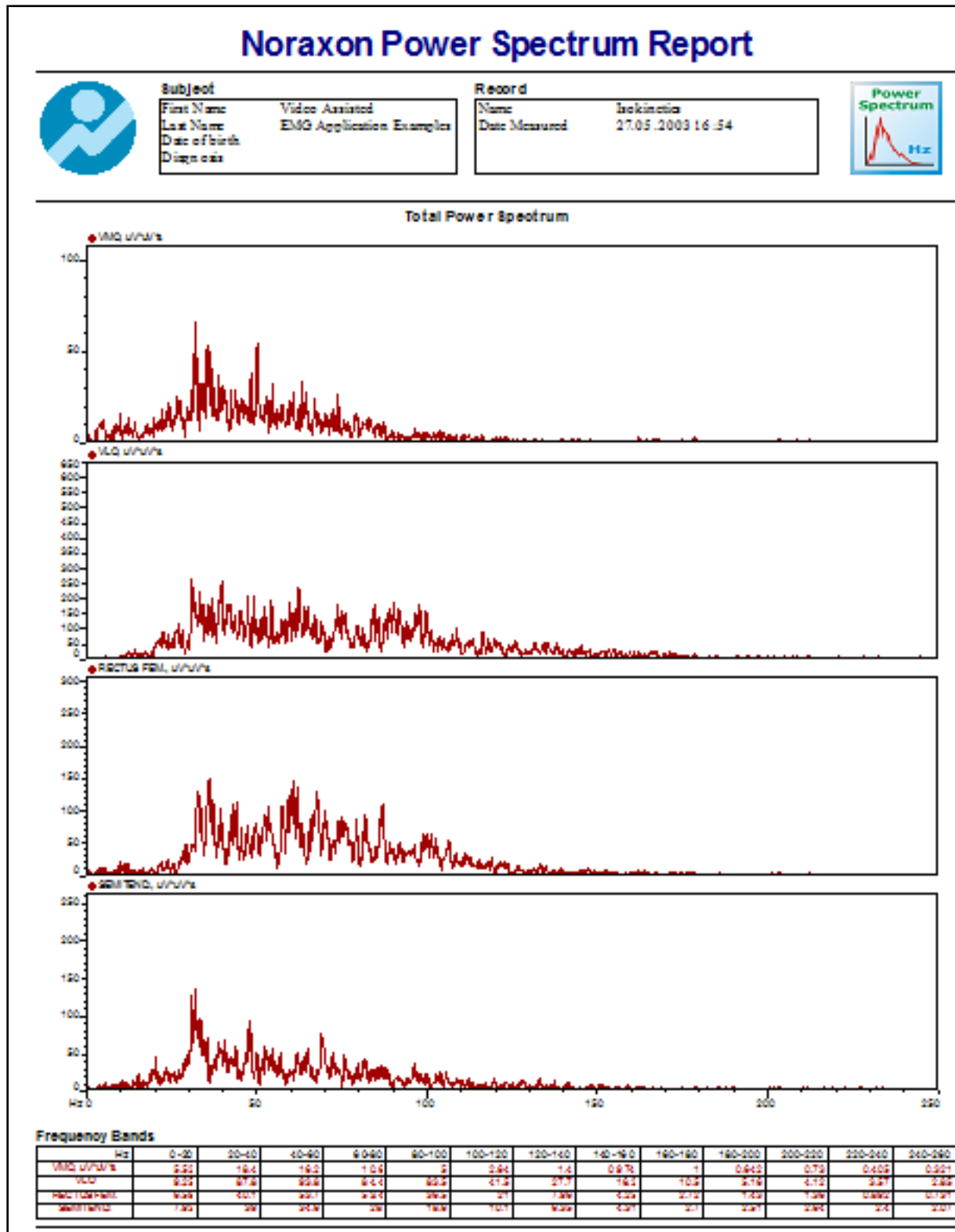


Figure (B-5) the power spectrum report for Noraxon EMG test for Single axis foot.

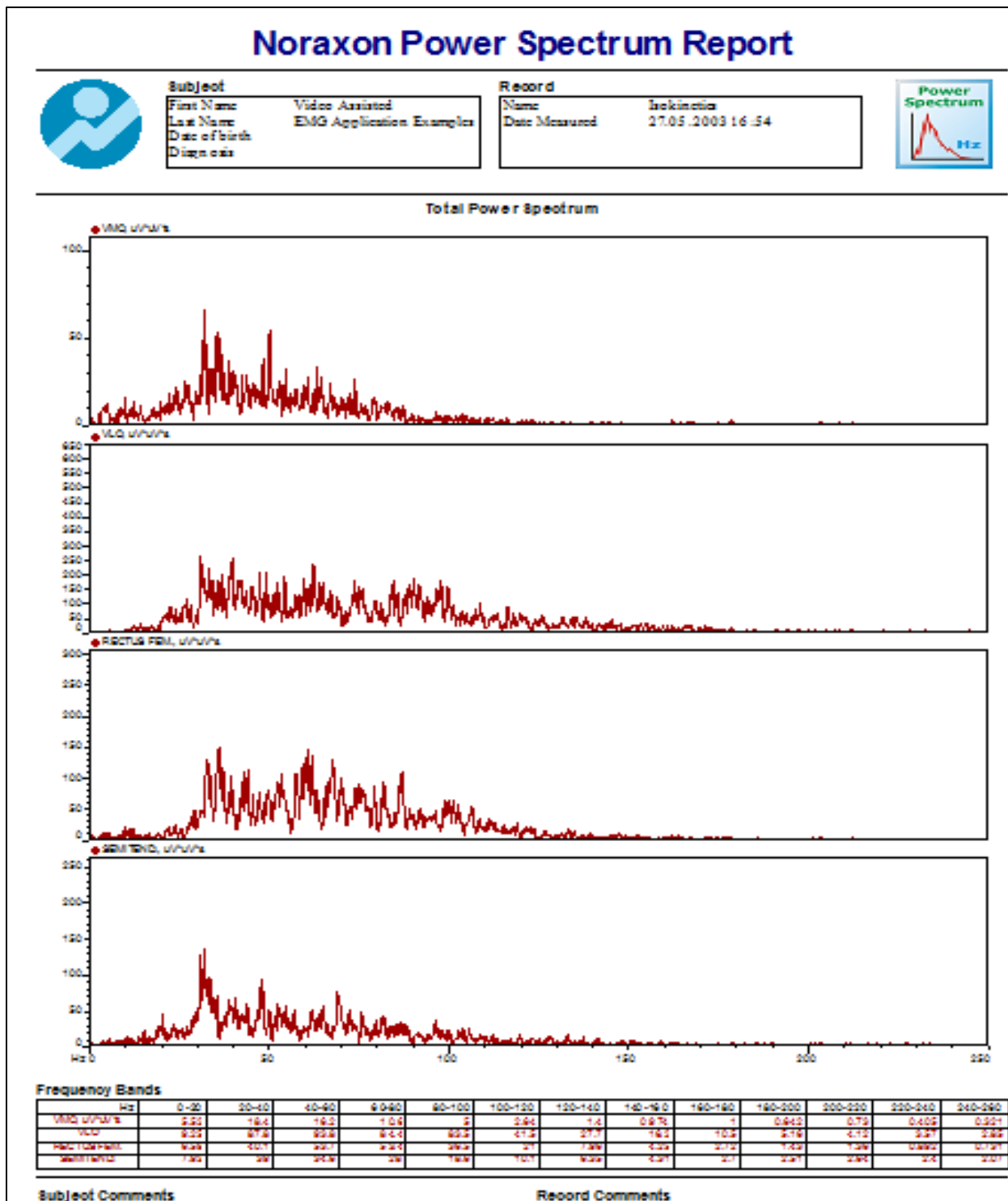


Figure (B-6) the power spectrum report for Noraxon EMG test for Multi axis foot.

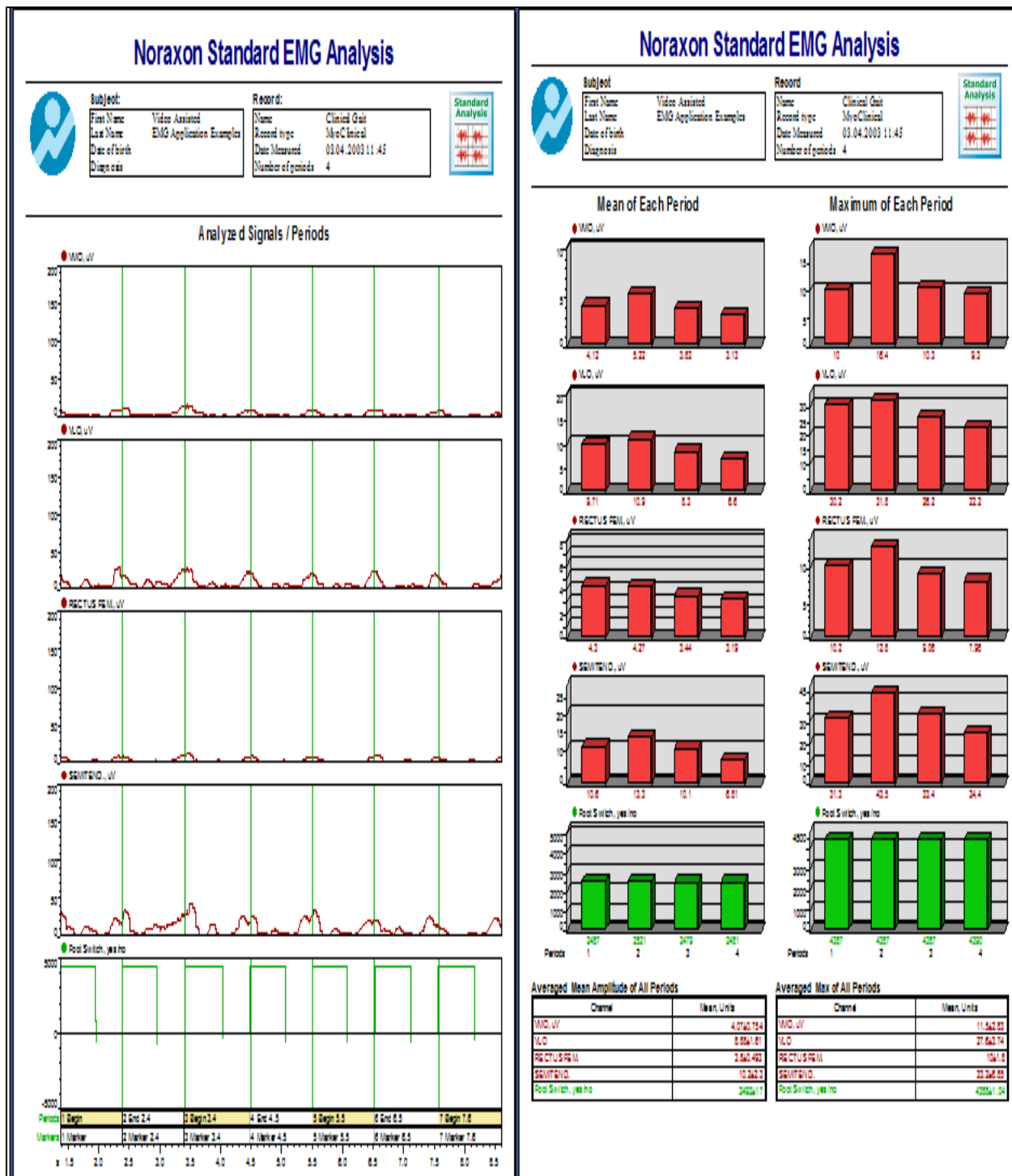


Figure (B-7) show the standard EMG analysis report for the test for Single axis foot.

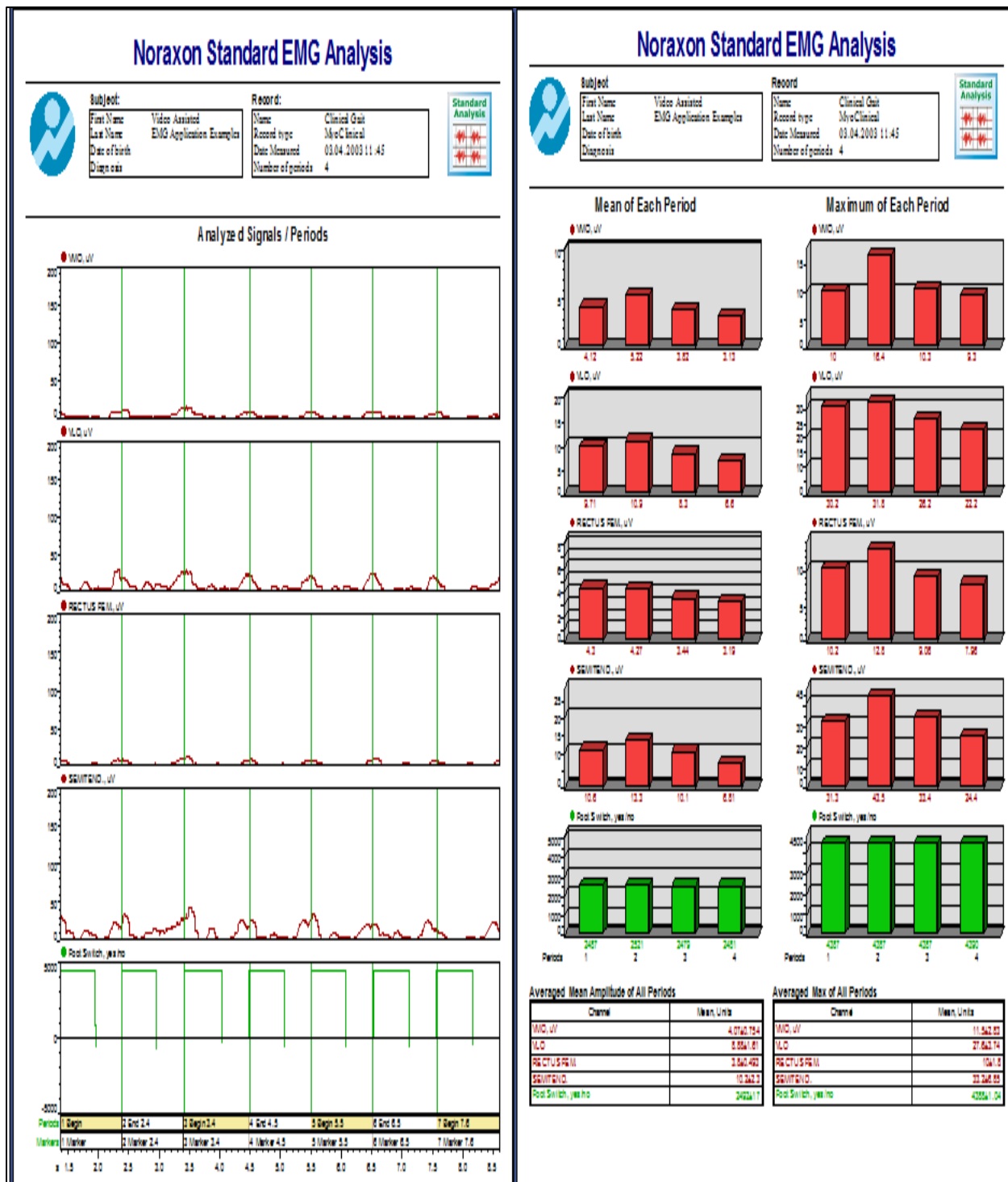


Figure (B-8) show the standard EMG analysis report for the test for Multi axis foot.

دراسة تأثير نوع القدم الاصطناعية على الاهتزازات والإجهادات التي تتعرض لها الأطراف الاصطناعية أسفل الركبة

رسالة مقدمة إلى كلية الهندسة

جامعة البصرة

كجزء من متطلبات نيل شهادة الماجستير في علوم

الهندسة الميكانيكية

تقدم بها

حيدر رحيم معيد

شباط 2025

الخلاصة

تهدف هذه الدراسة إلى تقديم رؤى يمكن أن تؤدي إلى تقدم في تكنولوجيا الأطراف الصناعية، مما يعزز تجربة المستخدم العامة للأشخاص الذين تم بتر أرجلهم أسفل الركبة، من خلال التحقيق في كيفية تأثير أنواع الأطراف الصناعية المختلفة على الاهتزازات والضغوط لدى هؤلاء المرضى.

تم اختيار رجل يبلغ من العمر 34 عاماً، فقد قدمه الأيسر في عام 2016، كعينة دراسية للبحث الحالي ، من خلال تصوير مقطعي محوسب في مستشفى الكاظمية التعليمي لتحديد أبعاد الجزء المبتور. تستخدم هذه التقنية شعاعاً ضيقاً من الأشعة السينية يدور حول الجسم لتوليد صور مقطعية.

لتقييم القوى المؤثرة على ثلاثة أنواع من الأطراف الصناعية (SACH، الأحادية المحور، متعددة المحاور) تم قياس قوة رد الفعل الأرضي باستخدام منصة Tekscan Walkway وتم قياس توزيع ضغط الواجهة باستخدام مستشعر F-socket بين الطرف الاصطناعي والطرف المتبقى ، تم تحليل ضغط العضلات في الساق المبتورة باستخدام مستشعرات EMG Myotrace 400 المثبتة على الفخذ، كما تم تحويل قيم التسارع إلى قيم اهتزاز باستخدام تحويل فورييه السريع (FFT) وتم تحليلها عبر الجذر التربيعي المتوسط (RMS) للمقارنة بين أنواع الأطراف. بالإضافة إلى ذلك، تم إجراء نمذجة عدبية ومحاكاة باستخدام برنامج ABAQUS 6.5 جنباً إلى جنب مع الاختبارات الواقعية.

سجل الطرف الصناعي SACH أدنى قيمة لقوة رد الفعل الأرضي (663.116 نيوتن)، بينما أظهر الطرف الصناعي متعدد المحاور أعلى قيمة (703.024 نيوتن). وهذا يشير إلى أن الطرف متعدد المحاور قد يوفر امتصاصاً وتوزيعاً أفضل للطاقة أثناء المشي، مما قد يعزز خصائص الأداء ويؤدي إلى تحسين التنقل وجودة الحياة للمستخدمين.

فاس اختبار F-socket الضغوط المركزية القصوى: 227,53 كيلوباسكال لطرف SACH، و 275,79 كيلوباسكال لطرف الأحادية المحور، و 241,3 كيلوباسكال لطرف متعددة المحاور. تشير هذه النتائج إلى أن الطرف متعدد المحاور هو الخيار الأفضل بين الأنواع الثلاثة نظراً لتوزيع الضغط الفائق، والأداء الديناميكي، والراحة، مما يجعله أكثر ملائمة للتكيف مع الأسطح المختلفة الضرورية لنمط حياة نشط.

تكشف تحليلات EMG أن نشاط العضلات في الطرف السفلي، وخاصة في عضلة الفخذ المستقيمة، لا يتأثر بشكل كبير بنوع الطرف الاصطناعي المستخدم .

أظهرت قيم RMS للاهتزاز أن الطرف SACH هو الخيار الأفضل لتقليل الحركة الزائدة وتوفير الاستقرار، خاصة في الاتجاهين الجانبي والرأسي. تشير قيم RMS المنخفضة في المحاور Y و Z إلى أداء أفضل مقارنةً بالأطراف الأحادية والمتعددة. بينما يتفوق الطرف الأحادي في المحور X ، إلا أنه لا يضاهي استقرار الطرف SACH بشكل عام. في النهاية، يعتمد الخيار الأفضل على احتياجات الأفراد وظروف المشي، لكن الطرف SACH يظل الخيار الأفضل من حيث الاستقرار والراحة.

المحاكاة العددية للدراسة اجريت لحساب توزيع الضغوط في الطرف الصناعي تحت ثلاث حالات تحميل: طرف SACH عند kPa227.53 ، والطرف متعدد المحاور عند kPa241.3 ، والطرف الأحادي المحور عند kPa. 275.79 أظهر الطرف الأحادي أعلى الضغوط، بقيم متوسطة في المحاور X و Y و Z (9.3، 10.1، و 11.2) بسبب محدودية الحركة. بينما أظهر الطرف متعدد المحاور ضغوطاً معتدلة (7.4، 7.9، و 8.3) نتيجة لتوزيع القوى بشكل فعال ولكنه يفتقر إلى امتصاص الصدمات. كان للطرف SACH أدنى الضغوط (6.3، 6.8، و 7.1) بفضل تصميمه الذي يمتص الصدمات. تسلط هذه التحليل الضوء على أهمية اختيار الطرف الاصطناعي المناسب بناءً على مستوى النشاط والتوازن بين توزيع الضغوط والوظائف.

في الختام، يعد الطرف متعدد المحاور هو الخيار الأفضل بشكل عام من حيث الأداء البيوميكانيكي والراحة، ما لم يتم إعطاء الأولوية للاستقرار، وفي هذه الحالة يكون الطرف SACH هو المفضل.